Utilizing Noise to implement Logical operations in Bistable Systems

Manaoj Aravind V

A thesis submitted for the partial fulfillment of

the degree of Doctor of Philosophy

Department of Physical Sciences

Indian Institute of Science Education and Research (IISER) Mohali

Knowledge city, Sector 81, SAS Nagar, Manauli PO, Mohali 140306, Punjab, India.

January, 2020

To my *family* who've always been *there* for me.
To my *friends* who've always been *here* for me.

Certificate of Examination

This is to certify that the dissertation titled *"Utilizing noise to implement logical operation in bistable systems"* submitted by **Mr. Manaoj Aravind V** (Reg. No. MP12011) for the partial fulfillment of Doctor of Philosophy programme of the Institute, has been examined by the thesis committee duly appointed by the Institute. The committee finds the work done by the candidate satisfactory and recommends that the report be accepted.

Dr. Kamal P. Singh

Dr. Ananth Venkatesan

Professor Sudeshna Sinha

(Supervisor)

Declaration

The work presented in this dissertation has been carried out by me under the guidance of Prof. Sudeshna Sinha at the Indian Institute of Science Education and Research Mohali.

This work has not been submitted in part or in full for a degree, a diploma, or a fellowship to any other university or institute. Whenever contributions of others are involved, every effort is made to indicate this clearly, with due acknowledgment of collaborative research and discussions. This thesis is a bona-fide record of original work done by me and all sources listed within have been detailed in the bibliography.

Manaoj Aravind V

(Candidate)

In my capacity as the supervisor of the candidate's doctoral thesis, I certify that the above statements by the candidate are true to the best of my knowledge.

Professor Sudeshna Sinha

(Supervisor)

Acknowledgements

I thank the people who've nurtured and guided me through various stages of my life, without whose support and care, I would not be what I am today and this thesis would not exist.

I wholeheartedly thank Prof. Sudeshna Sinha for guiding me through my noisy research endeavor. I owe all the competence I have currently acquired in research to her persistence and patience. Thank you for showing me sometimes all it takes is a constant bias.

I thank Dr. K. Murali of Anna University, for the hands-on introduction to nonlinear dynamics and driving home the importance of the real world application of research. His constant advice and support throughout has been crucial in making this thesis possible.

I thank members of my thesis committee, Dr. Kamal P. Singh and Dr. Ananth Venkatesan, for their support and guidance.

I thank IISER Mohali, for nurturing and funding my research and providing a home away from home for seven years.

I thank my friends at IISER, for making a home out of an institute. I thank my friends far away, for shaping me into who I am.

I thank my family, for bringing me up, loving me to the core and accommodating innumerable hardships just to let me follow my heart.

Thank you all.

Manaoj Aravind V

Preface

The central theme of this thesis is the study of bistable dynamical systems in the presence of noise and the subsequent use of this understanding to implement highly reliable logic gates that work in the presence of noise. Specifically, we identify the various regimes of behaviours that arise when bistable systems interact with noise and use this understanding to construct logic gates and identify the parameter ranges where reliable operation is achieved.

In the first part of this thesis, we explore the behaviour of two coupled bistable systems that are subject to noises from two independent uncorrelated noise sources. The influence of the uncorrelated noise sources hinder the onset of synchronization, whereas the coupling between the two systems aids it. The noise in the two systems promote the random escapes from the locally stable states, while the coupling between the systems pulls them towards the same wells. This interaction of mutually opposing trends may give rise to counter intuitive behaviours in such systems. Thus the central question we raise is the following: When do the random hopping events induced by noise, become synchronous in coupled bistable systems? To answer this question we study a variety of bistable systems subject to different kinds of noises over an entire range of coupling and noise strengths.

We observe that depending on the coupling and noise strength four different regimes of behaviours emerge: (a) no synchrony and no hopping, (b) unsynchronized hopping, (c) synchronized hopping and (d) synchrony without hopping. We quantify these qualitative behaviours and characterize the newly observed phenomenon of synchronized random hopping, using the two measures synchronization error and probability of hopping. We identify that the phenomenon of synchronized hopping is non-trivial as the dependence of both synchronization error and hopping probability is non-monotonic with respect to coupling and noise strengths. We demarcate these different regimes of behaviour in a parameter space of coupling and noise strengths by introducing thresholds on the two measures to quantify reasonable synchrony and sufficiently frequent switching.

In order to establish the generality of these results we study same results in a bistable synthetic gene network model and a piece-wise linear bistable circuit model. We also investigate the behaviour of the above system in the presence of uncorrelated uniform noises instead of Gaussian noises. In all these cases we observe the results are completely consistent with the main observations. To establish the real world prevalence of the phenomenon we also construct and couple two of the piece-wise linear circuits mentioned

above. We clearly observe the four different regimes of behaviour in the oscilloscope traces of state variables of the circuit. Thus we study, characterize and experimentally verify the four behavioural regimes including synchronized random hopping that arise in coupled bistable systems that are subject to uncorrelated noises.

The understanding of coupled bistable systems subject to uncorrelated noises lead to the question of using such systems as a natural progression from single bistable elements to perform Logical Stochastic Resonance (LSR). The clear advantage of such a system being employed in the generation of reliable logic is that the two inputs can be fed to the two bistable subsystems in completely different noise environments. Thus the second part of this thesis demonstrates the use of coupled bistable systems to produce reliable logic operations in spite of the presence of two uncorrelated noise floors in the two subsystems.

Logical Stochastic Resonance (LSR) is a phenomenon that has been demonstrated in previous works, where a single bistable system produces reliable logic outputs when driven by a sum of the two input signals in the presence of a moderate noise floor. In this work, we go beyond a single bistable system and demonstrate that when we have two coupled bistable sub-systems each individually driven by an input signal, the coupled system yields outputs that can be mapped to specific 2-input logic gate operations in a robust manner, in an optimal window of noise strength. It is to be noted here that the individual signals are fed separately into each subsystem rather than being added as in the previous implementations of LSR. The collective response of the system due to coupling, in the presence of the noise floor leads to reliable logic operations. We term this phenomena coupling induced Logical Stochastic Resonance (cLSR).

We simulate the stochastic differential equations governing the above system using the Euler-Maruyama method. We observe that consistent logic operation is obtained neither at low nor high noise strengths but only in a moderate window in between. It is important to note that the robust operation of such a system is possible only if the coupling and noise strengths in the system are tuned to be in the 'synchrony without hopping' regime from the first part of this thesis. If either of the two subsystems begin to hop as in the other regimes demonstrated in part one, consistent logic wouldn't be possible. This highlights the crucial bearing that the study in part one has on the useful practical implementation in this work.

To clearly quantify this range of coupling and noise strengths where robust logic outputs are obtained we plot the probability of reliable logic versus noise strengths for various values of coupling constants. This provides the exact window of noise where ro-

bust operations occur. We see broad window of noise strengths where this probability approaches 1, thus demonstrating the reliability of this method under varying noise conditions. Moreover, we see larger coupling yields larger windows of consistent operation, underscoring the crucial importance of coupling in this phenomenon. Additionally, we show the system can effectively switch the logic response by adjusting a bias parameter. Thus the bias acts as a morphing control to robustly implement different logic gates using the same physical system.

We go further and build a proof of principle physical implementation of the above system using two bistable piece-wise linear circuits coupled via a resistor. We see through the oscilloscope traces of the system output that reliable logic operations are indeed obtained in the moderate noise window. Thus in the second part of this thesis we demonstrate how the constructive interplay between noise-floor, coupling and nonlinearlity can be exploited to obtain extremely reliable logic gate output from coupled bistable systems.

In part three of this thesis, we demonstrate the implementation of a noise-aided logic gate using LSR in a second order autonomous memristive circuit. Memristors are resistors with memory which have been considered promising candidates to implement neuromorphic computing architectures. In this work we construct, simulate and measure the reliability of operation of an LSR based logic gate in a memristive circuit. We demonstrate that in an optimal window of noise the memristive circuit produces a very reliable logic output. Further we show that due to the inherent symmetry in this system, complementary logic outputs are obtained in parallel from the response of the second state variable. We also show the output can be morphed into different logic functions by a simple switch of the constant bias. Lastly, we investigate two coupled memristive circuits and demonstrate the occurrence of coupling induced Logical Stochastic Resonance (cLSR) that was explored in the second part of this thesis. Thus we show an LSR based memristive logic gate that could further expand the scope of memcomputing.

In conclusion, in this thesis we explore and quantify the behaviour of nonlinear bistable systems interacting with noise and use the understanding to physically implement robust noise-aided logic gates using both simple piece-wise linear elements and memristors which will further the future forms of computing. So our results help propel the idea of noise-aided design using richer dynamics of nonlinear systems.

List of Publications

1. **Manaoj Aravind V**, K. Murali and Sudeshna Sinha, "Synchronized Hopping induced by interplay of coupling and noise". In Walter Lacarbonara, Balakumar Balachandran, Jun Ma, J. A. Tenreiro Machado and Gabor Stepan (eds), *Nonlinear Dynamics and Control*, pp 325–334, Springer Cham, 2020.

2. **Manaoj Aravind V**, K. Murali, and Sudeshna Sinha. "Coupling induced Logical Stochastic Resonance" *Physics Letters A*, **382**, 1581-1585, 2018.

3. **Manaoj Aravind V**, K. Murali and Sudeshna Sinha, "Implementation of Noise-aided logic in Memristive Circuits" Submitted to *International Journal of Bifurcation and Chaos*.

List of Figures

Contents

Chapter 1

Introduction

"Begin at the beginning..."

- Lewis Carroll, *Alice in Wonderland.*

Everything changes with time.
Everything, from colliding galaxies to organized life, are all processes that *evolve* in time.

1.1 Dynamical Systems

Dynamics, is the study of this *time evolution*. To quantitatively study the changes that constitute such evolution, we first describe the system we're studying using a set of variables that uniquely describe the current *state* X of the system, where $X = (x_1, x_2, ..., x_n)^T \in R^n$, is an n-dimensional vector. This set of *state variables* uniquely correspond to a point in an abstract *state space* (or phase space). The time evolution of our system can then be seen as a *trajectory* in this state space. Such a space of state variables and the rule for time evolution of those state variables, together constitute a *dynamical system*.

1.1.1 Types of Dynamical Systems

A dynamical system is *deterministic* if there is a unique consequent state to every state or *stochastic* if the consequent state is determined by a probability distribution of consequent states. The time evolution of a dynamical system can happen in *discrete time* or *continuous time*. A deterministic dynamical system with discrete time can be defined by a *map*,

$$X_1 = F(X_0) \tag{1.1}$$

where F is a set of functions that gives the set of state variables X_1 arising from the initial state X_0 at the next time value. After arbitrary n-steps the map is given as,

$$X_n = F_n(X_0) \tag{1.2}$$

where F_n is the n-th iterate of the function F. This an be alternatively written as,

$$X_n = F(X_{n-1}) \tag{1.3}$$

A deterministic system evolving in continuous time are given by *flows*. A smooth flow can be differentiated through out the state space and hence the rules of time evolution here can be represented as a set of first order differential equations. If X represents the

state of the system, rules for time evolution are given by the vector equation,

$$\dot{X} = F(X) \tag{1.4}$$

where, $\dot{X}$ represents the time derivative of X. Expressed in terms of the constituent state variables,

$$\begin{aligned} \dot{x_1} &= F_1(x_1, x_2, ..., x_n) \\ \dot{x_2} &= F_2(x_1, x_2, ..., x_n) \\ &... \\ &... \\ \dot{x_n} &= F_n(x_1, x_2, ..., x_n) \end{aligned} \tag{1.5}$$

A dynamical system is said to be *linear*, only when, the relationship given in Eq. 1.4 can be written as,

$$\dot{X}(t) = A \cdot X(t) \tag{1.6}$$

where, A is a constant matrix, i.e. all the time derivatives of the state variables depend simply on a linear combination of the state variables. Thus methods like normal modes, fourier analysis, superposition arguments, etc., can be used effectively to solve complex linear problems [1].

All other dynamical systems (which are not of the form given by Eq. 1.6) are *nonlinear*.

1.2 Nonlinear Dynamical Systems

Nonlinear dynamical systems are those in which the functions determining the time evolution of the state variable are nonlinear. Thus, the various components of the system cannot be separated in any sense and the principle of superposition fails in these systems. Also, nonlinear dynamical systems rarely have closed form solutions and are mostly solved using computational methods. Nonlinear systems, in different parameter regimes, exhibit a wide variety of dynamic behavior like, equilibrium points, limit cycles and a sensitive dependence to initial conditions - termed as chaos.

One simple example of a nonlinear system that exhibits all such behaviour is a Chua's circuit. The non-dimensional equations governing the evolution of a Chua's circuit are the following,

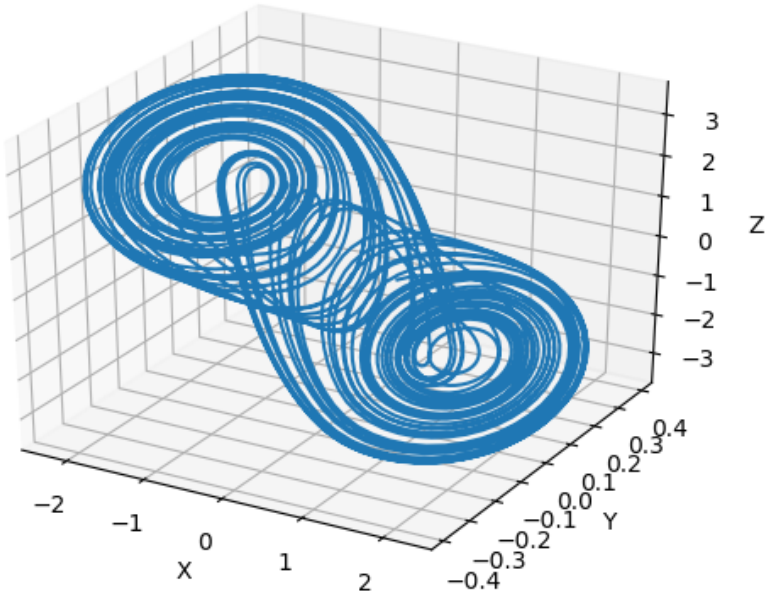

Figure 1.1: Simulation of a Chua's circuit equations given by Eqns. 1.7 and 1.8, depicting a chaotic "double-scroll" attractor. The parameter values used here are, $\alpha = 15.6$, $\beta = 28.0$, $m_0 = -0.714$ and $m_1 = -1.143$.

$$\begin{aligned} \dot{x} &= \alpha(y - x - g(x)) \\ \dot{y} &= x - y + z \\ \dot{z} &= -\beta y \end{aligned} \tag{1.7}$$

where, α and β are tunable parameters and $g(x)$ is the simple piece-wise linear function with three line segments. m_0 is the slope of the two outer line segments and m_1 is the slope of the inner line segment. So g(x) takes the form,

$$\begin{aligned} g(x) &= m_0 x + m_0 - m_1, \quad \text{if} \quad x < -1 \\ &= m_1 x, \quad \text{if} \quad -1 \leq x \leq +1 \\ &= m_0 x - m_0 + m_1 \quad \text{if} \quad x > +1 \end{aligned} \tag{1.8}$$

Figure 1.1 shows the simulation of a double scroll attractor obtained in the chaotic regime of a Chua's circuit.

1.2.1 Nonlinear Circuits

Even though the detailed dynamics of a nonlinear system can be obtained through numerical simulations of the system. The computational power and time required may be very large to explore large parameters spaces. An extremely useful tool to identify and explore nonlinear phenomena within systems with more than one parameters, is an analogue nonlinear circuit [2]. These circuits can be built to represent any nonlinear system under consideration and may help explore behaviour in such systems with no computational requirement. Nonlinear circuits are also a subject of study in their own right as applications of nonlinear dynamics are being increasingly applied in current technology and rich dynamics available in nonlinear systems may provide different ways of overcoming challenges in modern electronics.

In a general sense, a nonlinear circuit is an electronic circuit with one or more nonlinear elements, i.e. circuit components whose characteristic curves are nonlinear. A simple example of a nonlinear resistor is a Chua's diode, whose characteristic curve is piecewise linear. A more complex, but very important nonlinear circuit element with major current technological relevance is a memristor, which will be discussed in detail in section 1.5. The simplest autonomous chaotic circuit constructed using a Chua's diode is the Chua's circuit. The schematic representaion of the Chua's circuit is shown in figure 1.2. Figure 1.3 shows the wide range of dynamics that is seen in nonlinear systems, obtained experimentally from the oscilloscope traces of a Chua's circuit.

Electronic analogue simulations of nonlinear equations are of particular interest as they can mimic the behaviour of any given dynamical system. The measurable quantities of such an electronic circuit are designed to obey the same mathematical rules as the governing equations. All basic mathematical operations that occur in a differential equation such as summing, multiplication, sign inversion and integration can be achieved by active networks involving operational amplifiers (or op-amp). Thus a network of these elements can be used to experimentally simulate any mathematical equation. In this thesis we show analogue electronic circuits (c.f. Figures 4.1 and 3.14) constructed for certain governing equations (c.f. Equations 2.7 and 3.2). Experiments performed using those analogues are used to confirm results obtained from numerical simulations.

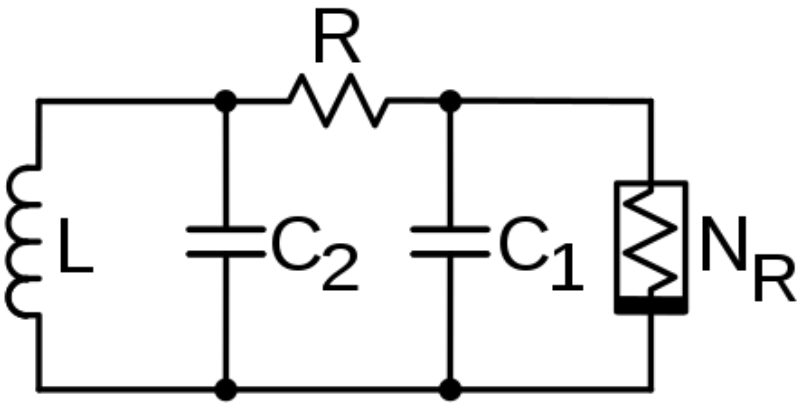

Figure 1.2: The schematic of the Chua's circuit. The component N_R depicted here is a nonlinear resistance called Chua's diode, which has a piece-wise linear V-I characteristic curve.(Source: `https://commons.wikimedia.org/wiki/File:Chua%27s_circuit_with_Chua_diode.svg`)

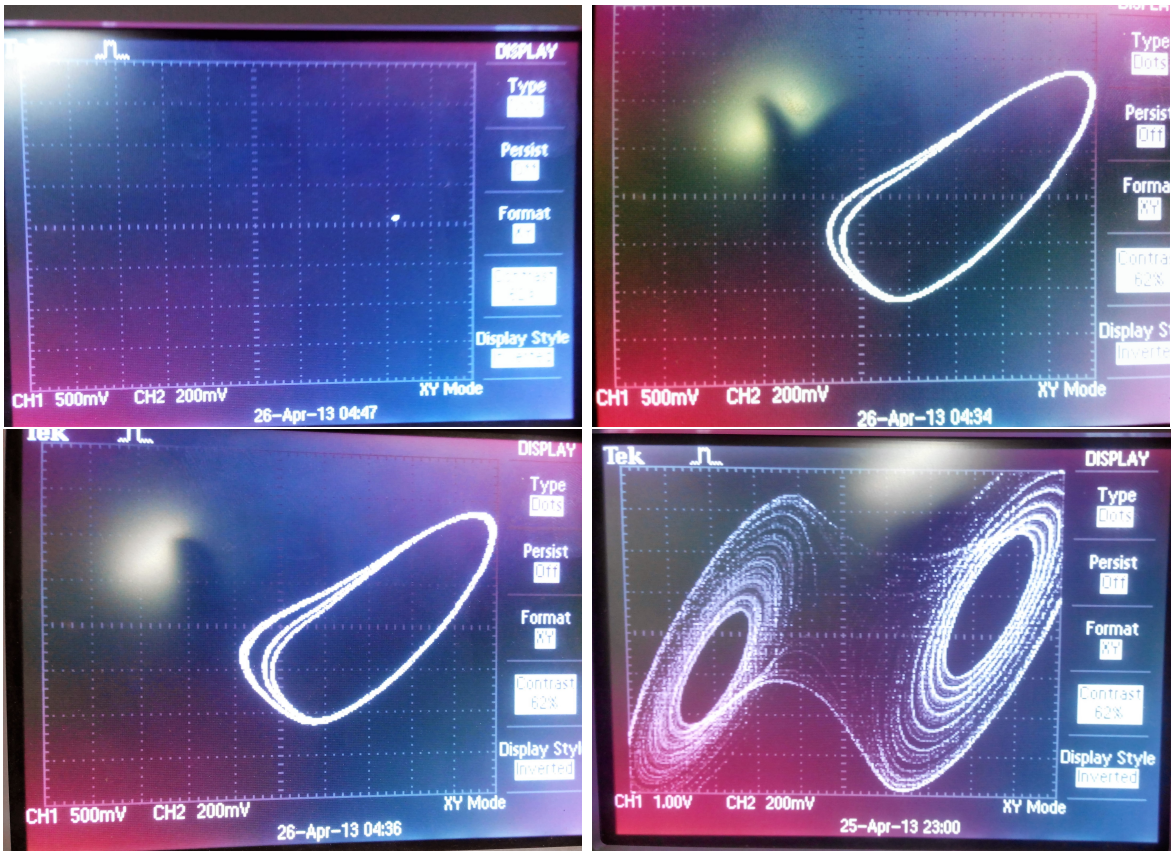

Figure 1.3: Oscilloscope traces of the voltages across capacitor C_1 and C_2, obtained from the circuit implementation of Chua's circuit shown in Fig. 1.2. The images depict a period doubling route to chaos with (top-left) a fixed point solution, (top-right) a period-2 limit cycle, (bottom left) a period-4 limit cycle and (bottom right) chaotic double-scroll attractor.

It is important to note that we use electronic circuit implementation as a proof of principle and test of robustness of a computational result, because all electronic implementations are limited by the component tolerances. As the absolute values of the components used (resistors, capacitors, diodes, etc.) and hence the intended parameter values in the governing equation are subject to variation. Thus, when computational results are reproduced in an electronic implementation, we infer that the results are robust to operational fluctuations and realizable in other experimental systems. For all circuits described and implemented in this thesis, we have used resistors and diodes with a tolerance rating of $\pm 5\%$ and capacitors with a tolerance rating of $\pm 10\%$.

For the entirety of this thesis, all electronic circuit experiments presented, have been performed using Agilent or Keysight 33522A, Function/Arbitrary Waveform Generator, as a source for reliable signal generation and production of noise signals with specific characteristics. Agilent or Keysight DSOX2012A oscilloscopes have been used to obtain all measurements and waveform traces.

1.2.2 Bistable Systems

A class of nonlinear systems, the real world application of which is the prime focus of this thesis, is the bistable system. A bistable system is a dynamical system which has two equilibrium states that are stable for a given set of parameter values. A simple example of a bistable mechanical device is an electrical switch, which can stay in either ON or OFF position. The core idea involved in this thesis to use bistable systems as logic gates, also relies on the mapping of the two stable equilibriums in a bistable system to the ON(1) and OFF(0) states of digital signals.

One of the simplest bistable systems that has been used extensively in this thesis is the following,

$$\dot{x} = f(x) = a(x - bx^3) + c \tag{1.9}$$

Here the term c represents a constant bias to the system. When the bias is zero the two wells are symmetric. The bias term can be used to tilt the potential wells in one direction or the other and hence to externally drive the bistable system. Figure 1.4 shows $f(x)$ and the potential surface (integral of $f(x)$) for specific a, b and c values (from [3]).

Bistable systems, have been crucial to our understanding of a wide range of phenom-

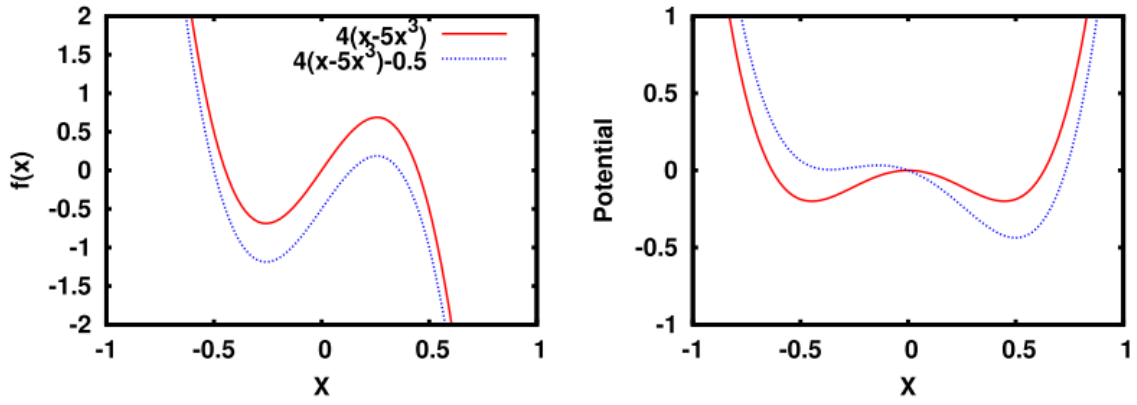

Figure 1.4: The functional form f(x) (left) and the effective potential (right) are plotted from Eq. 1.9 for parameter values $a = 4$, $b = 5$, $c = 0$ (red solid) and $c = 0.5$ (blue dotted). (Figure used from [3]).

ena in various disciplines. For example, in electronic systems they're used to encode one bit of data, in biological systems to model decision making processes in a cell, in chemical systems to study relaxation kinetics and non-equilibrium thermodynamics and in mechanical systems to model multi-stable devices like rachet-and-pawl. The results obtained in this thesis also has this wide scale of applicability across disciplines.

1.3 Noise and Nonlinearity

The influence of noise on nonlinear systems is an important area of active research as every real system, physical to physiological, evolve in the presence of noisy driving forces. Though noise in linear systems may simply have a blurring effect on the resulting dynamics, interaction of dynamic noise (noisy driving forces) with nonlinear systems produce effects which do not have a deterministic counterpart. For instance, noise can make finding bifurcation points of nonlinear systems very difficult even for the simplest of bifurcations and may cause noise induced transitions [4]. Another direction of enquiry is, can one use these counter-intuitive interactions between noise and nonlinearity for engineering applications. One such interesting outcome of this interplay is a phenomenon called stochastic resonance which has found wide applications and interest across disciplines. It occurs in bistable systems where noise facilitates the transition between the two stable states even when driven by a sub-threshold signal [5].

While modelling dynamical systems with noise in them, it is important to note that

there are different kinds of noise that can be found in real systems. Based on the frequency distribution and the source, noises have been classified into several kinds. Thermal noise that is found in any real system with temperatures above absolute zero, shot noise in electronic devices when charge carriers traverse a gap, $1/f$ noise or flicker noise widely found across real systems, the exact source of which is still debated, and more. For the purpose of this thesis we mostly concentrate on Gaussian white noise. This is because most work covered in this thesis is focused on modelling and utilizing the natural noise found in electronic circuits. Thermal noise of an ideal resistor is usually modelled as white noise, i.e. the power spectral density is constant across the frequency spectrum and when the bandwidth is finite, white noise has an almost Gaussian amplitude distribution.

1.4 Logical Stochastic Resonance

Stochastic resonance (SR), was the counter intuitive phenomenon where dynamic noise in a bistable system amplifies the subthreshold signal driving the system, thus causing a sharp increase in the signal-to-noise ratio (SNR) when the noise is within an optimal window of noise strengths [5]. Going beyond just detection of subthreshold signals, in 2009, Murali et al. demonstrated that when such a bistable system is driven by the sum of two input signals (encoded in two square waves), in the presence of a constant bias, the output response of the bistable system reliably mapped to 2-input logic. This robustly occurred in a wide window of moderate noise strength [6, 7]. This phenomenon was named Logical Stochastic Resonance (LSR) [8].

One of the main focuses of this thesis is the extension of this LSR to coupled bistable systems. Hence, let's look at this phenomenon in further detail. The general model considered is the following,

$$\dot{x} = F(x) + D\eta(t) + I \tag{1.10}$$

here, F(x) can be any function that gives rise to a bistable potential. η is zero mean Gaussian noise with unit variance, I is a low amplitude signal which is the sum of two aperiodic pulses, $I_1 + I_2$. The schematic representation of the system is shown in Fig. 1.5. This scheme was experimentally implemented in [7] and the experimental circuit results are shown in Fig. 1.6. It is clear from the figure that Logical Stochastic Resonance (LSR) enables the implementation of robust flexible logic gates using the interplay of noise and nonlinearity.

Since its implementation in 2009, LSR has garnered wide-ranging research interest

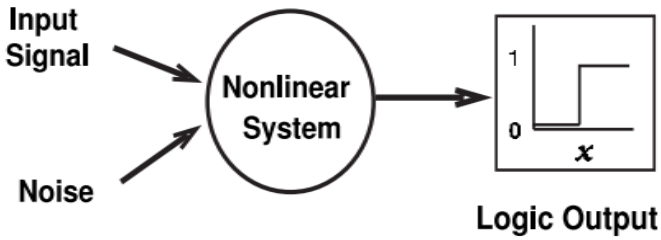

Figure 1.5: Schematic of Logical Stochastic Resonance showing system being driven by input signal $I = I_1 + I_2 + b$ and noise. Output of the system $x(t)$ reliably maps to two input logic NOR/NAND depending on the value of the bias strength b. (Figure used from [7]).

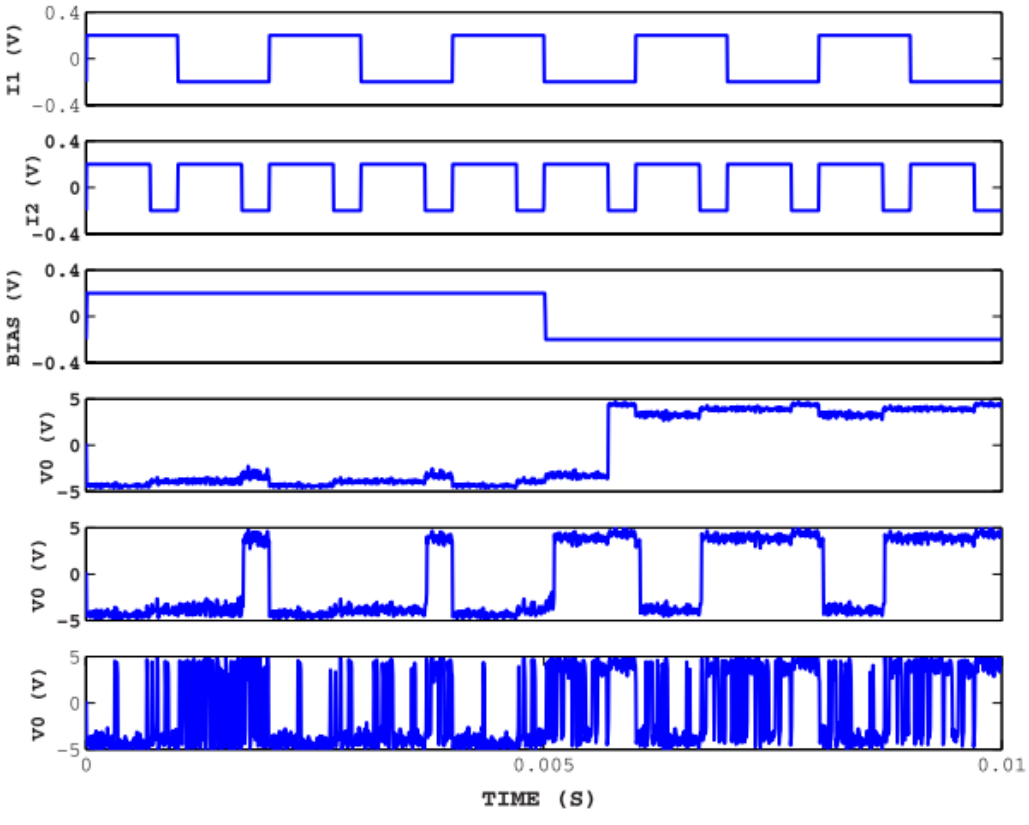

Figure 1.6: Experimental circuit results. From top to bottom: panels 1 and 2 show streams of inputs I1 and I2, which take value 0.2 V when logic input is 0 and value 0.2 V when logic input is 1. Panel 3 shows the constant bias signal varying from $0.2V$ (0–5 ms) to $-0.2V$ (5–10 ms). Panels 4, 5, and 6 show the waveforms obtained from the circuit implementation of LSR under noise levels D: (i) 0.4 V, (ii) 1 V, and (iii) 2 V. When the noise levels is in an optimal band, D=1 V, the desired NOR logic output (when b=0.2 V) or NAND logic output (when b=0.2 V), while for small or larger noise, one does not obtain the necessary response. (Figure used from [7]).

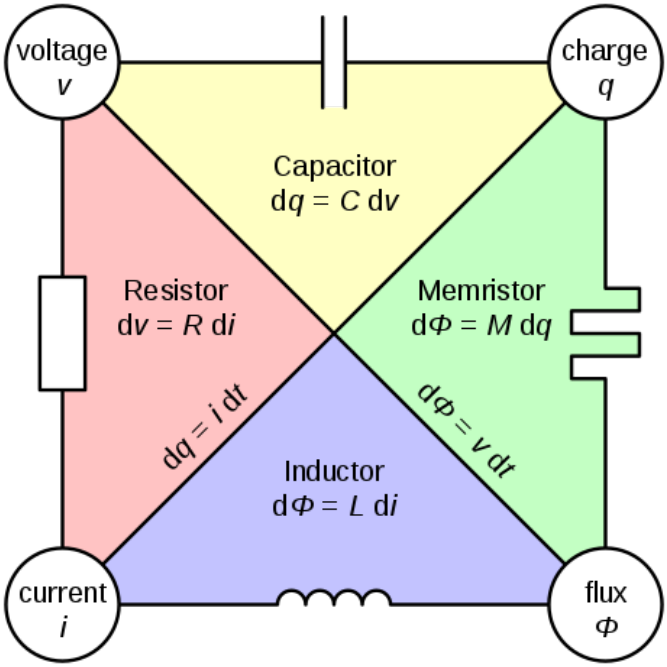

Figure 1.7: Conceptual symmetries of resistor, capacitor, inductor and memristor. Using this symmetry arguement L. O. Chua proposed the exixtence of a memristor linking charge and flux in a ciruit. (Source: `https://commons.wikimedia.org/wiki/File:Two-terminal_non-linear_circuit_elements.svg`)

[9–18]. Over the years it has been successfully realized in systems ranging from electronic circuits [3, 7, 19] and coulomb-coupled quantum dots [20] to synthetic genetic networks [18, 21–26], optical systems [27–29] and nanomechanical devices [30].

In Chapter 2 and 3 of this thesis, we shall focus on what are the challenges that need to be dealt with and improvements in terms of implementation can be obtained by introducing coupling in such systems. How the interplay of noise, nonlinearity and coupling could give rise to a new paradigm of coupled bistable elements performing logic operations.

1.5 Memristors

Finally, to make apparent the importance and the current relevance of the work done in chapter 4 of this thesis, we introduce the memristor, a nonlinear circuit element with peculiar properties that was envisioned by L. O. Chua in 1971. This has sparked interests again after 40 years when it was physically realized for the first time by HP labs in 2008.

In 1971, Leon O. Chua extrapolated the conceptual symmetry between the nonlinear resistor, nonlinear capacitor and nonlinear inductor (see Fig. 1.7). He argued the possibility a fourth passive fundamental circuit element called memristor (a portmanreau of memory resistor) linking flux and charge [31]. This passive two terminal circuit element maintains a functional relationship between time integral of current (charge) and time integral of voltage (flux). This idea has been further expanded to include any class of two terminal devices called memristive systems by Di Ventra et al. in [32]. The general form of an n-th order voltage controlled memristive system is given by the relations,

$$\begin{aligned} I(t) =& G(x, V, t)V(t) \\ \dot{(x)} =& f(x, V, t) \end{aligned} \tag{1.11}$$

where, x denotes the n state variables that describe the internal state of the system, V and I are the current and voltage across the device and G denotes the memductance of the device.

There's renewed interest and active research in the area since Hewlett Packard (HP) labs published their serendipitous discovery of the missing memristor, implemented using a thin film of titanium oxide [33]. Memristors are now seen as prime candidates for neuromorphic computing [34]. Thus, the relevance of the memristor emerges from the fact that passive elements that store information will represent a paradigm shift in electronics. Given that the values stored are actually continuous in nature, this may help analogue computation take over its digital counterpart. Our efforts in chapter 4 of this thesis are towards using this passive memory element to construct a very simple autonomous circuit that can robustly perform logic operations, in the presence of noise.

1.6 Outline of the Thesis

Now that the concepts necessary to fully understand the contents of this thesis have been introduced, we present a broad overview of this thesis. The core work presented in this thesis is divided among three chapters.

In chapter 2 of this thesis we study in detail the range of emergent behaviors that arise when, two simple bistable systems with independent uncorrelated Gaussian noise floors, are diffusively coupled to one another. We show that four qualitative regimes of behaviours emerge in such cases and those regimes of behavior are quantitatively characterized using the two simple, potent measures of synchronization error and probability

of hopping (between the two stable wells). We note the presence of one regime where the random hopping event induces by noise in the two system synchronize because of strong coupling in the system. We identify this behaviour as *synchronized hopping*. We use the quantitative measures to demarcate the regimes of behaviour in a parameter space of coupling strength and noise strength, thereby identifying the exact region of parameter space where this synchronized hopping occurs. We establish prevalence of our results for the case of uniform noise floors. Further we exhibit the generality of our result by demonstrating the same results in two other well known bistable systems. Finally we establish the robustness of our findings by experimentally coupling two bistable circuits and demonstrating all the four regimes of behaviours.

In chapter 3 of this thesis, we use our understanding of coupled noisy bistable systems to implement an alternate way of performing Logical Stochastic Resonance using coupled systems. The major difference here, is that the two streams of input are separately fed into different bistable subsystems and the logical operation occurs purely due to coupling. Hence, we show that this is a new paradigm in noise aided logic. We show that, when two coupled bistable subsystems are each driven by a sub-threshold signal, in the presence of moderate noise, the output of both subsystems robustly map to 2-input logic of the input streams. Also, the bias of the two bistable systems can act as a morphing control to change between different possible logic gates. We call this phenomenon *coupling induced Logical Stochastic Resonance*. We further demonstrate this phenomena experimentally and establish the real world prevalence of this possibility.

In chapter 4 we suggest a new possibility for the real world implementation of both LSR and cLSR. We demonstrate that robust noise aided logic using both methods can be obtained using a simple autonomous memristive circuit. We demonstrate this result both using numerical simulations of the circuit equation and proof of principle circuit implementations of both these cases. We find that extremely reliable logic operations are achieved in wide windows of moderate noise for both cases. Further we use a rigorous quantitative measure to demarcate the regions of the complete parameter space where reliable logic operations are achieved. Hence, we have opened up a brand new use case for memristors in computation.

Thus, in this thesis we will present in detail the three sections of work, all of which further our understanding of the interaction between noise and nonlinearity and also present possible use cases of this interaction in noise aided and dynamics based design.

Chapter 2

Synchronized Hopping in Coupled Bistable Systems

Adapted from the work published in [35] :

Manaoj Aravind V, K. Murali and Sudeshna Sinha,
"Synchronized Hopping Induced by Interplay of Coupling and Noise",
Lacarbonara W., Balachandran B., Ma J., Tenreiro Machado J., Stepan G. (eds)
Nonlinear Dynamics and Control pp 325-334, Springer, Cham (2020)

2.1 Introduction

Synchronization has emerged as a very significant phenomenon in fields as diverse as electronic circuits and biological systems. The key element in synchronization is the coupling. It has been observed in a large class of systems that, increasing the coupling strength induces the onset of synchronization [36].

In another direction, the phenomenon of escape from locally stable states induced by noise has seen long-standing attention. It has crucial bearing on fields ranging from chemical kinetics to diffusion in solids.

The central focus of this work is to combine these two important threads: first, noise induces hopping in bi-stable systems and the second is the onset of synchronization in the presence of sufficient coupling. The question we investigate is the following: when does the random hopping events induced by noise become synchronous in coupled bi-stable systems? Importantly, the systems here are subject to *independent random influences*. This uncorrelated noise *is expected to hinder synchronization*, as it does not provide a common drive to the sub-systems. On the other hand, noise will *aid frequent switches* between the locally stable wells. A balance of these two opposing trends may yield synchronized switching of states. The aim of this work is to explore this possibility in a range of bi-stable systems, under different kinds of noise.

Note that the phenomenon we are exploring is distinct from the phenomenon of stochastic resonance, and also distinct from the phenomenon of synchronization aided by common noise. In stochastic resonance, the effect of increasing noise on a bi-stable system has revealed counter-intuitive phenomena: it has been found that noise can enhance the response of the bi-stable system to weak sub-threshold signals, periodic driving or wide-band input signals. This phenomenon, known as stochastic resonance [5], has been demonstrated in many natural and engineered systems, and has also been utilized to increase reliability of computations [6] [37]. However, here we have *no external signal* driving the coupled bi-stable systems, and so if synchronized hopping emerges in our system, its origin cannot be understood in terms of an external drive.

The phenomenon here is also distinct from noise-aided synchronization, which arises in systems experiencing *common noise* or the parameters of the system experience common random fluctuations [38]. Here on the other hand the noise on the two sub-systems is *uncorrelated*, and is therefore expected to *inhibit* synchronization.

2.2 Model

Consider a system of coupled bi-stable systems whose dynamical equations have the general form:

$$\begin{aligned} \dot{x_1} &= F(x_1) + c(x_2 - x_1) + D\ \eta_1(t) \\ \dot{x_2} &= F(x_2) + c(x_1 - x_2) + D\ \eta_2(t) \end{aligned} \tag{2.1}$$

where F is a nonlinear function that gives rise to a bi-stable potential, and the coupling is linear and bidirectional.

We consider the additive noise $\eta_1(t)$ and $\eta_2(t)$ in the two sub-systems to be independent and uncorrelated, and we have considered both (a) uniform noise drawn from a uniform distribution in the range $[-1 : 1]$, and (b) zero mean Gaussian noise with variance 1, with the parameter D indicating the noise strength, with $D \in [0 : 1]$.

We start with the illustrative example where F in Eq. 1 is a simple nonlinear function of the form

$$F(x_i) = a_1(x_i - a_2 x_i^3) \tag{2.2}$$

Specifically, with no loss of generality, we choose the values $a_1 = 4$ and $a_2 = 5$. This system gives rise to two stable fixed points $x_+ > 0$ and $x_- < 0$, separated by an unstable fixed point (the "barrier") at zero. We denote the state characterized by positive-valued state variables as the "positive well", and the state characterized by negative-valued state variables as the "negative well".

We focus on two features of the dynamical patterns of the state variables x and y of the two sub-systems. First is the propensity of the sub-systems to jump between the two wells, i.e. the probability of *hopping*. The second feature of significance is *synchrony*. Note that synchrony here *does not imply complete synchronization*, where $x_1(t) = x_2(t)$ for all t after transient time. Rather it implies that the two sub-systems are confined to the same well, with both x_1 and x_2 being in the neighbourhood of the same fixed point, i.e both sub-systems are in the basin of attraction of x_+, or both are in the basin of x_-. The combination of these two features dictates the different classes of dynamical patterns.

Our central observation in this system is the following:

Depending on the noise strength and coupling strength four behavioural regimes emerge.

(i) The first regime occurs when both coupling and noise are low, and is characterized by no hops at all during the time of observation (which was very long) and additionally there was no synchrony either.

(ii) The second type of behaviour arises for low coupling strengths and high noise strengths, and is characterized by the sub-systems switching between the wells. However this hopping is not synchronized. So when one sub-system is in the positive well, the other subsystem may be in the negative well.

(iii) Thirdly, for strong coupling and weak noise one finds that the two sub-systems are synchronized and remain confined to the same well during the entirety of the long run-time, i.e. there is synchrony without hopping.

(iv) Lastly, for a specific range of noise strength D and coupling constant c, the system exhibits random hopping between the two wells in a synchronous manner. That is, the two sub-systems jump together from one well to another. We label this special dynamical pattern as *synchronized hopping*.

Fig 2.1 displays these different behaviors, observed in different ranges of coupling c and noise strength D. In this work we explore the the range $c \in [0, 6]$ and $D \in [0, 1]$.

Note that an early result on coupled bistable systems driven by independent noise sources [39] had indicated that the stochastic processes in the subsystems become coherent when the strength of coupling achieves a critical value (namely, the dynamical pattern iv). However, the full implications of the *interplay* of coupling strength and noise strength on the emergence of synchronized hopping was not explored. Also, the dynamical patterns in the regions outside synchronized hopping, in the extended parameter space of coupling strength and noise strength, were not obtained. In this work we will address these open questions. We will also obtain an understanding of the range of coupling, as well the range of noise, that yields synchronized hopping, and the relationship between them. This will allow us to judge the prevalence of the phenomena. Lastly, we will verify our results in electronic circuit experiments.

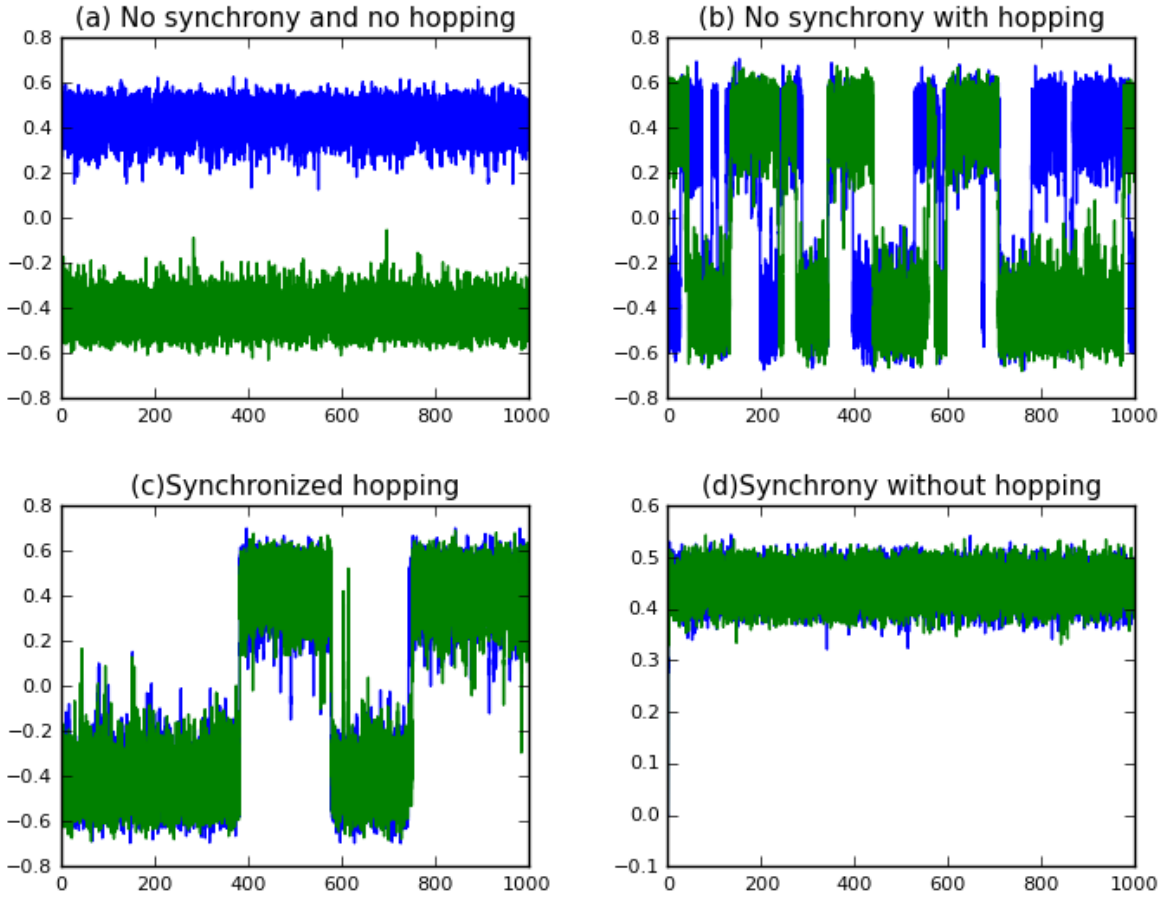

Figure 2.1: Timeseries of the two state variables x_1(blue) and x_2(green) of the two subsystems, for four illustrative values of noise stength D and coupling strength c, displaying different dynamical patterns: (a) no synchronization and no hopping, when $D = 0.2$, $c = 0.1$ (b) unsynchronized hopping, when $D = 0.3$, $c = 0.2$ (c) synchronized hopping, when $D = 0.32$, $c = 1$ (d) synchrony without hopping, when $D = 0.1$, $c = 1$.

2.3 Characterization

Now we will attempt to quantify the qualitative behaviour observed above, using a measure analogous to synchronization error, along with an estimate of the probability of hopping. The aim here was to precisely characterize the observed synchronized hopping in the system by finding the window of coupling strengths and noise strengths where there is a concurrence of *reasonable synchrony* and *sufficiently frequent switching*.

First we introduce a variant of synchronization error Z, defined as the probability of the states of the two systems to be in different wells. This is estimated by following the states of the two systems over long times, and finding the fraction of time the two systems reside in different wells.

When $Z = 0$, the states of the two systems are always in the basin of attraction of the same fixed point, namely the states of the systems are on the same side of the barrier, i.e. both states are in the "positive well" or both in the "negative well". Note that our measure of synchronization error is not the usual measure reflecting deviation from complete synchronization. Rather it reflects the degree to which the two multi-stable systems reside in the same well. Note that when the systems are in the same well (i.e. either both are positive, or both negative) the sign of the product of the state variables of the two sub-systems x_1 and x_2 at a given instant of time is positive. On the other hand, if the systems are in different wells, the sign of the product of the state variables of the two sub-systems at a given instant of time is negative. So our synchronization error Z is easily defined mathematically as,

$$Z = \frac{1}{N} \sum_{i=1}^{N} H(x_1[i] \times x_2[i]) \tag{2.3}$$

This quantity then serves as an order parameter that can reflect the transition from the case where both systems are in the same well at all times, to the case where they inhabit different wells for significant amounts of time.

The second important quantity is the probability of hopping h, which is estimated through the number of jumps between the two wells, in either system, over a prescribed very long (though necessarily finite) period of time. The key feature to note when the systems switch between positive and negative wells is that the sign of the product of the state variables just before the hop and just after the hop is negative. So the hopping

probability can be estimated readily by:

$$h = \frac{1}{N-1}\sum_{i=1}^{N} H(x_1[i] \times x_1[i-1]) \tag{2.4}$$

where N is the total number of timesteps in the observed timeseries, with N being very large, and H given as:

$$H(x_i) = \begin{cases} 1 & x_i < 0 \\ 0 & x_i \geq 0 \end{cases}$$

Both Z and h are averaged over a large sample of initial conditions, chosen randomly from the interval $[-1, 1]$.

Fig. 2.2a-b shows the dependence of the synchronization error on coupling and noise strengths. It is clear that for low coupling and low noise, the states of the sub-systems are almost uncorrelated. Since the synchronization order parameter is averaged over a sample of initial conditions uniformly distributed across the two wells, the two sub-systems maybe in the same well, or in different wells, with equal probability. So Z is close to 0.5 when c and D are very small. As coupling strength increases (cf. Fig. 2.2a), synchronization between the sub-systems is induced. It is also evident from Fig. 2.2b that for high coupling strengths the synchronization error increases monotonically after a minimum noise threshold. However, interestingly, *for low coupling strengths the degree of synchronization varies non-monotonically with noise strength.* For low noise strengths the system is largely unsynchronized, after which there is a *window of moderate noise where the synchronization error is very low*, i.e. we observe *noise induced synchronization in a window of intermediate noise strength.* For noise strengths beyond this window the synchronization error again rises, as is intuitively expected.

The second measure, the probability of switches, simply reflects how often the sub-systems switch between the two wells. This gives a measure of the average amount of time spent in a particular well, under varying D and c. As clearly evident from Figs. 2.4, 2.5, 2.6 and 2.7 that the *hopping probability varies non-monotonically with increasing coupling strengths.* That is, there exists an optimal value of coupling strength c for which the probability of switches in maximised. The value of the optimal coupling strength is dependent on noise strength D. This can be rationalized by noting that coupling has two distinct effects. It can aid hopping as a coupled system can be dragged out of a well due to coupling to a sub-system that is pushed to another well under a stochastic kick, thereby increasing its probability to hop. However, when coupling is larger than a critical amount it can inhibit hopping, as the pull of coupling prevents a sub-system

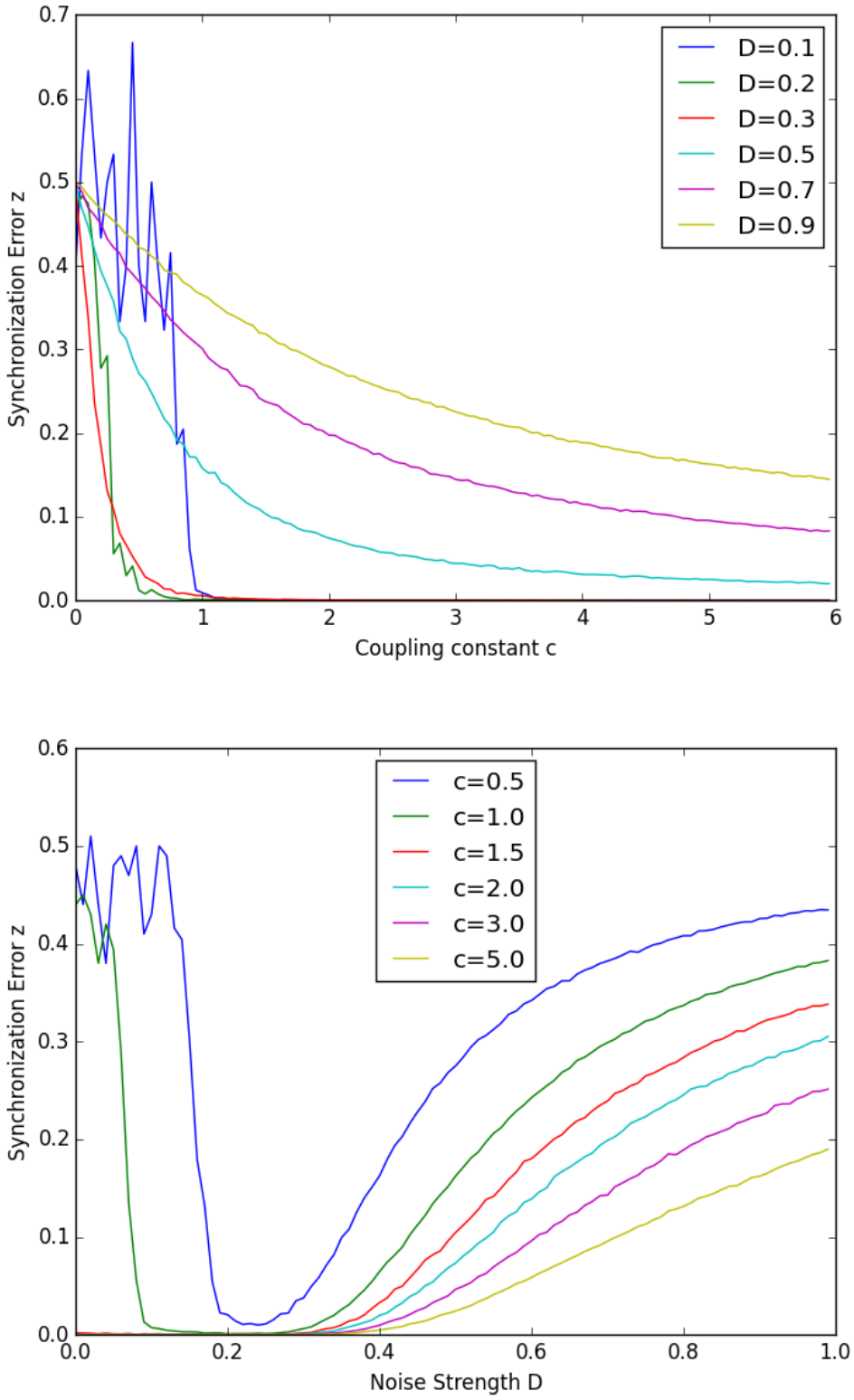

Figure 2.2: Dependence of the Synchronization Error Z on (top) coupling strength c, and (bottom) noise strength D.

from escaping to the other well under a stochastic push. At the cross-over of these two contrasting behaviour lies the critical value of coupling where the probability of hopping is most favoured. It is also expected then that the balance of the push due to noise in comparison with the pull due to coupling determines the critical coupling strength where the probability of hopping is maximised. Hence the dependence of the peak in Figs 2.5-2.7 on noise strength. It is also expected that the optimal coupling should increase with noise strength as stronger coupling is needed to counter the larger stochastic kicks. This is indeed the observed trend in Figs 2.5- 2.7.

The switching is significant only after a minimum noise threshold as observed in Fig. 2.3. This is expected, since a minimum strength of noise is needed in order to drive a system to cross the barrier to the other well. So there is a monotonous increase in the probability of hopping with increasing noise strength D. The threshold of noise strength D, after which synchronization error Z and probability of hopping assume significant finite values is the same (within statistical error)(cf. Fig. 2.8).

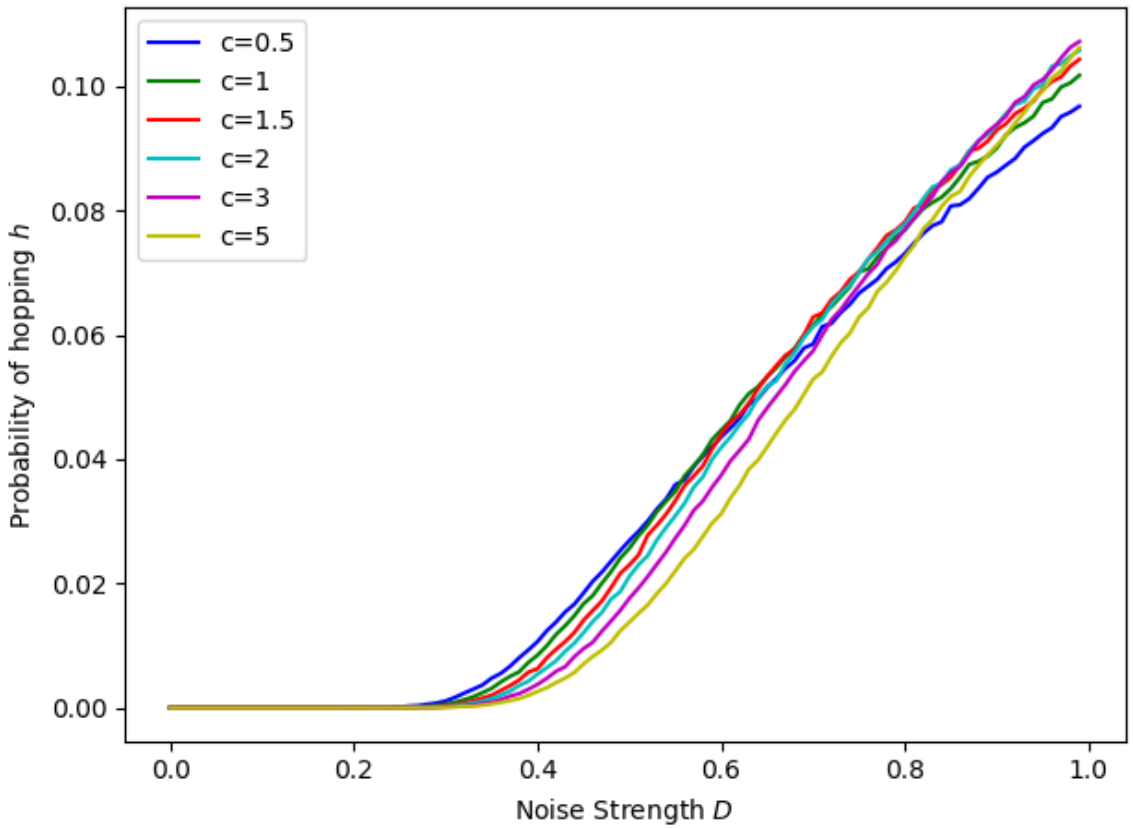

Figure 2.3: Dependance of probability of hopping h on the noise strength D for various values of coupling strengths c.

So, for sufficiently large noise strengths, the noise can push the sub-systems to hop

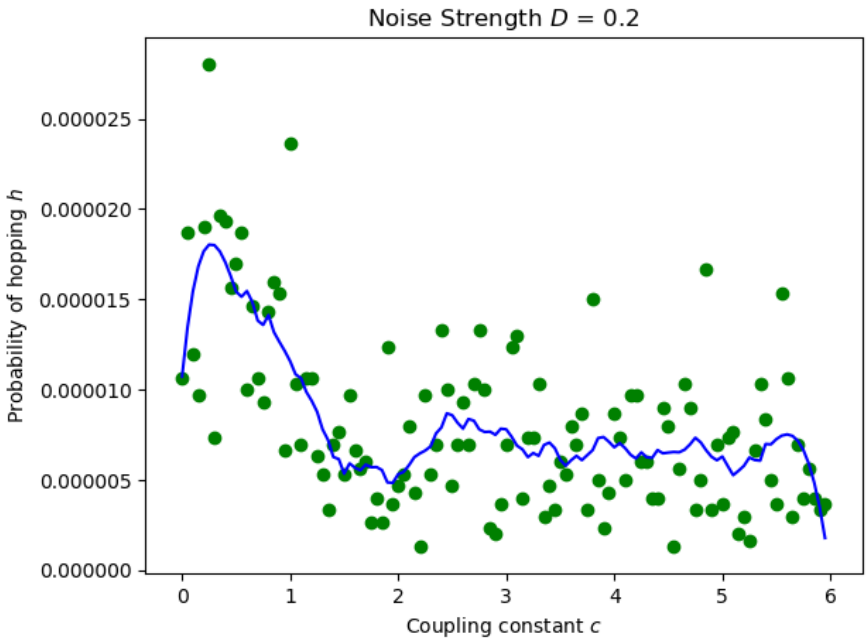

Figure 2.4: Dependence of the probability of hopping on coupling constant c, for noise strengths $D = 0.2$.

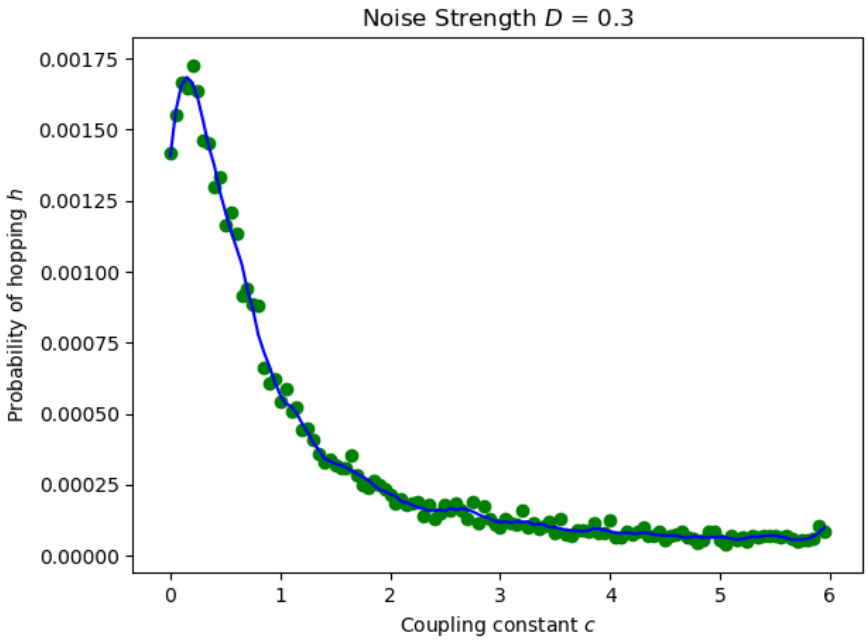

Figure 2.5: Dependence of the probability of hopping on coupling constant c, for noise strengths $D = 0.3$.

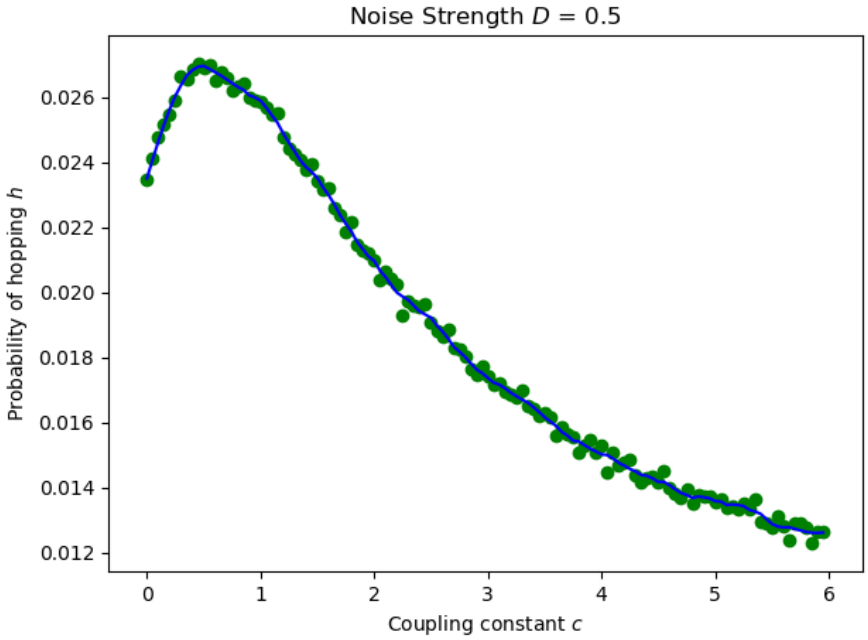

Figure 2.6: Dependence of the probability of hopping on coupling constant c, for noise strengths $D = 0.5$.

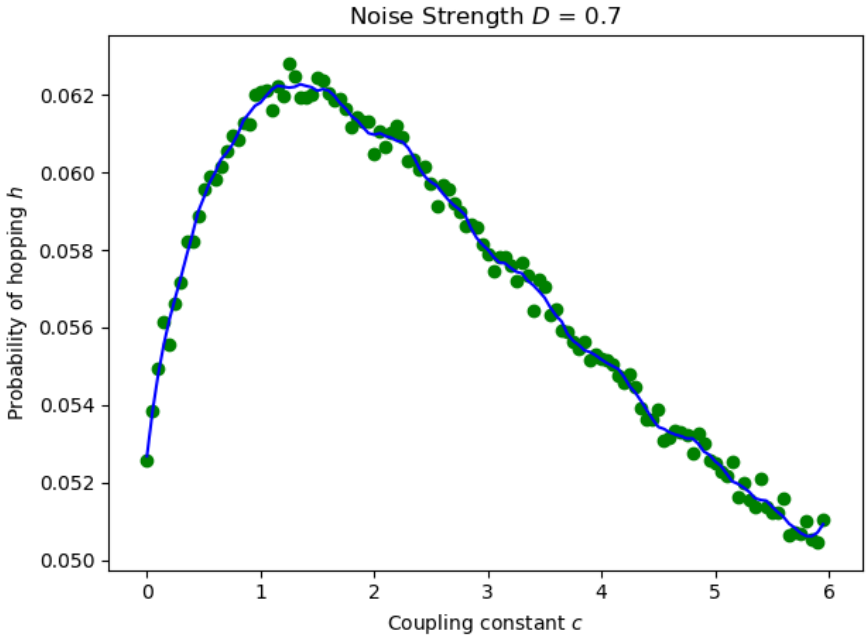

Figure 2.7: Dependence of the probability of hopping on coupling constant c, for noise strengths $D = 0.7$.

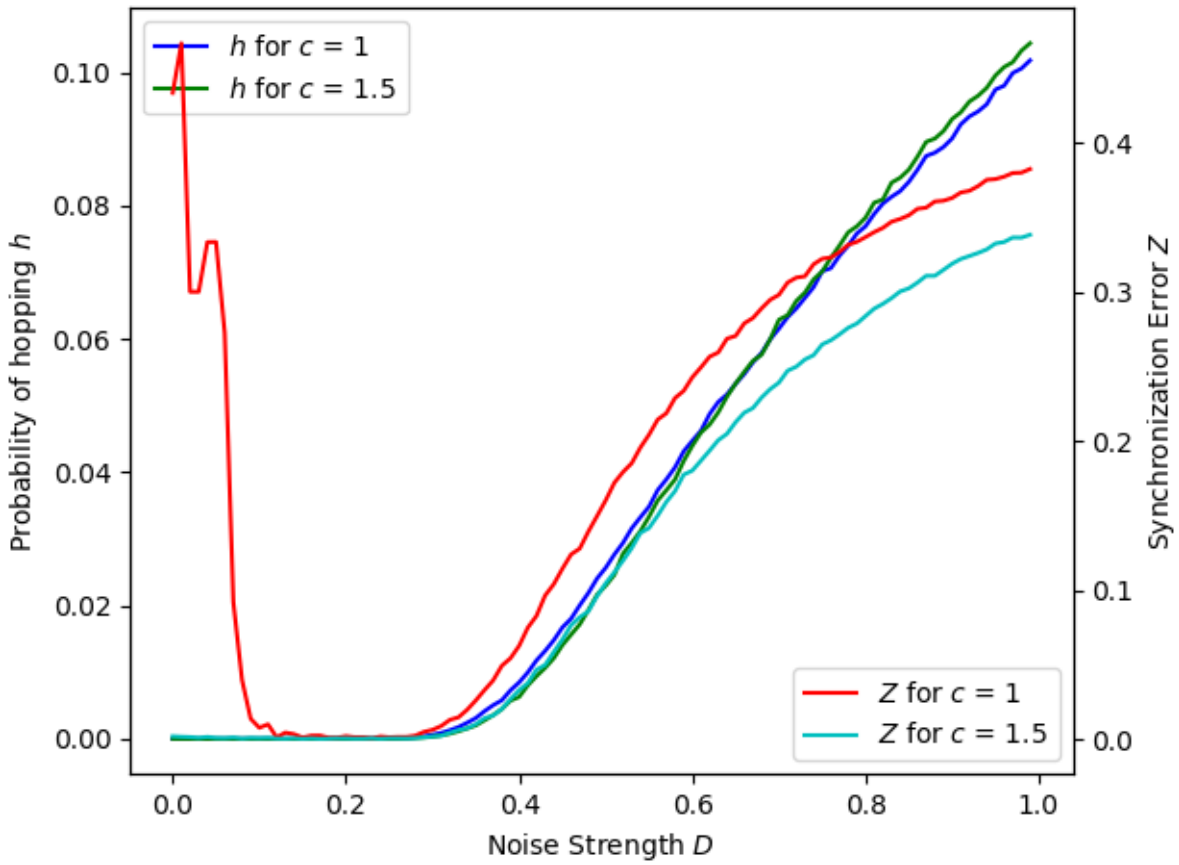

Figure 2.8: Comparison of minimum thresholds of noise strength D after which synchronization error Z and probability of hopping h assume finite values. The threshold for both is at ($D \approx 0.28$).

between the two wells. At these high noise strengths, if the coupling is also sufficiently high, the sub-systems switch between wells in synchrony: namely, we observe synchronized random hops. Such a phenomena will be seen only if the system lies in the window of noise where synchronization error is small and the probability of hopping is sufficiently large, provided these two windows have a reasonable overlap. Further the system has to simultaneously lie in the window of coupling strengths that is sufficiently high to induce approximate synchronization between the sub-systems, and the window of coupling where the probability of hopping is sufficiently large. Again if this intersection of parameter regions is a null set, we will not obtain the synchronized hopping phenomena. Note that the synchronized hopping phenomena is also non-trivial as the dependence of both synchronization and the hopping probability is non-monotonic with respect to coupling and noise strength. In general, the synchronized hopping phase lies on the boundary of the the dynamical phase of unsynchronized hopping and synchrony with (almost) no hopping.

To quantitatively demarcate the different behaviours in parameter space, we first introduce a threshold for both synchrony and hopping probability. We consider the following: if synchronization error $Z < 0.01$ then the two systems are considered synchronised, and if the probability of switching $h > 5 \times 10^{-5}$ then we consider the system to be "hopping". Using these conditions the various behaviours in parameter space are shown in Fig. 2.9(c). We see synchronized hopping occurs in a somewhat narrow region of parameter space (marked by orange). The exact boundaries of the region is dependent of the synchronization and hopping probability threshold chosen to describe the phase. However, qualitatively the phenomena emerges independent of the exact thresholds employed in the definition of the dynamical phase.

We have checked the generality of the observations above for the case of uniformly distributed noise. The synchronized hopping again occurs in a region of moderate noise and sufficiently high coupling, as evident from the results displayed in Fig. 2.10.

2.4 Generality of the phenomenon

To firmly establish the robustness, generality and wide prevalence of our observations, we study the dynamics of two other bi-stable systems. First we consider a single gene synthetic genetic network model developed in [40]. It describes the regulation of the operator region of a λ phage, whose promoter region consists of three operator sites.

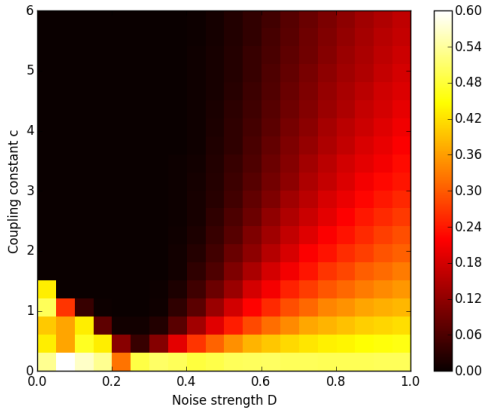

(a) Synchronization error Z

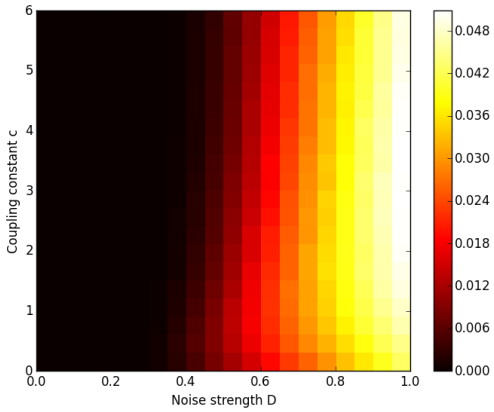

(b) Frequency of hopping h

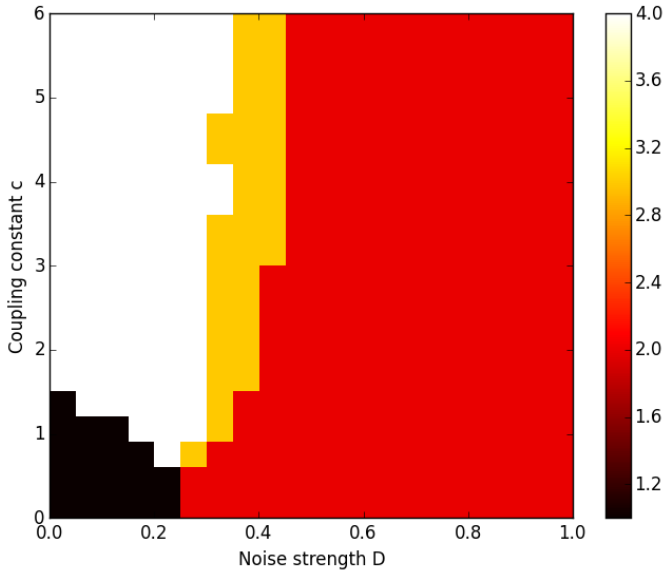

(c) Dynamical phases

Figure 2.9: (a) Dependence of the Synchronization Error Z on coupling strength c and noise strength D. (b) Dependence of the Probability of hopping h on the coupling strength c and noise strength D. (c) Different dynamical behaviour in the parameter space of coupling strength and noise strength. The colors indicate the following: BLACK - No synchrony, and extremely low probability of hopping; RED - No synchrony, with reasonable probability of hopping; ORANGE - Synchronized hopping, namely where there is reasonable synchronization as well as reasonable probability of hopping; WHITE - Synchronized sub-systems with extremely low probability of hopping.

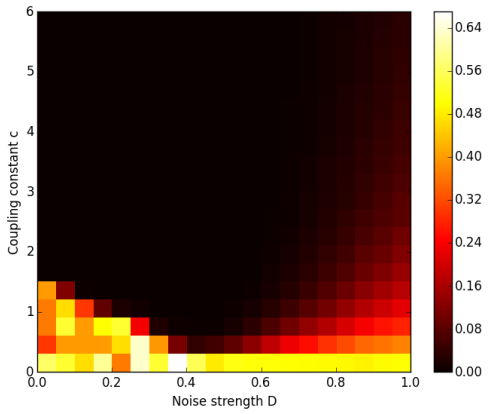

(a) Synchronization Error Z

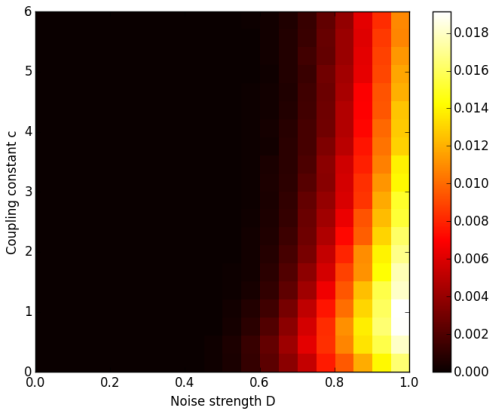

(b) Probability of Hopping h

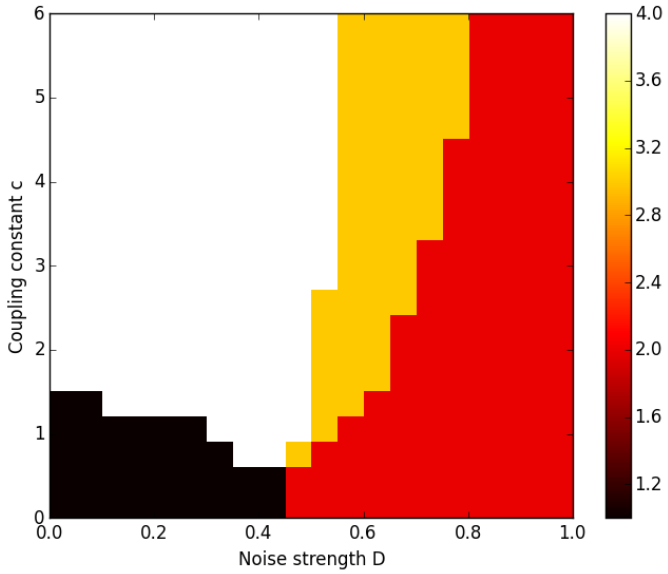

(c) Dynamical Phases

Figure 2.10: Characterization of system behaviour under uniform noise in the parameter space of noise strength D and coupling strength c. (a) Dependence of the Synchronization Error Z on coupling strength c and noise strength D. (b) Dependence of the Probability of hopping h on the coupling strength c and noise strength D. (c) Different dynamical behaviour in the parameter space of coupling strength and noise strength. The colors scheme is the same as indicated in Fig 2.9(c).

With suitable rescaling and considering the total concentration of DNA promoter sites to be constant, the reactions describing this network attain the form,

$$\dot{x} = \frac{m(1 + x^2 + \alpha\sigma_1 x^4)}{1 + x^2 + \sigma_1 x^4 + \sigma_1\sigma_2 x^6} = F(x) \tag{2.5}$$

where, x is the concentration of the repressor. $\sigma_1 = 2$, $\sigma_2 = 0.08$ and $\alpha = 11$ for the operator region of the λ phage and number of plasmids $m = 1$.

This biological model exhibits bi-stability and given that biological systems are intrinsically noisy, it is of considerable interest to see if synchronized hopping emerges here as well.

We further investigate another coupled system, relevant for electronic circuits (Eq. 2.7). It is clearly evident from Figs. 2.11-2.12, that our results hold for these bi-stable systems as well. This suggests that the phenomenon of synchronized hopping is quite general and occurs whenever coupling is sufficiently high and the noise is in a moderate window.

2.5 Experimental Implementation

In order to establish the robustness of the observed phenomena we constructed two simple bistable piecewise linear circuits and coupled them via a resistor. Fig. 2.13 shows the schematic representation of the constructed circuit. The non-dimensionalised equation governing the circuit is as follows,

$$\begin{aligned} \dot{x_1} &= F(x_1) + c(x_2 - x_1) + D\ \eta_1(t) \\ \dot{x_2} &= F(x_2) + c(x_1 - x_2) + D\ \eta_2(t) \end{aligned} \tag{2.6}$$

where F is a piecewise linear function given by,

$$F(x_i) = \begin{cases} -(x_i + 1) & x_i < -0.5 \\ x_i & -0.5 \leq x_i \leq 0.5 \\ -(x_i - 1) & x_i > 0.5 \end{cases}$$

The time trails of the two capacitor voltages for various values coupling and noise strength are also shown in Fig. 2.14. The four dynamical regimes of behavior are clearly evident, thus establishing the wide real world prevalence of the phenomenon.

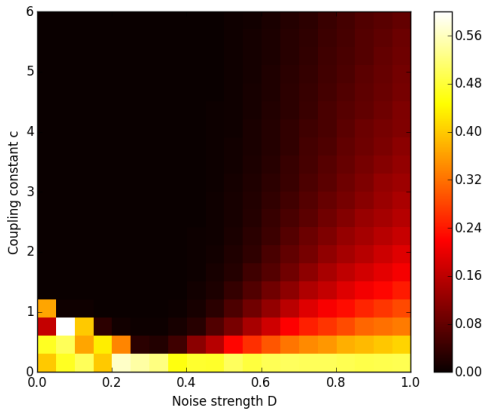

(a) Synchronization Error Z

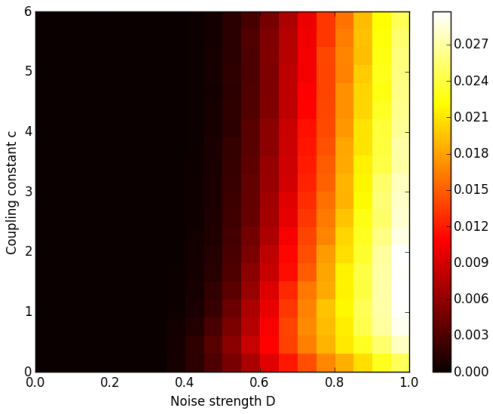

(b) Probability of Hopping h

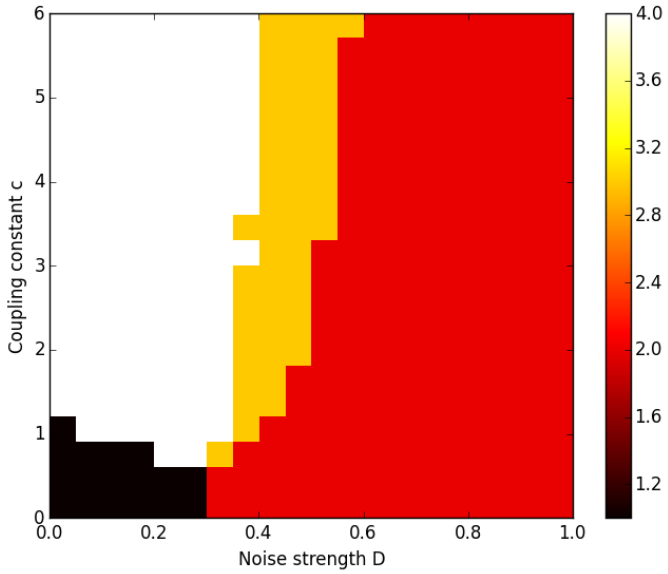

(c) Dynamical Phases

Figure 2.11: Characterization of the synthetic genetic network model given by Eq. 2.5 in the parameter space of noise strength D and coupling strength c. (a) Dependence of the Synchronization Error Z on coupling strength c and noise strength D. (b) Dependence of the Probability of hopping h on the coupling strength c and noise strength D. (c) Different dynamical behaviour in the parameter space of coupling strength and noise strength. The colors scheme is the same as indicated in Fig 2.9(c).

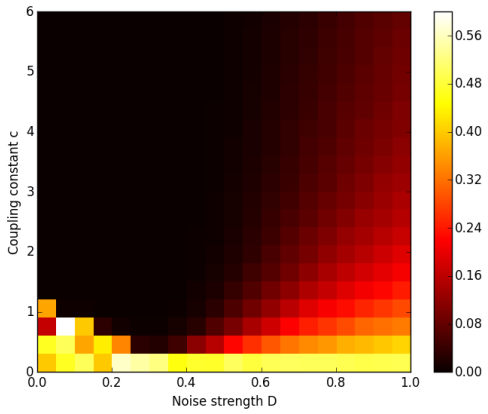

(a) Synchronization Error Z

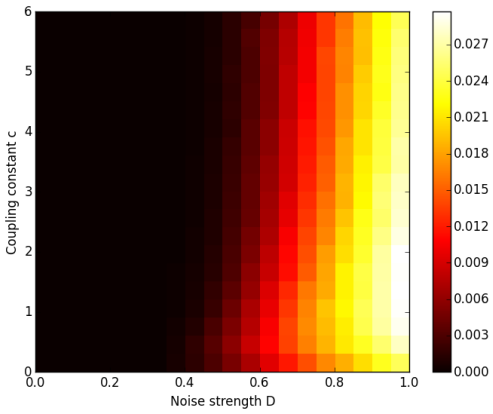

(b) Probability of Hopping h

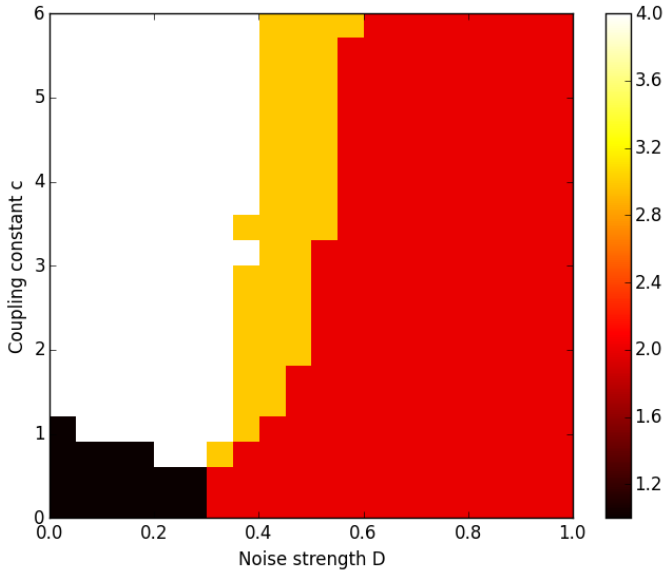

(c) Dynamical Phases

Figure 2.12: Characterization of the piece-wise linear circuit model given by Eq. 2.7 in the parameter space of noise strength D and coupling strength c. (a) Dependence of the Synchronization Error Z on coupling strength c and noise strength D. (b) Dependence of the Probability of hopping h on the coupling strength c and noise strength D. (c) Different dynamical behaviour in the parameter space of coupling strength and noise strength. The colors scheme is the same as indicated in Fig 2.9(c).

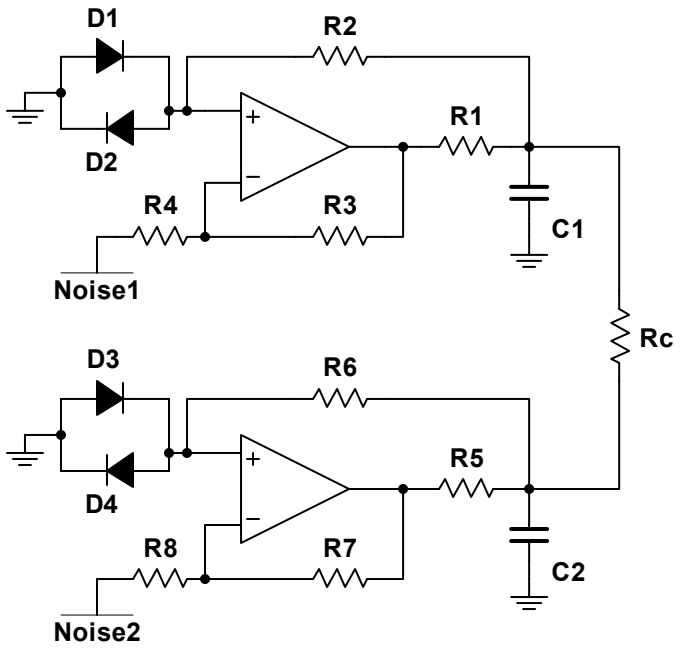

Figure 2.13: Schematic representation of the circuit. Here, resistances R_1, $R_5 = 70\Omega$, R_2, R_3, R_4, R_6, R_7, $R_8 = 10k\Omega$ and capacitances $C_1, C_2 = 470\mu F$.

2.6 Conclusions

In summary, we explored the behavior of coupled bistable systems subject to noise from two independent noise sources, over a range of coupling and noise strengths. We found that the interplay of coupling and noise lead to the emergence of four behavioral regimes: no synchrony and no hopping; unsynchronized hopping; synchronized hopping; synchrony without hopping. We demonstrated the occurrence of this phenomenon in a variety of bistable systems, in the presence of both uniform and Gaussian noise. Further, we experimentally verified the different regimes of behaviour in coupled bistable electronic circuits, thus establishing its robustness. Different theoretical approaches to analyze the phenomena is an open problem. Information theoretic measures to characterize the observed phenomena and solving the relevant Fokker-Plank equations [41] would be useful directions for future work.

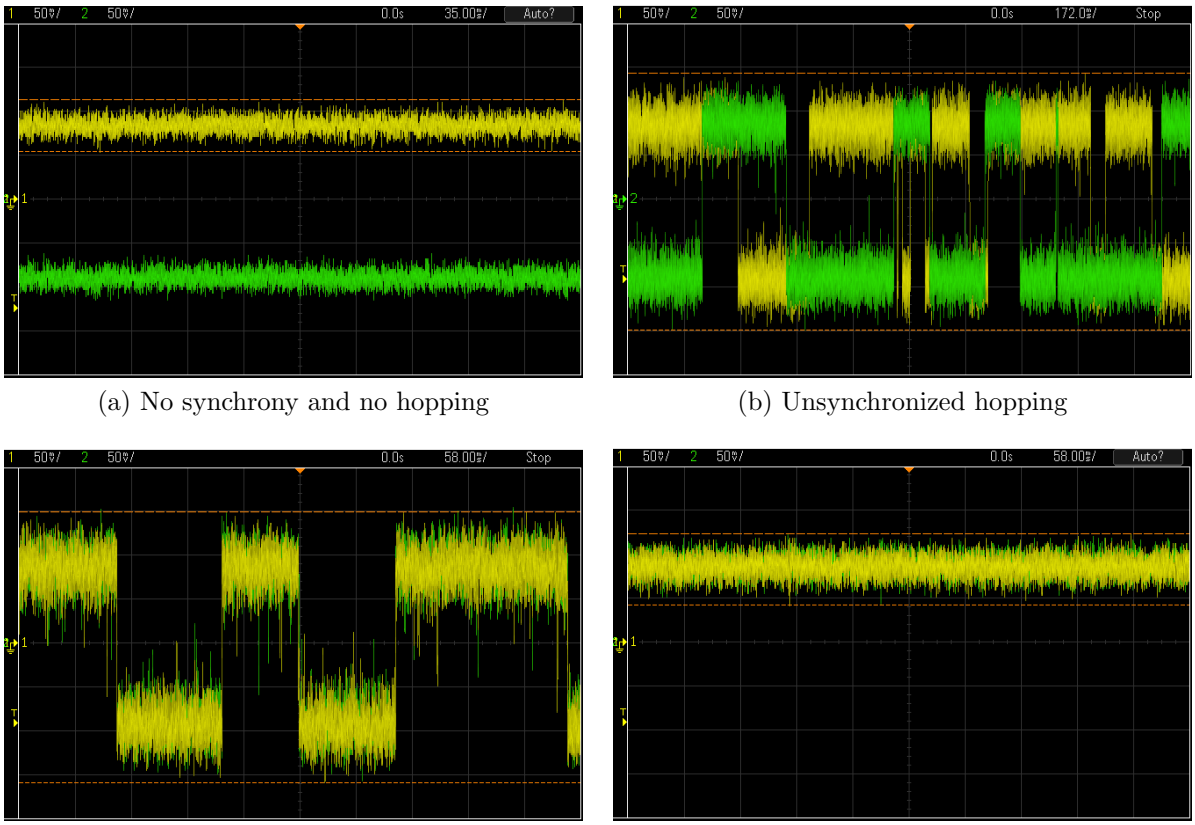

(a) No synchrony and no hopping

(b) Unsynchronized hopping

(c) Syncronized hopping

(d) Synchrony without hopping

Figure 2.14: Experimental observation of the four different behavioural patterns, including synchronized hopping, for different values of coupling resistance R_c and noise amplitude D. (a) $R_c = 1k\Omega$, $D = 450mV$ (b) $R_c = 9.15k\Omega$, $D = 950mV$ (c) $R_c = 180\Omega$, $D = 1.30V$ (d) $R_c = 180\Omega$, $D = 700mV$.

Chapter 3

Coupling induced Logical Stochastic Resonance

Adapted from the work published in [37] :

Manaoj Aravind V, K. Murali and Sudeshna Sinha,
Physics Letters A, 382(24), 1581-1585, 2018.

3.1 Introduction

As discussed in section 1.4 a single bistable system, when driven by the sum of two external signals, can consistently work as a logic gate in a window of moderate noise. This phenomenon, termed *Logical Stochastic Resonance*, has drawn wide research interest.

In this chapter, we will go beyond a single bistable system, and demonstrate the following result: when we have two coupled bistable sub-systems, with each driven separately by an input signal, the coupled system yields outputs that can be mapped to specific 2-input logic gate operations in a robust manner, in an optimal window of noise. So the *interplay of coupling and noise allows the system to operate as flexible logic gates*. Importantly, the two external input signals are not added into a single input signal to drive the bistable system, as in previous work on Logical Stochastic Resonance. Rather they are given separately to each sub-system, without necessitating addition of signals. The collective response of the system, due to the coupling, in the presence of a noise floor, maps consistently to that of a logic operation. We term this phenomenon *coupling induced Logical Stochastic Resonance*.

3.2 Model

We first test our idea through numerical simulations of a representative system comprised of two first order sub-systems, which are coupled linearly and bidirectionally, given by the following equations,

$$\begin{aligned} \dot{x} &= a_1(x - a_2x^3) + b + c(y - x) + I_1 + D\ \eta_1(t), \\ \dot{y} &= a_1(y - a_2y^3) + b + c(x - y) + I_2 + D\ \eta_2(t). \end{aligned} \tag{3.1}$$

Specifically, we consider parameter values $a_1 = 4$ and $a_2 = 5$, where each sub-system is bistable with two potential wells at $x_+ > 0$ and $x_- < 0$. Here c is the coupling strength, b is a bias provided to both the sub-systems, and $\eta_1(t)$ and $\eta_2(t)$ are additive zero mean Gaussian noise with variance 1 and noise strength D. The external drive I_1 and I_2 are low-amplitude input signals encoding the two binary inputs. In particular, we consider (with no loss of generality) logic input 0 to be encoded by -0.8 and logic input 1 to be encoded by 0.8.

The output of the system is determined by the state of the system. If x or y is negative, Logic Output is 0, and if x or y is positive, Logic Output is 1. Namely, when the sub-system is in the positive well the output is taken to be 1, and when the system is in the other well the output is 0.

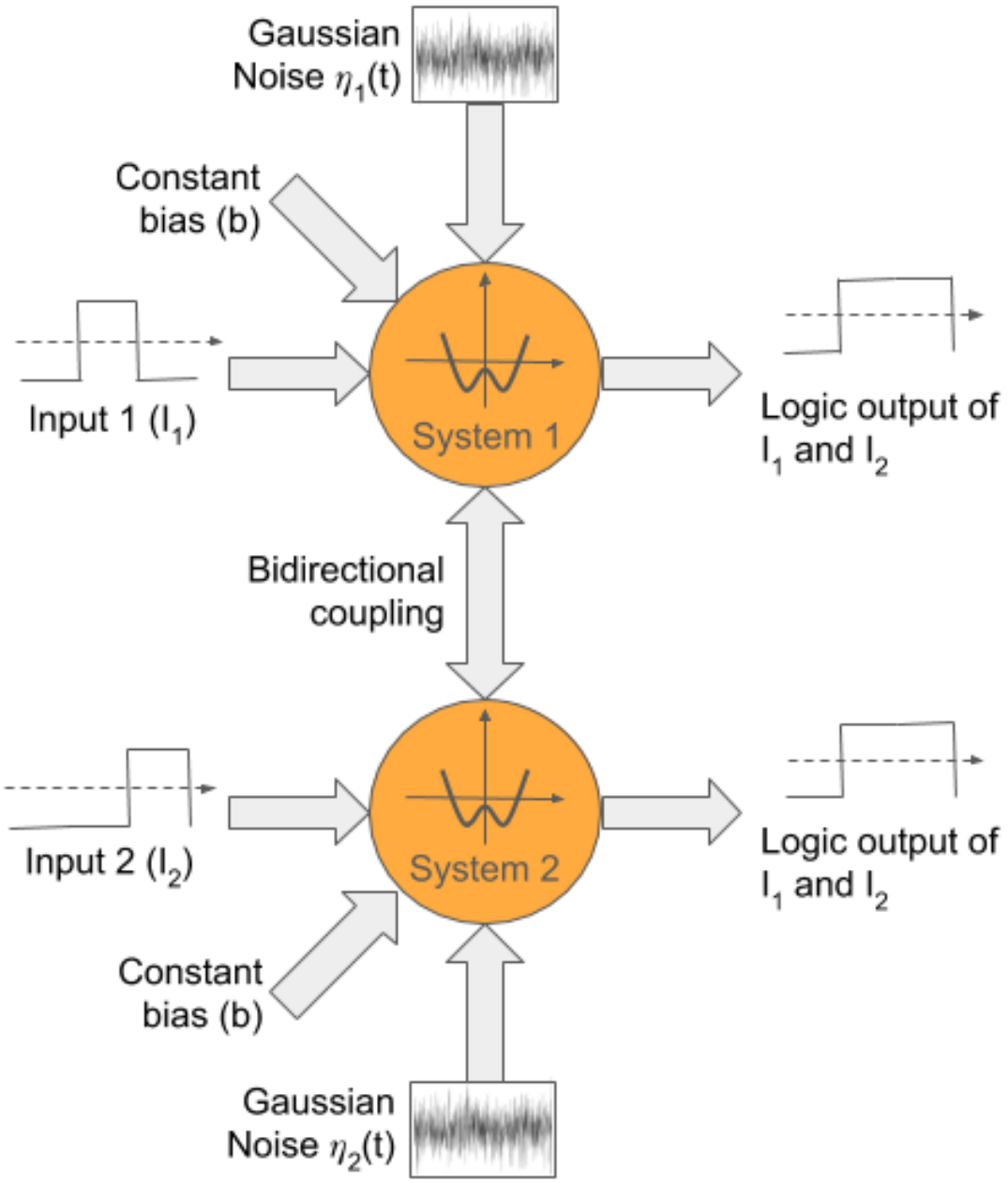

Figure 3.1: Schematic representation of coupling induced Logical Stochastic Resonance

So I_1 and I_2 are two external uncorrelated signals that drive the two sub-systems, and we need to have a consistent correspondence between these separate streams of inputs and the output of the coupled system. Notice that coupling is crucial here, as a 2-input

logic operation needs information from both inputs, and these are provided separately to two bistable sub-systems. So the inherent coupling of the sub-systems is the only mechanism by which the system can yield an emergent response that is in accordance with the truth tables of fundamental 2-input logic operations [42], such as AND or OR.

3.3 Results

We first display results from numerical simulations of the stochastic differential equation describing the coupled bi-stable systems (cf. Eqn. 3.1), using the Euler-Maruyama method. In Figs. 3.2 and 3.3 the states x and y of the two sub-systems are shown in blue and orange respectively. As defined earlier, the state corresponds to the output. It is clear that the state switches (from the positive well to the negative well, and vice versa) in response to the inputs, in a manner that mirrors the input-output correspondence of the fundamental AND and OR logic operations. Importantly, by changing the bias b, one can switch the type of logic operation obtained, and so the system behaves as a *flexible logic gate*. For instance, when bias is negative the coupled system behaves as an AND gate and when the bias is positive it behaves as an OR gate. Also it is clear that the states of the two sub-systems is largely synchronized. So one can map either x or y to obtain a consistent logic output.

A *quantitative measure* of how reliably this system performs logical operations is obtained by comparing the output of the system with the expected logical output, by driving the system with a stream consisting of a large number of (I_1 - I_2) sets, namely the system is subject to many different random combinations of I_1 and I_2 over time and its response to this random stream of inputs is explored. The fraction of time where one obtains the desired logic output successfully, gives a measure of the probability of obtaining that specific logic, denoted as P(OR) or P(AND). When this measure approaches 1 we have completely reliable logic outputs. Specifically, in this work we sample 500 randomly chosen input sets. Further, we do not remove transience, and so this measure also reflects latency in the system, and is therefore a stringent measure of the efficacy of the logic operation.

In Figs. 3.4, 3.5, 3.6, 3.7, 3.8, 3.9, 3.10 and 3.11 we show the dependence of this measure, P(AND) and P(OR), on noise strength D. It is clearly evident that there is an optimal window of noise strength D, for which AND and OR logic is consistently obtained, for negative bias and positive bias respectively. Note that *larger coupling yields*

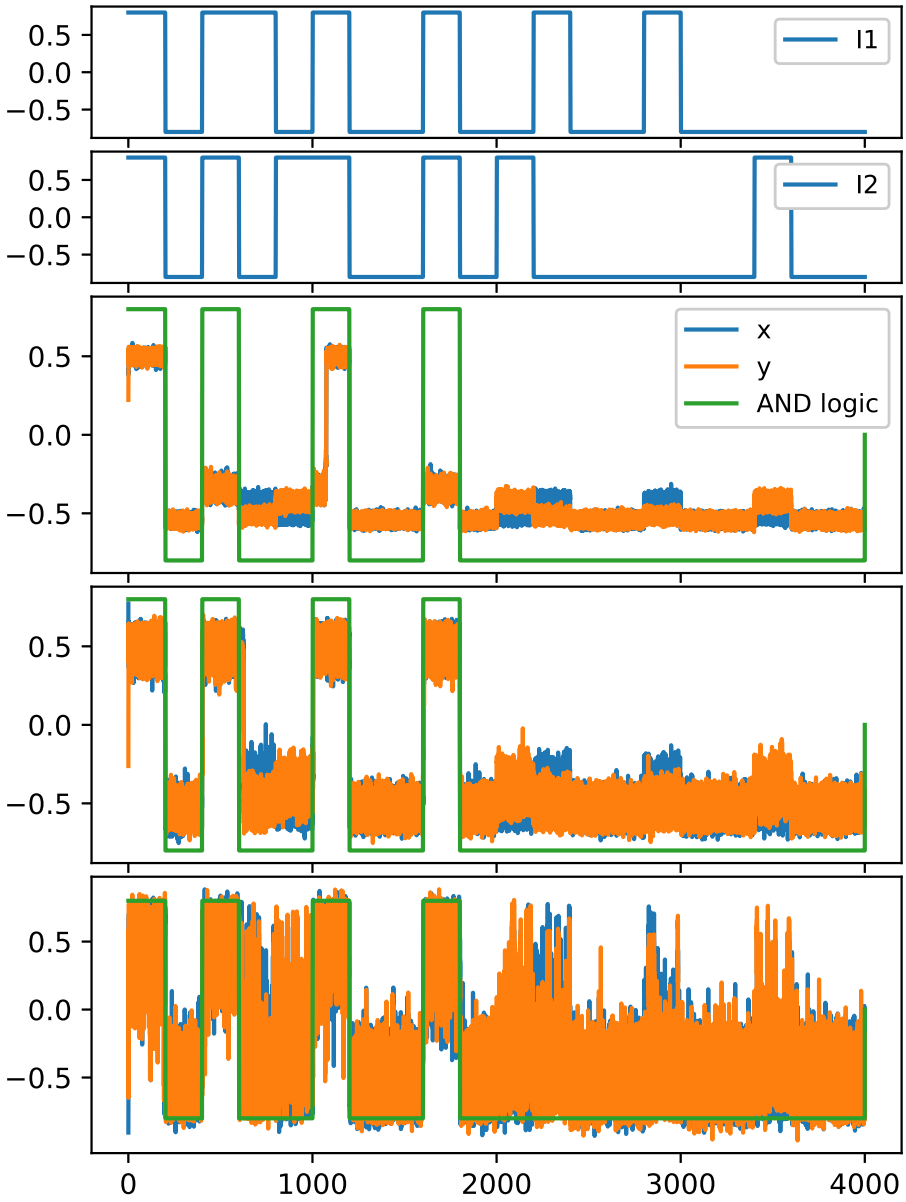

Figure 3.2: From top to bottom: panels 1 and 2 show streams of inputs I_1 and I_2, which take value -0.8 when logic input is 0 and value 0.8 when logic input is 1. Panels 3, 4 and 5 show the waveforms of the state of the two sub systems, $x(t)$ (blue) and $y(t)$ (red), obtained from numerical simulations of the system given in Eqn. 3.1 under noise levels $D = 0.1$, $D = 0.28$, and $D = 0.6$, with coupling constant $c = 4$ and **bias b** $= -0.28$. Clearly panel 4 (moderate noise) yields a consistent **AND logic** output. Note that assigning output value 1 to $x(t)/y(t) < 0$, and output value 0 to $x(t)/y(t) > 0$, yields the complementary logic NAND operations.

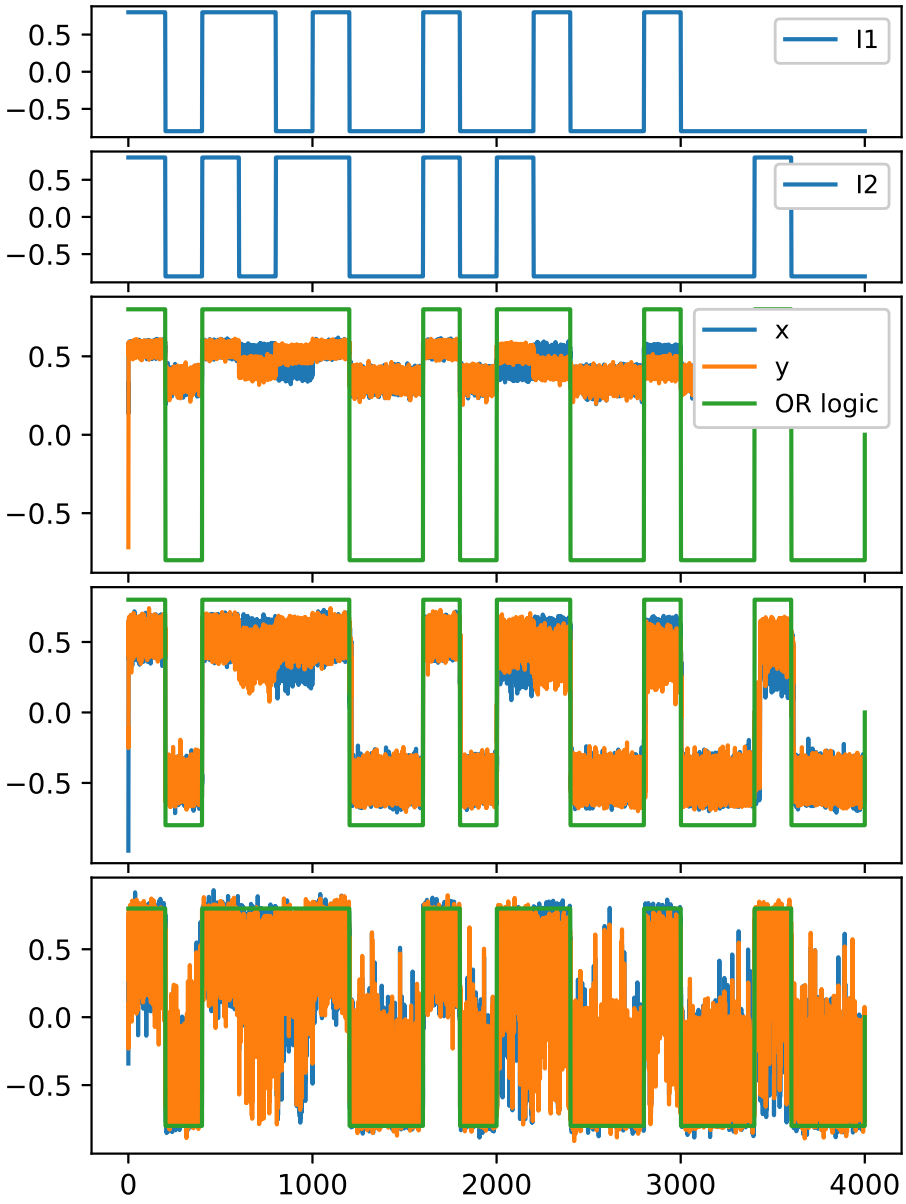

Figure 3.3: From top to bottom: panels 1 and 2 show streams of inputs I_1 and I_2, which take value -0.8 when logic input is 0 and value 0.8 when logic input is 1. Panels 3, 4 and 5 show the waveforms of the state of the two sub systems, $x(t)$ (blue) and $y(t)$ (red), obtained from numerical simulations of the system given in Eqn. 3.1 under noise levels $D = 0.1$, $D = 0.28$, and $D = 0.6$, with coupling constant $c = 4$ and **bias b** $= +\mathbf{0.28}$. Clearly panel 4 (moderate noise) yields a consistent **OR logic** output for bias $b = +0.28$. Note that assigning output value 1 to $x(t)/y(t) < 0$, and output value 0 to $x(t)/y(t) > 0$, yields the complementary NOR logic operation.

larger windows of consistent operation, underscoring the crucial importance of coupling in this phenomenon. Further we explicitly show the dependence of P(AND) and P(OR) on coupling constant c in Figs. 3.12 and 3.13. It is clear that on increasing coupling strength one observes a very sharp transition to consistent logic operations after a critical coupling strength.

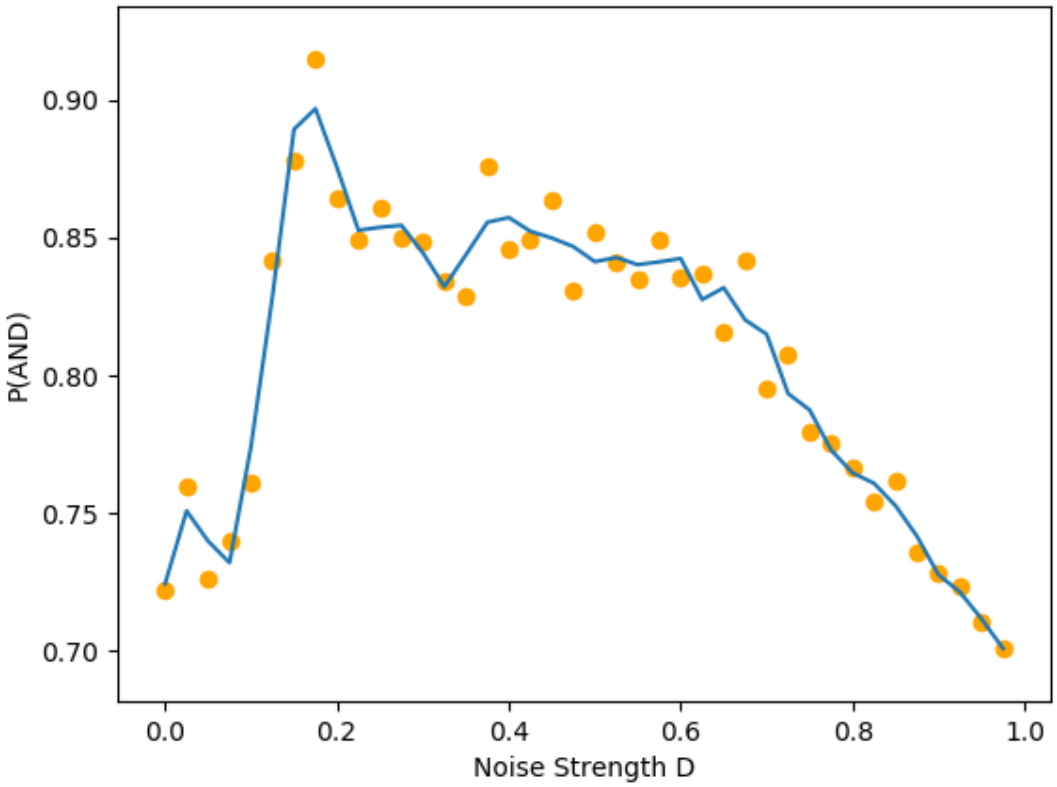

Figure 3.4: Dependence of the probability of obtaining AND logic operation, P(AND), on noise strength D, for coupling strength $c = 1$ and bias $b = -0.28$.

The advantage this system has over the typical logical stochastic resonance set-ups is that this eliminates the need to include an adder in the circuit, in order to sum up the two input signals fed to the system. Here one logic input I_1 drives the first system, and the other logic input I_2 drives the second system, as indicated in Eqn. 3.1. The output from any *one* of the two coupled systems may be extracted to obtain the appropriate logic output of the two inputs I_1 and I_2.

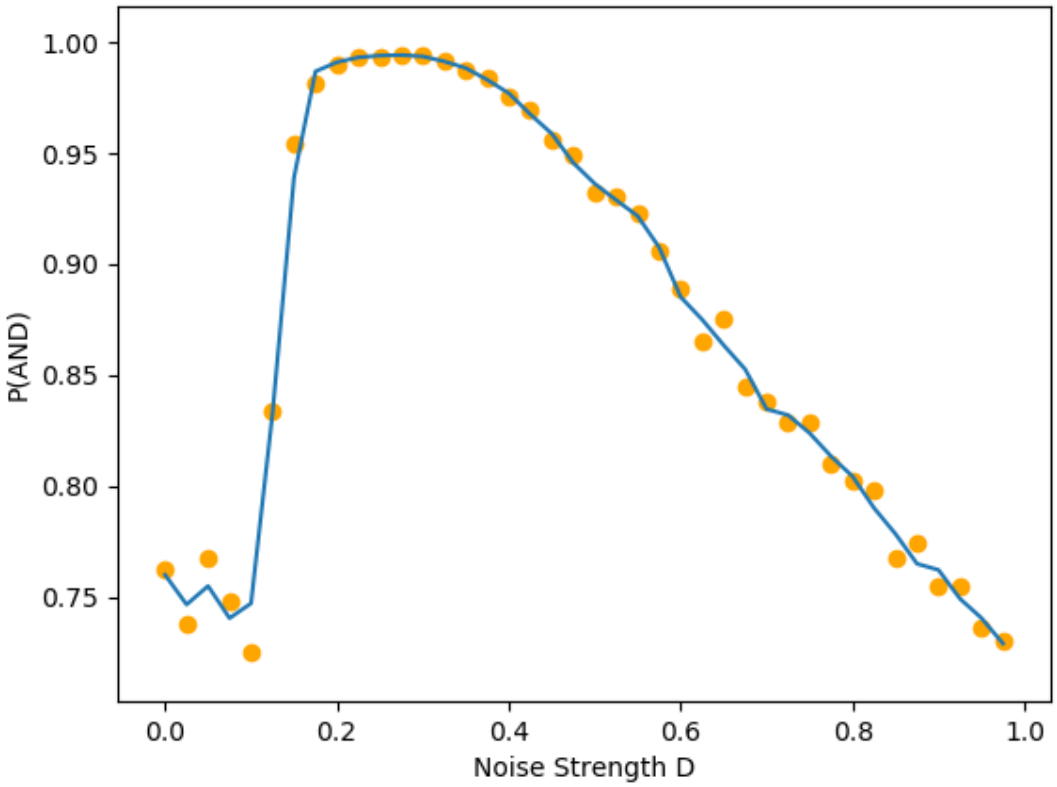

Figure 3.5: Dependence of the probability of obtaining AND logic operation, P(AND), on noise strength D, for coupling strength $c = 2$ and bias $b = -0.28$.

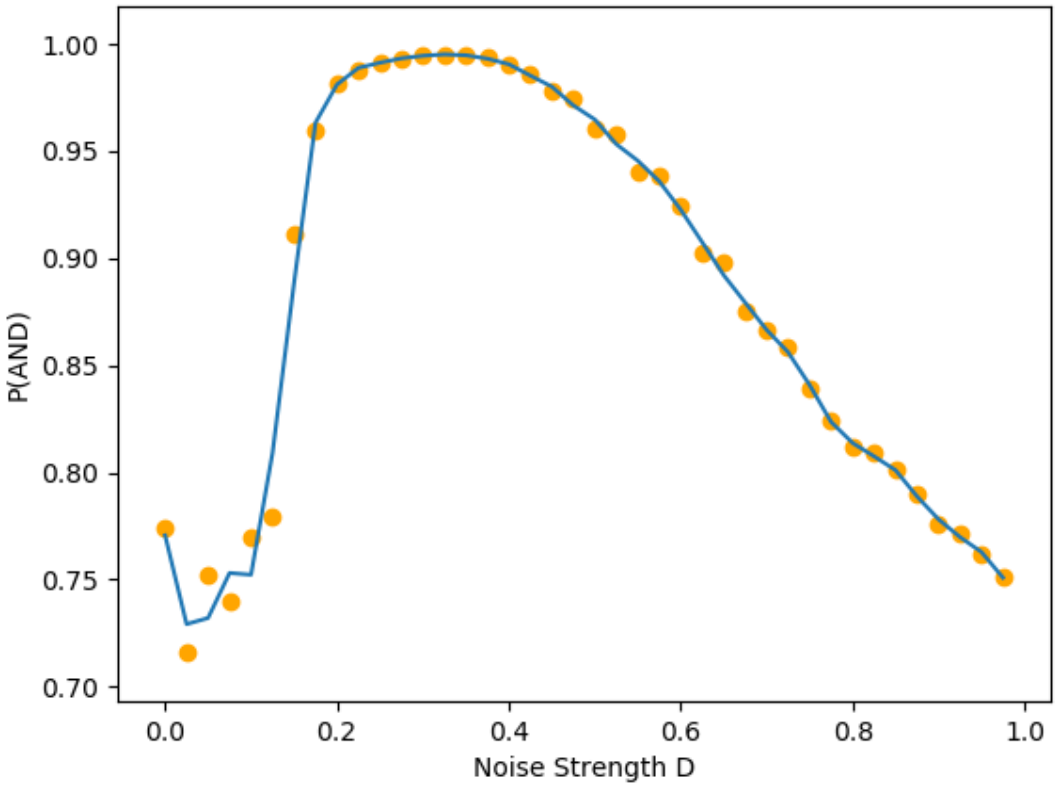

Figure 3.6: Dependence of the probability of obtaining AND logic operation, P(AND), on noise strength D, for coupling strength $c = 3$ and bias $b = -0.28$.

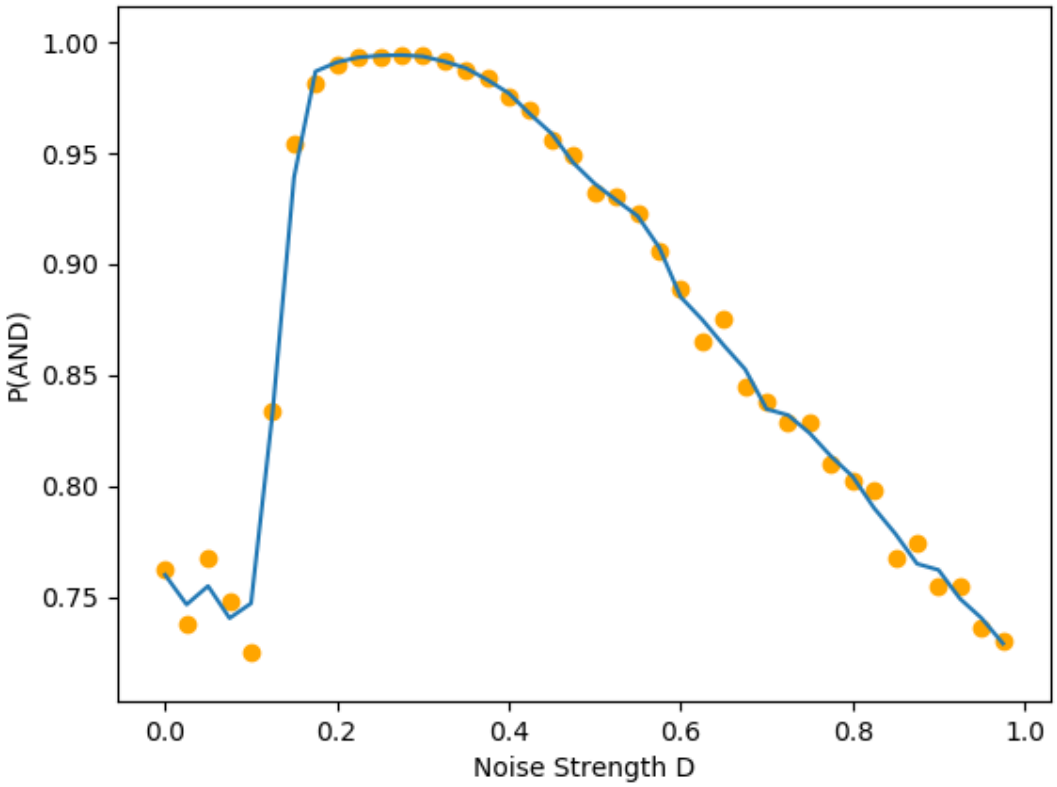

Figure 3.7: Dependence of the probability of obtaining AND logic operation, P(AND), on noise strength D, for coupling strength $c = 5$ and bias $b = -0.28$.

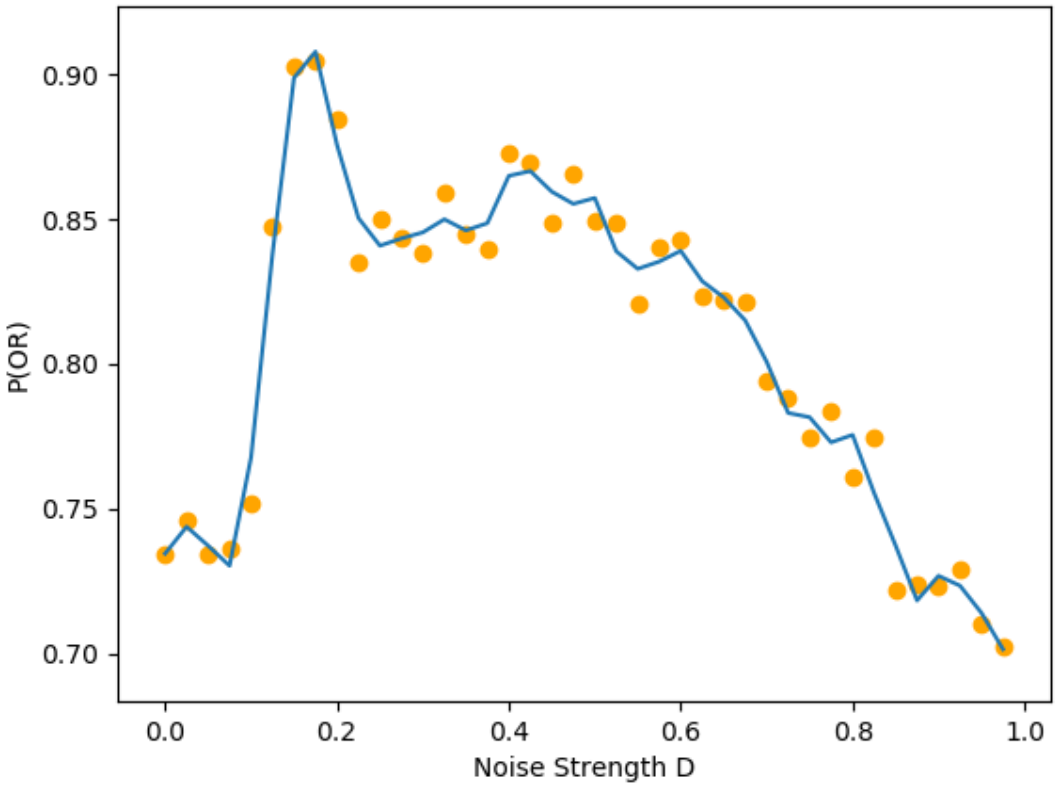

Figure 3.8: Dependence of the probability of obtaining OR logic operation, P(OR), on noise strength D, for coupling strength $c = 1$ and bias $b = -0.28$.

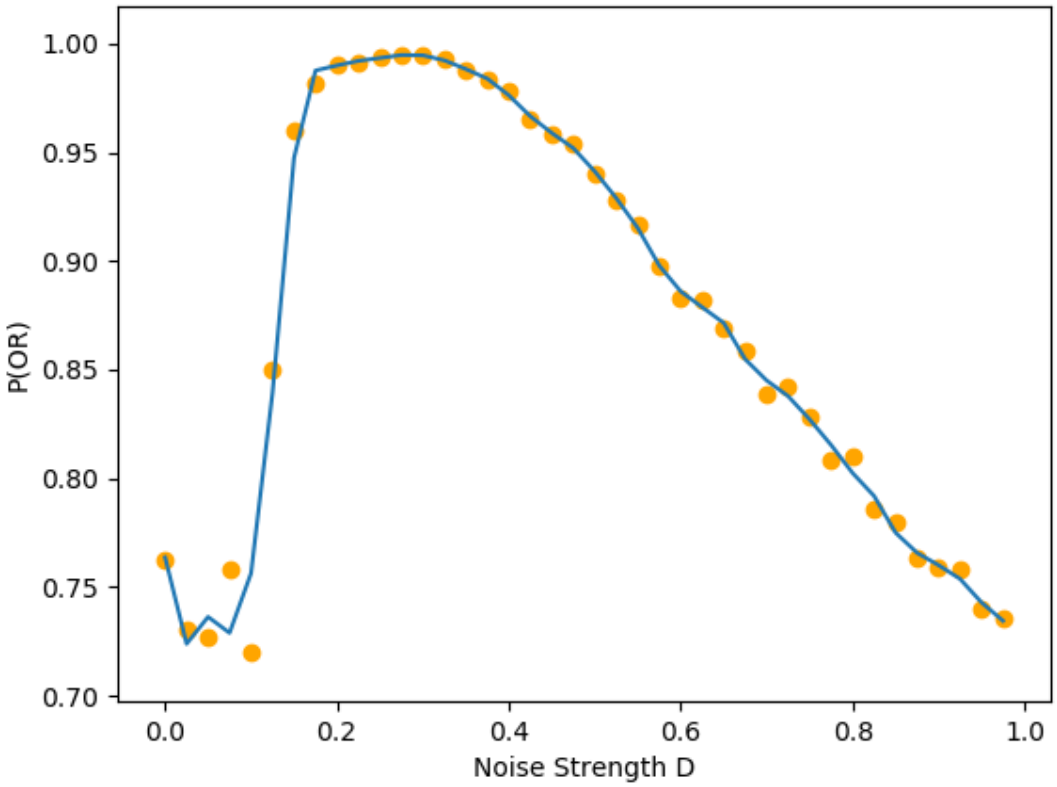

Figure 3.9: Dependence of the probability of obtaining OR logic operation, P(OR), on noise strength D, for coupling strength $c = 2$ and bias $b = -0.28$.

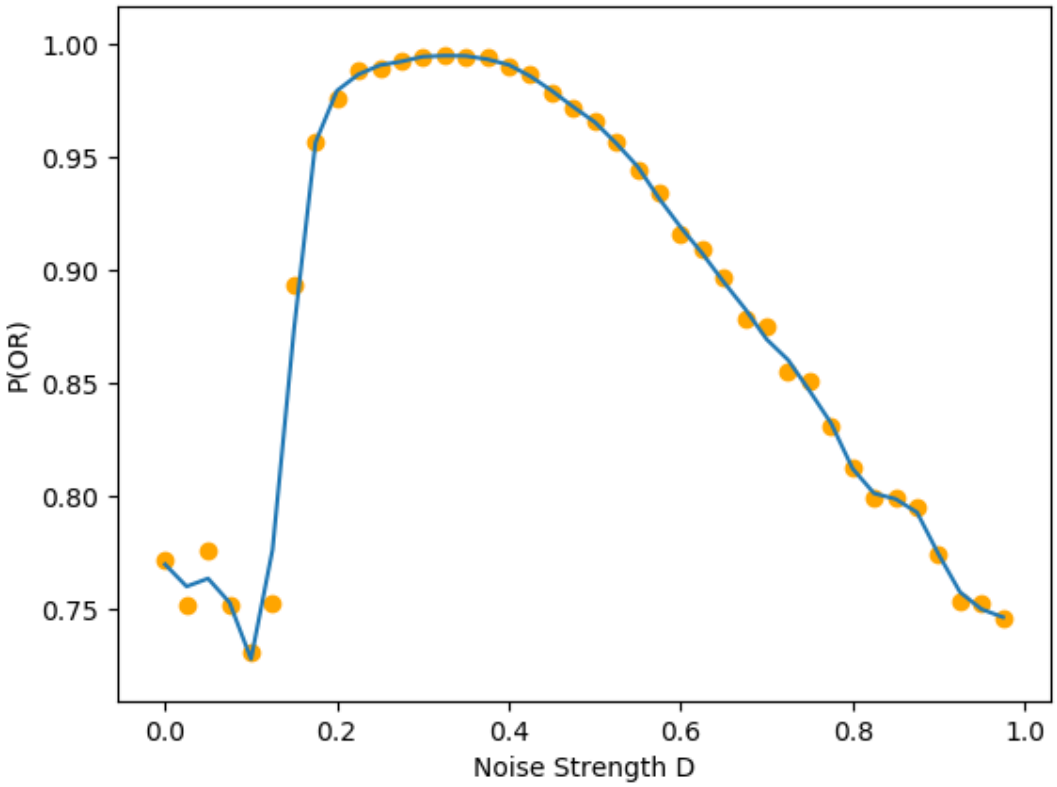

Figure 3.10: Dependence of the probability of obtaining OR logic operation, P(OR), on noise strength D, for coupling strength $c = 3$ and bias $b = -0.28$.

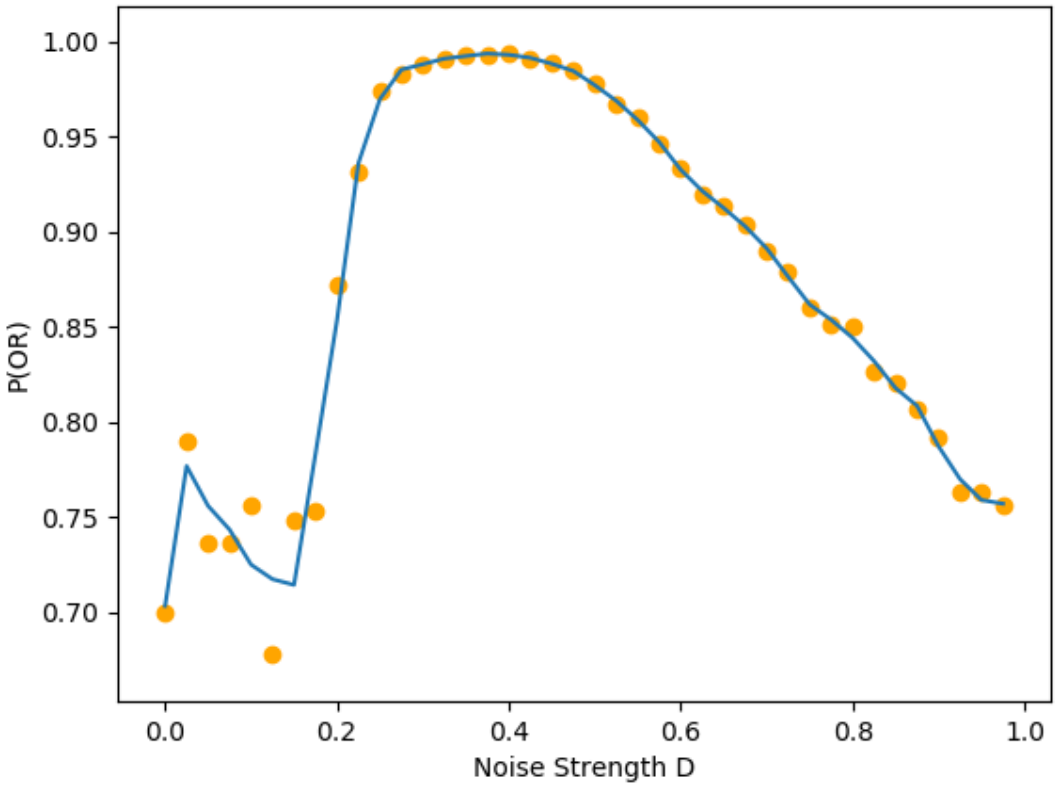

Figure 3.11: Dependence of the probability of obtaining OR logic operation, P(OR), on noise strength D, for coupling strength $c = 5$ and bias $b = -0.28$.

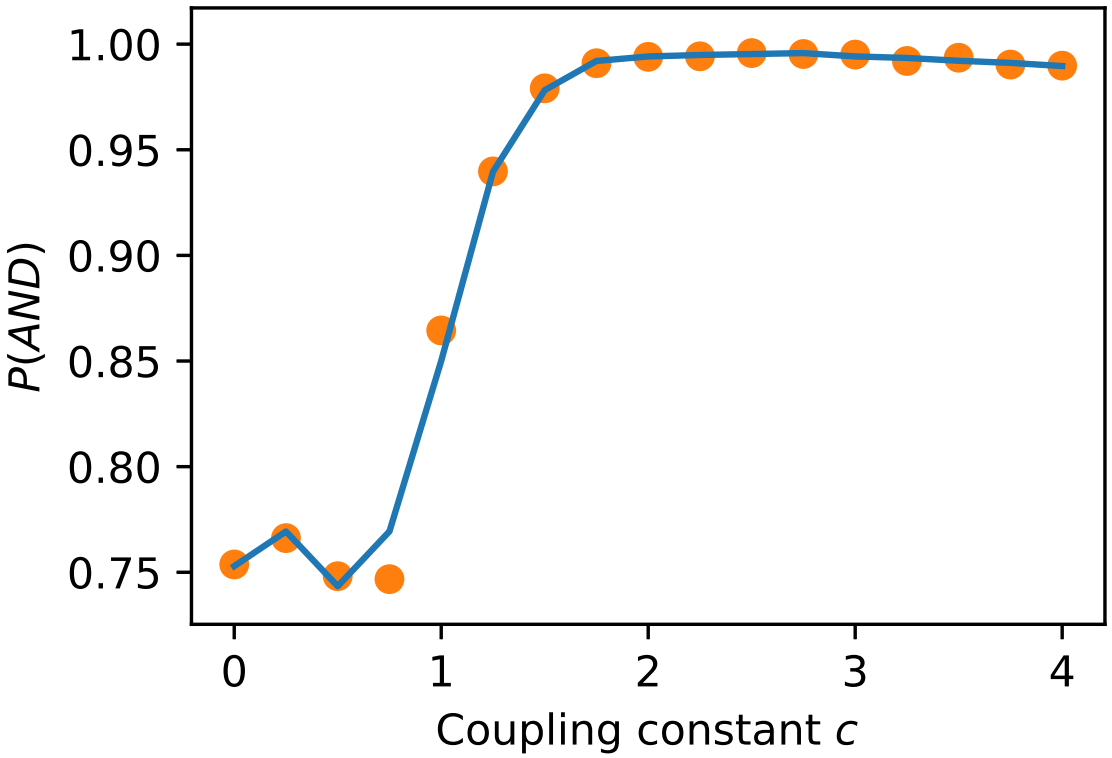

Figure 3.12: Dependence of probability of obtaining AND logic P(AND) on coupling constant c, for noise strength $D = 0.3$ and bias $b = -0.28$

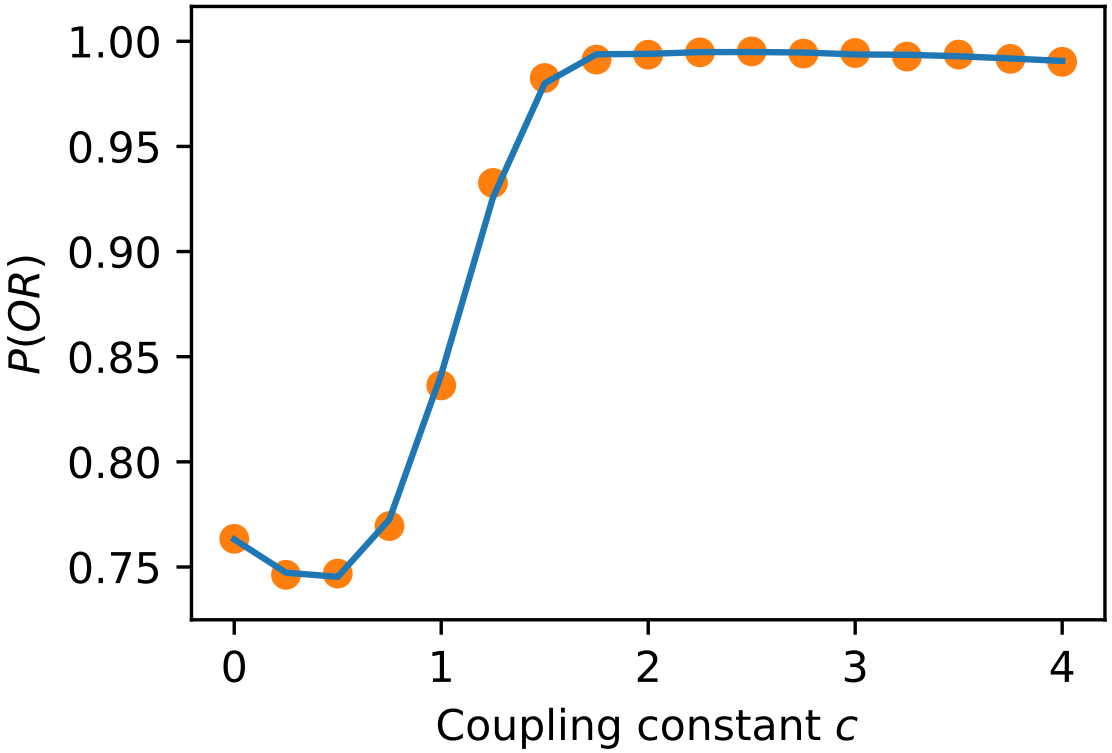

Figure 3.13: Dependence of probability of obtaining OR logic P(OR) on coupling constant c, for noise strength $D = 0.3$ and bias $b = +0.28$

3.4 Experimental Realization

As proof of principle of this idea we now present the experimental realization of this approach. *In order to demonstrate the robustness and generality of this phenomenon we implement the idea using a different bistable system.* Specifically, we use a piecewise linear bistable system. This system allows simple experimental realization with identical individual units, owing to the minimal number of components required in its construction.

The non-dimensionalized form of the circuit equations is as follows:

$$\begin{aligned} \dot{x} &= F(x) + b + c(y - x) + I_1 + D\ \eta_1(t) \\ \dot{y} &= F(y) + b + c(x - y) + I_2 + D\ \eta_2(t) \end{aligned} \tag{3.2}$$

where F is a piecewise linear function given by,

$$F(k) = \begin{cases} -(k+1) & k < -0.5 \\ k & -0.5 \leq k \leq 0.5 \\ -(k-1) & k > 0.5. \end{cases} \tag{3.3}$$

A schematic representation of the circuit is given in Fig. 3.14. The details of implementing the nonlinearity F experimentally are discussed in reference [43]. The time traces of this circuit, under varying noise, for positive and negative bias, are shown in Figs. 3.15 and 3.16. It is clearly evident that one obtains a consistent OR/NOR or AND/NAND logic operation in an optimal window of moderate noise strengths, depending upon the value of b in Eqn. 3.2. The system will behave either as logical OR or logical AND gate, if we consider logic state 0 (OFF) to be the negative input voltage (output voltage) and state 1 (ON) to be positive input voltage (output voltage). The *same* system can be made to work as complementary logic gates throughout the circuit by simply using the converse mapping of the negative input (output voltage) to be the ON state and positive input(output) voltage as OFF state throughout the circuit.

So, unlike all the previous work on Logical Stochastic Resonance, we do not need to first create a three-state signal of $(I = I_1 + I_2)$ and then add it to the system for logic extraction. In our method here the individual logic inputs I_1 and I_2 drive the individual systems separately. The idea behind this approach is that we have individual systems, each receiving independent logic inputs, and the individual systems co-operate and yield a collective response that gives the desired logic output. In terms of circuitry, this reduces

a resistor in each system in the input adder. However, the more significant thing is the broad idea that individual systems receive only *one* logic input each, but due to coupling they respond to give logic output that is a function of *both* inputs. This underlying idea may potentially lead to alternate implementations of other operations and computational tasks [44, 45].

3.5 Conclusions

In summary, we have shown how the constructive interplay between a noise-floor, coupling and nonlinearity can be exploited to obtain extremely reliable logic gate output from coupled bistable systems. Additionally, we have shown how the system can also switch the logic response by adjusting a bias parameter, thus allowing one to effectively manipulate the transfer characteristic of the system to optimize the logic response for a given noise-floor. So one can use the constant bias to robustly implement different logic truth tables. So one can use the constant bias in this coupled systems as a morphing control to robustly implement different logic gates. Further, it is interesting to note that the described coupled systems for logic gates are two dimensional in nature. Furthermore, due to the geometrical flexibility, it is possible to include additional systems (for example in the form of star network) having their respective logic input signals, towards the realization of multi-input logic gates without the need of separate adder circuits.

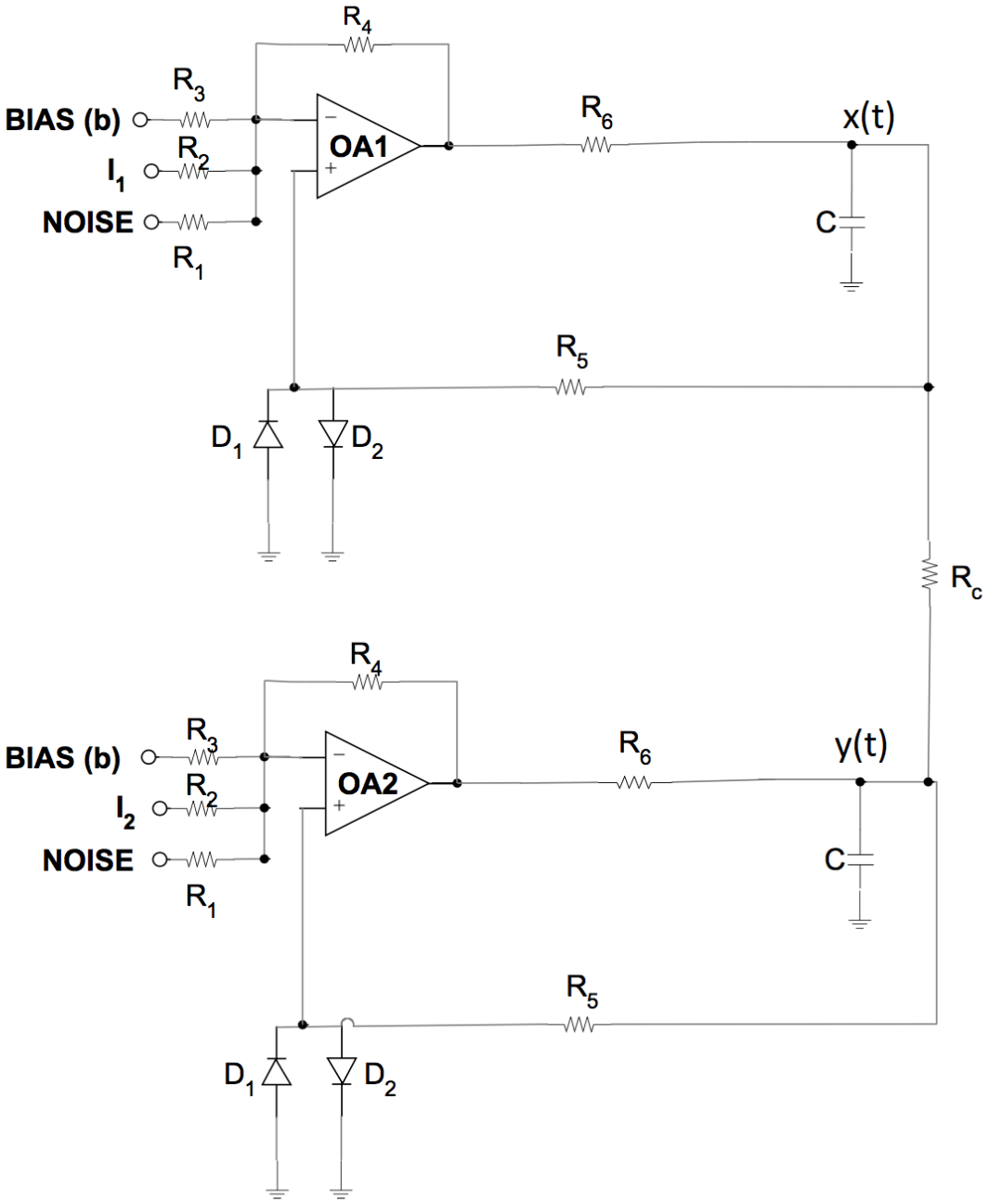

Figure 3.14: Circuit diagram of the coupled system represented by Eqn. 3.2.The op-amp used is μA741, capacitor value $C_1 = 470$ nF, resistances R_1, R_2, R_3, R_4, $R_5 = 10$ kΩ, $R_6 = 70$ Ω and coupling resistance $R_c = 173$ Ω

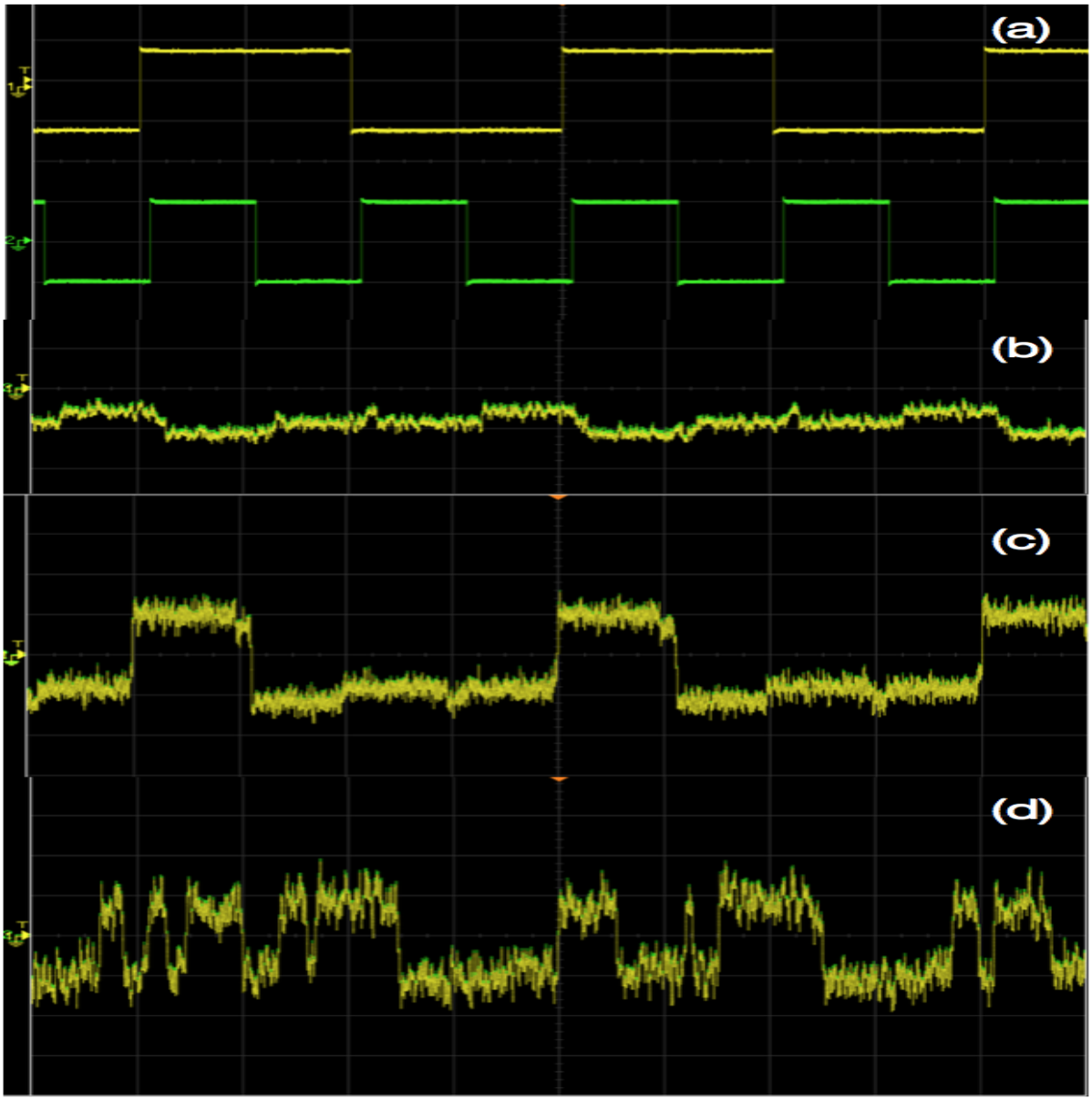

Figure 3.15: Progression of the response of either of capacitor voltages in the circuit of as marked in Fig. 3.14, in the presence of white noise (increasing from the top). The panels showing the capacitor voltage performing *AND/NAND logic*. The scale in the traces are: 200mV/Div (Y-axis) and 5 mS/Div (X-axis). For low noise strength (1.5 Vpp) the output is not able to produce reliable transitions between the two states. As the noise is increased, an optimal noise strength is reached (2.5 Vpp) in which the capacitor voltage switches logically with the inputs, obtaining in this way a reliable logic gate. Further increase of the noise strength (3.5 Vpp) leads to the occurrence of random switching destroying the reliability of the logic gates. The bias voltage b is fixed as -150 mV. The input logic signals levels are fixed as +400 mVpp (ON state) and -400 mVpp (OFF state). Here, colors yellow and green correspond to the capacitor voltages of upper and lower circuits respectively (Refer Fig. 3.14).

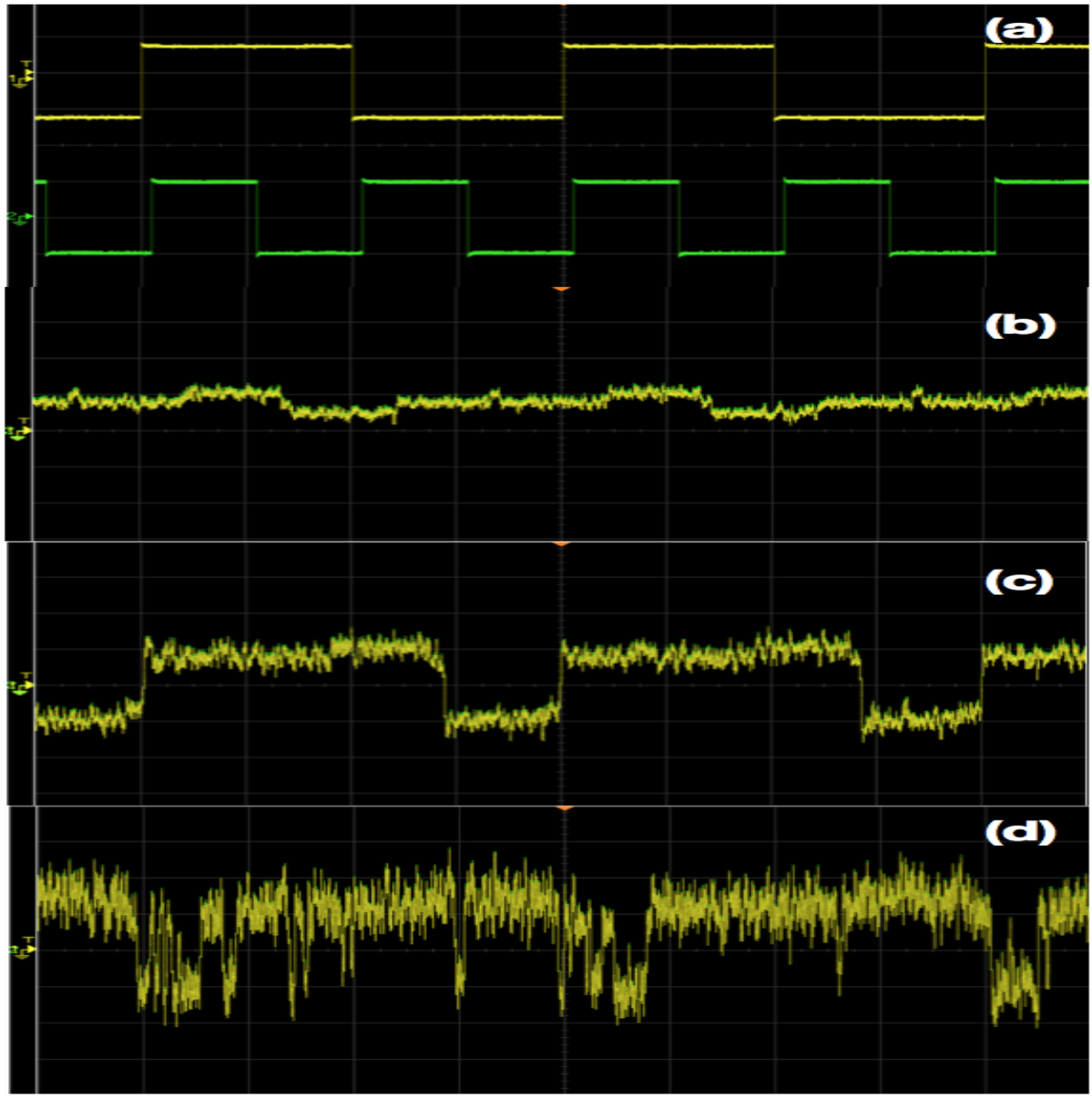

Figure 3.16: Progression of the response of either of capacitor voltages in the circuit of as marked in Fig. 3.14, in the presence of white noise (increasing from the top). The panels showing the capacitor voltage performing *OR/NOR logic*. The scale in the traces are: 200mV/Div (Y-axis) and 5mS/Div (X-axis). For low noise strength (1.5 Vpp) the output is not able to produce reliable transitions between the two states. As the noise is increased, an optimal noise strength is reached (2.5 Vpp) in which the capacitor voltage switches logically with the inputs, obtaining in this way a reliable logic gate. Further increase of the noise strength (3.5 Vpp) leads to the occurrence of random switching destroying the reliability of the logic gates. The bias voltage b is fixed as +150 mV. The input logic signals levels are fixed as +400 mVpp (ON state) and -400 mVpp (OFF state). Here, colors yellow and green correspond to the capacitor voltages of upper and lower circuits respectively (Refer Fig. 3.14).

Chapter 4

Implementation of Noise-aided Logic Gates with Memristive Circuits

Adapted from the work :

Manaoj Aravind V, K. Murali and Sudeshna Sinha,
Manuscript under review in *International Journal of Bifurcation and Chaos*

4.1 Introduction

Memristive devices (memristor) [see 1.5] are used principally for resistive switching memories, and these have been considered very promising candidates for developing novel state-of-the-art memory technology. Moreover, it has been established that networks of memristors may potentially help implement neuromorphic computing architectures [46,47]. The main advantages of computing with memristive elements is their low power consumption, and their ability to store and process information on the same physical platform. So our demonstration of noise-aided logic gates obtained from memristive elements in this work will significantly push forward the potential of memristive devices to provide promising alternatives to the conventional computing platforms, as well as expand the scope of [48].

4.2 LSR using Memristive circuit

Specifically, we have used a second order autonomous memristive circuit from Ref. [49] to implement Logical Stochastic Resonance (see section 1.4). In Fig. 4.1a we display the schematic of the circuit, which consists of a resistor, capacitor and memristor. We have used a simple, inductor free equivalent circuit to emulate the memristive behavior, as shown in Fig. 4.1b. The elaboration on how the given circuit has the functional form of a voltage controlled memristor and a complete analysis of its current-voltage characteristics can be found in ref. [49].

The dynamics of this circuit is dictated by two components, the capacitor C_1 and active voltage controlled memristor with memductance $W(v_0)$. Hence the circuit maybe modeled with voltage v_1 across capacitor C_1, and voltage v_0 as shown in Fig. 4.1, as the two state variables. This yields the governing equations:

$$\begin{aligned} \frac{dv_1}{dt} &= \frac{I(t) - v_1}{RC_1} + \frac{(1 - gv_0^2)v_1}{R_3C_1}, \\ \frac{dv_0}{dt} &= -\frac{v_1}{R_1C_0} - \frac{v_0}{R_2C_0} \end{aligned} \tag{4.1}$$

where $I(t)$ is the combined input given to the system and is the sum of Input streams I_1 and I_2, noise $D\eta(t)$ and bias b, i.e. $I(t) = I_1 + I_2 + D\eta(t) + b$. The noise term $\eta(t)$ is a zero mean delta-correlated Gaussian noise, with variance 1 and D is the noise

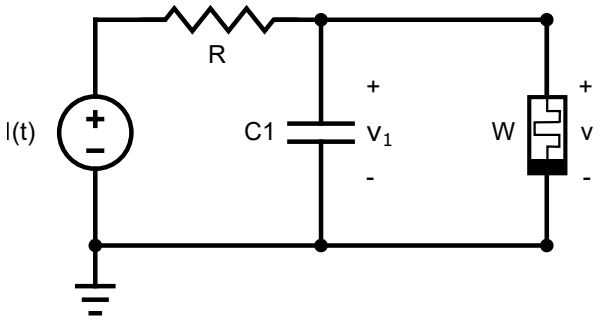

(a)

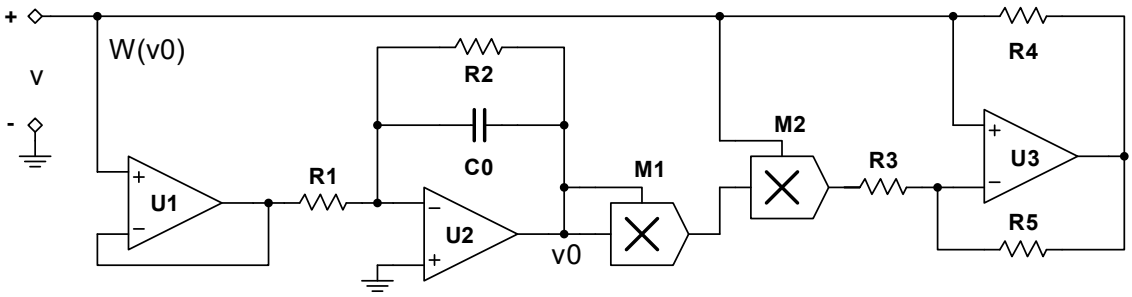

(b)

Figure 4.1: (a) Schematic of the single memristor based circuit. (b) Equivalent circuit of the memristor W. The multipliers (M1 and M2) are realized with AD633. The op-amps U1, U2, and U3 are realized with AD712. The circuit parameters are fixed as: $R_1 = 8\,k\Omega$, $R_2 = 4\,k\Omega$, $R_3 = 1.4\,k\Omega$, $R_4, R_5 = 2.2\,k\Omega$, $C_0 = 5\,nF$, $g = 1\,V^{-2}$, $R = 3\,k\Omega$ and $C_1 = 10\,nF$.

strength. The focus of our investigation here is the switching of the states of the system under varying noise strengths, and different bias parameters, and ascertaining whether this emergent switching can yield consistent logic outputs [42].

4.2.1 Computational Model

In order to computationally model the system we use the non-dimensionalized form of Eqn. 4.1

$$\begin{aligned} \dot{x} &= f_x(x,y) = -x + \alpha_1 x(1 - gy^2) + I(t), \\ \epsilon\dot{y} &= f_y(x,y) = -\alpha_2 x - \alpha_3 y \end{aligned} \tag{4.2}$$

Here, $I(t)$ is the sum of logic input streams I_1, I_2, Noise $D\eta(t)$ and bias b. i.e. $I(t) = I_1 + I_2 + D\eta(t) + b$. The noise term $\eta(t)$ is a zero mean Gaussian noise, with variance 1 and D is the noise strength. The output is determined by the sign of variable x (or y). For instance, if we can assign logic output value 1 to $x(t) > 0$, and output value 0 to $x(t) < 0$.

Figure 4.2 shows the timeseries of the two variables $x(t)$ and $y(t)$ for the corresponding input sequence I_1 and I_2, with bias $b = +1$. We see that *consistent logic output* is obtained for *moderate noise* at $D = 1$ and the reliability of the logic response is lost for both low noise strengths (for instance, $D = 0.4$) and high noise strengths (for instance, $D = 2.5$). Specifically, state variable $x(t)$ consistently produces an OR logic output, while the other state variable $y(t)$ produces the complementary NOR logic output, *in parallel*.

Most interestingly, given that the both signals are sub-threshold at $I_1, I_2 = \pm 1$ the logic response is considerably *amplified*. For the parameters used here, the response from $y(t)$ is *double* that of the input streams and $x(t)$ is *five* times that of the input streams (cf. Figs 4.2 and 4.3). This amplification is also apparent in the oscilloscope traces obtained from the experimental implementation shown in figs. 4.4 and 4.5.

Further, the bias b is the control parameter that determines the nature of the logic function being implemented. For instance, in this system when bias b takes value $+1$ one obtains a OR/NOR logic gate, and when it takes value -1 one obtains a AND/NAND logic gate. Figure 4.3 shows consistent AND logic being obtained for moderate noise (for instance $D = 1$) when bias $b = -1$. So a simple change of the bias allows us to

morph between fundamental logic functions, and lays the building block for potentially reconfigurable computing devices.

4.2.2 Experimental verification

We verify the computational results by constructing the circuit shown in Fig. 4.1. The time traces of the voltage across capacitor C_1 for different values of noise strength D and bias b are shown in Figs. 4.4 and 4.5. We see that consistent logic is obtained only in the presence of a moderately strong noise.

4.2.3 Quantitative measure of reliability

A quantitative measure of how reliably this system performs logical operations is obtained by comparing the output of the system with the expected logical output, over long times, and for different input sets. The probability of obtaining the desired output is estimated by driving the system with a stream consisting of a large number of (I_1 - I_2) sets, where each run consists of the four input sets $(0,0)$, $(0,1)$, $(1,0)$, $(1,1)$, in different permutations. So the memristive system is subject to a many different random combinations of I_1 and I_2 over time and its response to this random stream of inputs is recorded. If the logic output, as obtained from $x(t)(y(t))$, matches the logic output in the truth table for *all* input sets in the run, it is considered a success. The probability, $P(logic)$, is the ratio of the number of such successful runs to the total number of runs sampled. The fraction of time where one obtains the desired logic output successfully, gives a measure of the probability of obtaining that specific logic, denoted as P(OR) or P(AND). When this measure approaches 1 we have completely reliable logic outputs. In Figs. 4.6 and 4.7 we show this measure, and it is clearly evident that there is an optimal window of noise strength D, for which OR/NOR and AND/NAND logic is consistently obtained.

4.3 Coupling induced LSR using Memristive circuit

In a recent advancement [37], it has been shown that highly reliable logic response can be obtained when the input signals (I_1 and I_2) are separately fed into two coupled bistable sub-systems with sufficient coupling strengths in an optimal window of noise. Here since the signals are fed into individual subsystems, the coupling between them is pivotal in

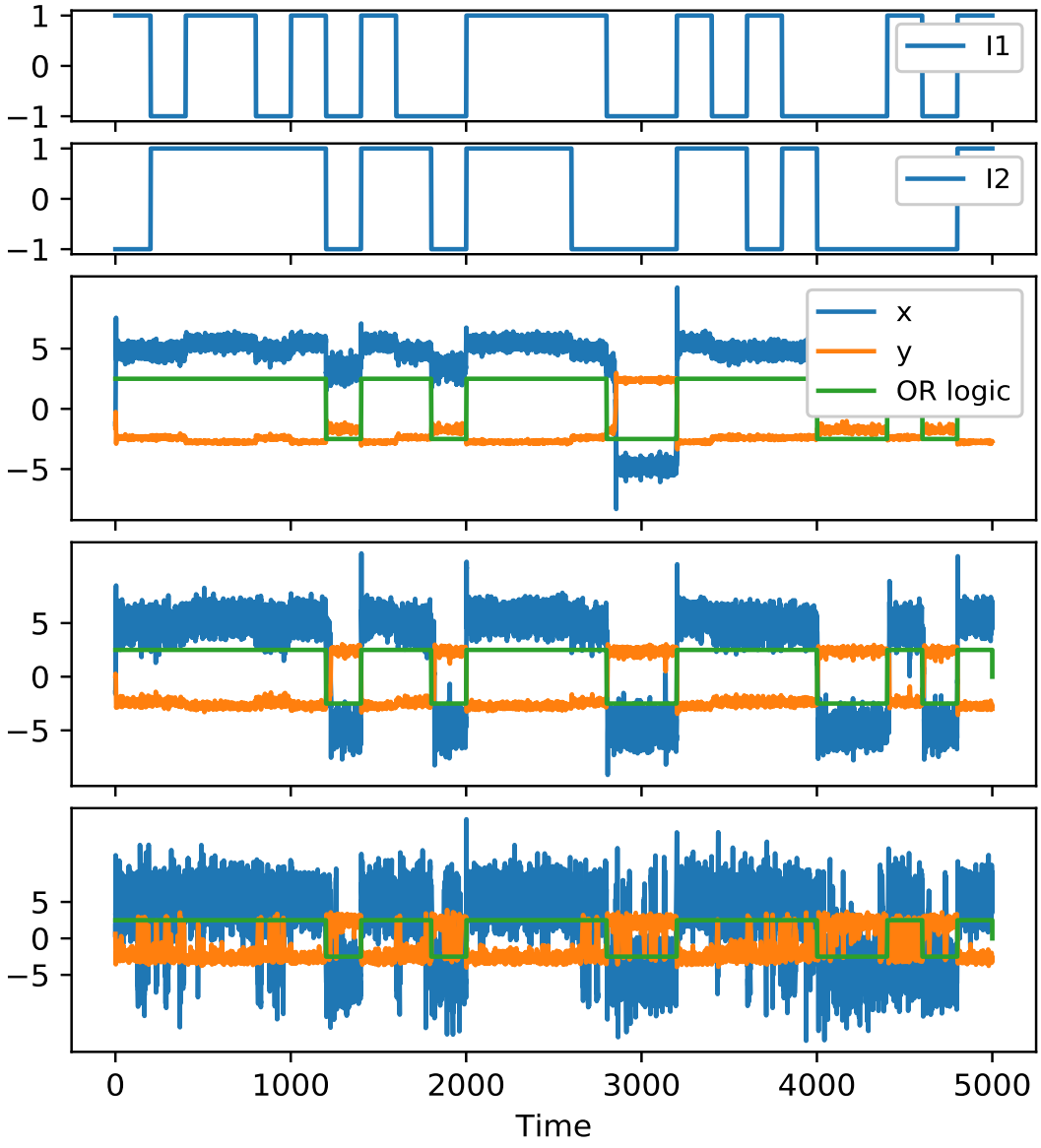

Figure 4.2: Timeseries of variables $x(t)$ and $y(t)$ obtained by simulating Eqns. 4.2, for three values of noise strength D, $D = 0.4$, $D = 1$, $D = 2.5$, with bias $b = +1$ yielding OR/NOR logic. The corresponding input streams I_1 and I_2 are also shown. Here $x(t) > 0$ (or $y(t) > 0$) corresponds to logic output 1 and $x(t) < 0$ (or $y(t) < 0$) corresponds to logic output 0. The parameter values used for the simulation are: $g = 0.1$, $\alpha_1 = 1.86$, $\alpha_2 = 0.325$, $\alpha_3 = 0.65$ and $\epsilon = 0.69$.

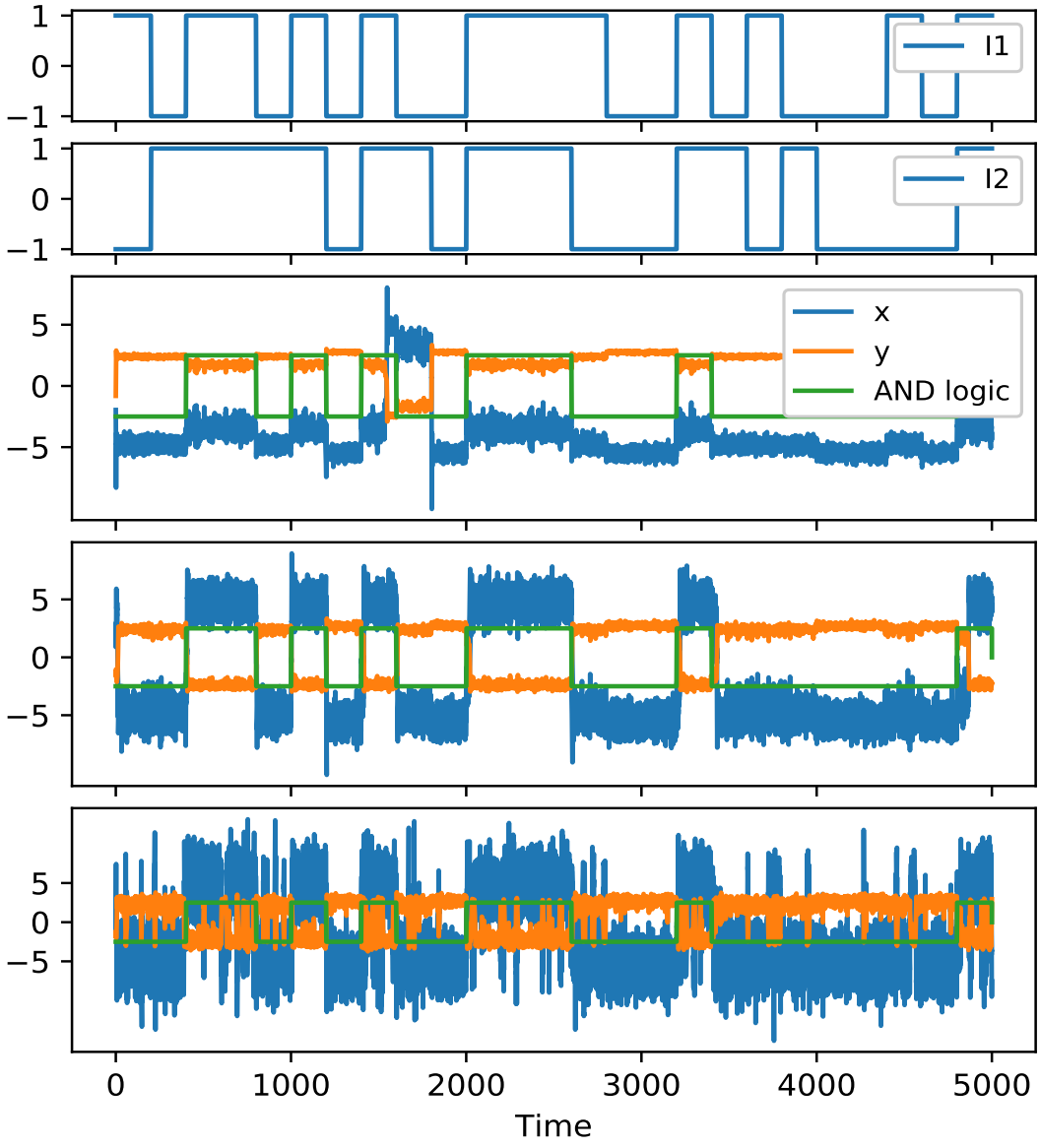

Figure 4.3: Timeseries of variables $x(t)$ and $y(t)$ obtained by simulating Eqns. 4.2, for three values of noise strength D, $D = 0.4$, $D = 1$, $D = 2.5$, with bias $b = -1$ yielding AND/NAND logic. The corresponding input streams I_1 and I_2 are also shown. Here $x(t) > 0$ (or $y(t) > 0$) corresponds to logic output 1 and $x(t) < 0$ (or $y(t) < 0$) corresponds to logic output 0. The parameter values used for the simulation are: $g = 0.1$, $\alpha_1 = 1.86$, $\alpha_2 = 0.325$, $\alpha_3 = 0.65$ and $\epsilon = 0.69$.

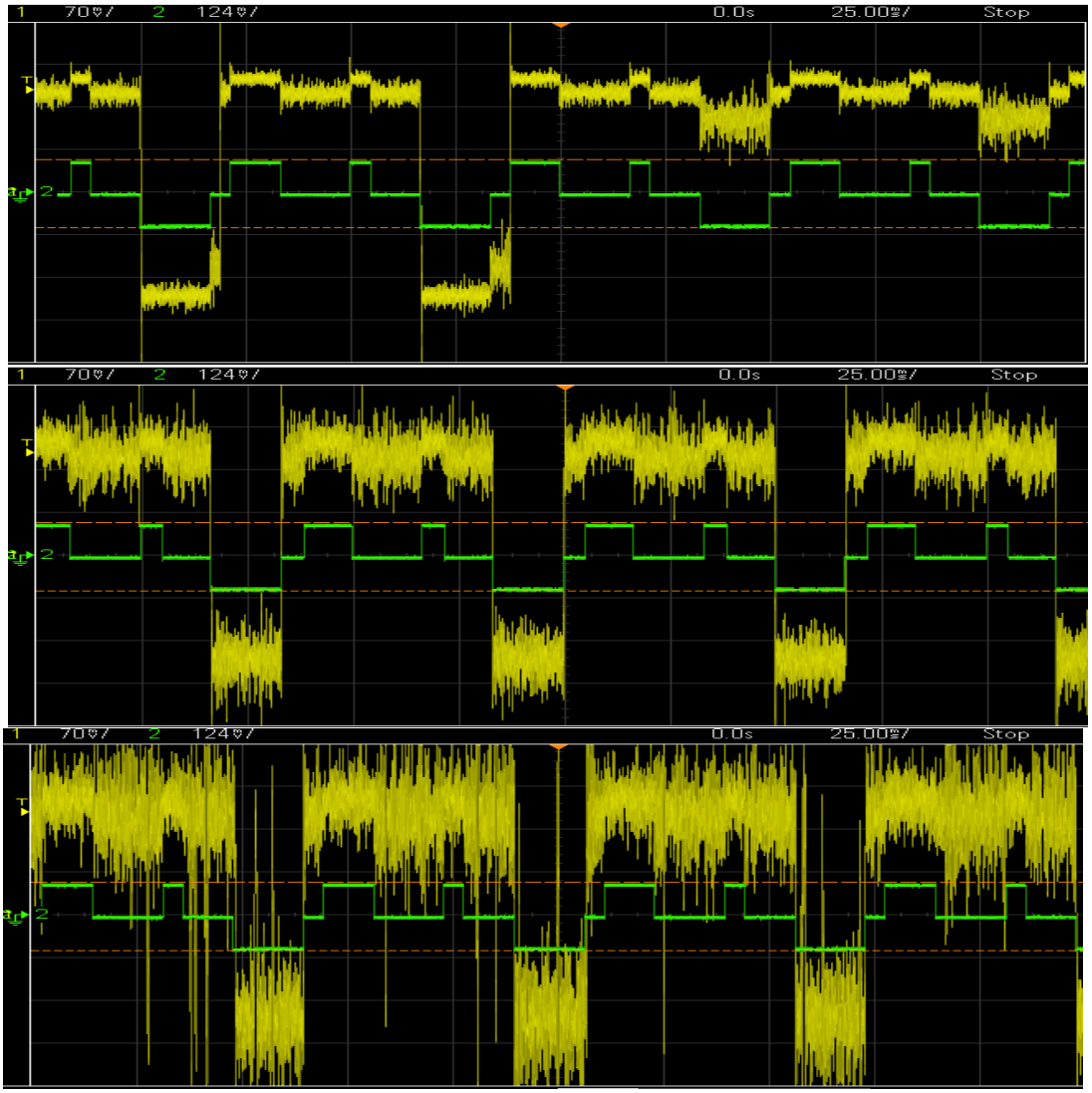

Figure 4.4: Waveforms of voltage across capacitor C_1 obtained from hardware implementation of the memristive circuit, for different noise levels: $D = 500mV$ (top) $D = 1.5V$ (middle) and $D = 2.5V$ (bottom). (Noise bandwidth 10 kHz) (cf. Fig.4.1). The panels also show the sum of the two input streams I_1+I_2 (green). I_1 and I_2 take value -0.5 V when logic input is 0 and value $+0.5$ V when logic input is 1. Here the bias b is set to $b = +250$ $mVpp$. Clearly the middle panel (moderate noise) yields a consistent OR logic output. The noise signal is drawn from Agilent or Keysight 33522A, Function/Arbitrary Waveform Generator. The oscilloscope used is Agilent or Keysight DSOX2012A. The scale of the traces are 70 mV/Div (Y-axis) and 25 mS /Div (X-axis).

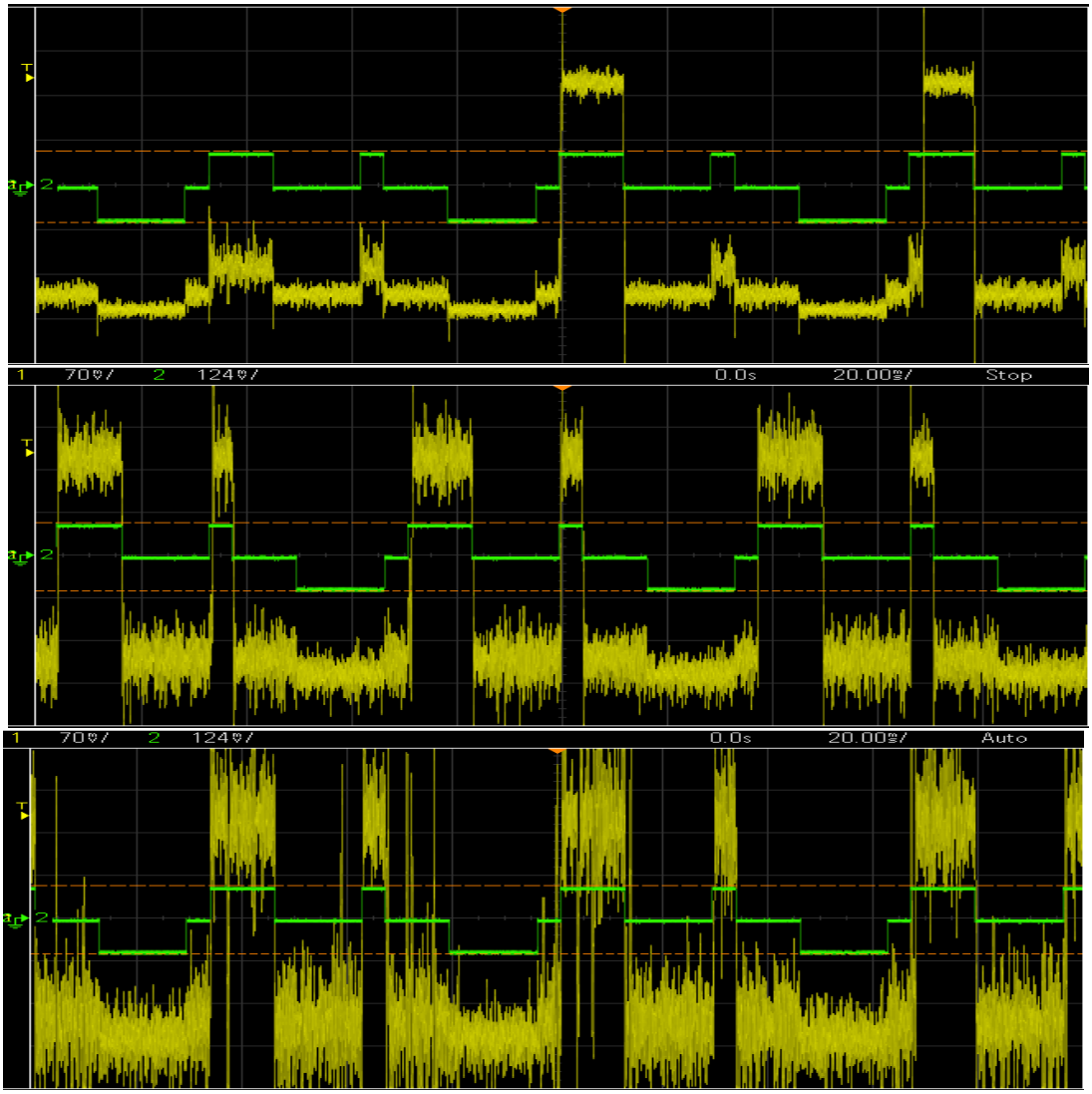

Figure 4.5: Waveforms of voltage across capacitor C_1 obtained from hardware implementation of the memristive circuit, for different noise levels: $D = 500mV$ (top) $D = 1.5V$ (middle) and $D = 2.5V$ (bottom). (Noise bandwidth 10 kHz) (cf. Fig.4.1). The panels also show the sum of the two input streams I_1+I_2 (green). I_1 and I_2 take value -0.5 V when logic input is 0 and value $+0.5$ V when logic input is 1. Here the bias b is set to $b = -250$ $mVpp$. Clearly the middle panel (moderate noise) yields a consistent AND logic output. The noise signal is drawn from Agilent or Keysight 33522A, Function/Arbitrary Waveform Generator. The oscilloscope used is Agilent or Keysight DSOX2012A. The scale of the traces are 70 mV/Div (Y-axis) and 25 mS /Div (X-axis).

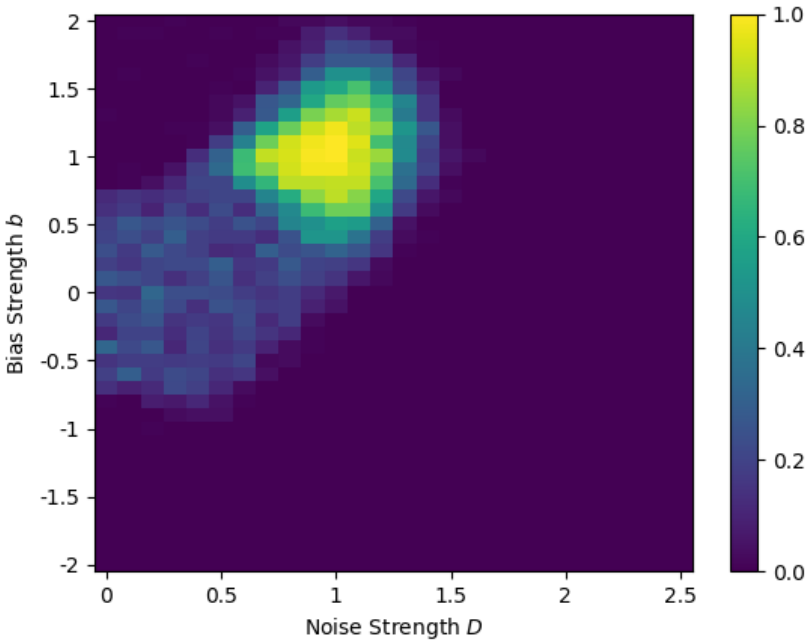

Figure 4.6: Dependence of the probability of obtaining OR logic operation, P(OR) on noise strength D, for system parameters: $g = 0.1$, $\alpha_1 = 1.86$, $\alpha_2 = 0.325$, $\alpha_3 = 0.65$ and $\epsilon = 0.69$ in Eqns. 4.2.

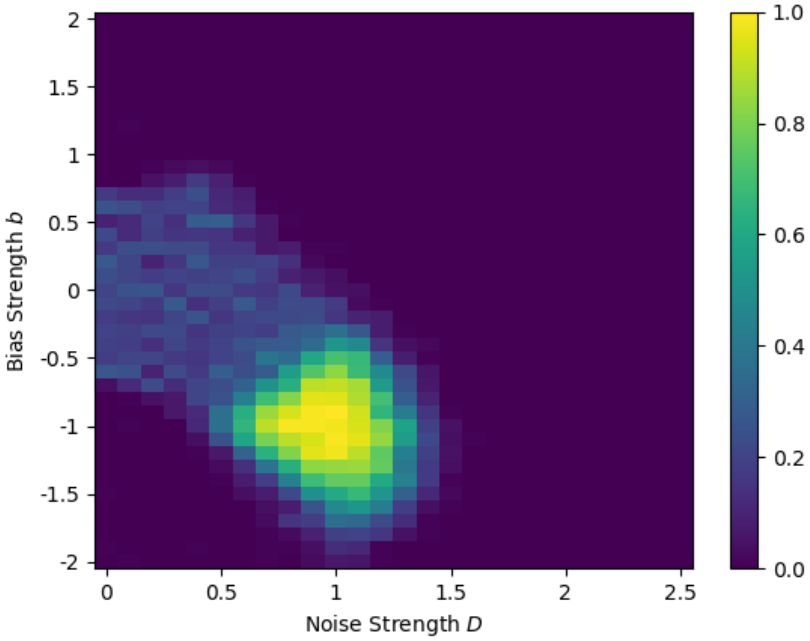

Figure 4.7: Dependence of the probability of obtaining AND logic operation P(AND), on noise strength D, for system parameters: $g = 0.1$, $\alpha_1 = 1.86$, $\alpha_2 = 0.325$, $\alpha_3 = 0.65$ and $\epsilon = 0.69$ in Eqns. 4.2.

obtaining the demonstrated logical response. We implement the aforementioned *coupling induced Logical stochastic resonance* using this memristive circuit to demonstrate another configuration in which consistent logic can be obtained.

4.3.1 Computational Model

We computationally model this coupled system, where each individual unit is given by Eqn. 4.2, by the following non-dimensionalized circuit equations:

$$\begin{aligned} \dot{x_1} &= f_x(x_1, y_1) + I_1(t) + b + D\eta_1(t) + c(x_2 - x_1) \\ \epsilon\dot{y_1} &= f_y(x_1, y_1) \\ \dot{x_2} &= f_x(x_2, y_2) + I_2(t) + b + D\eta_2(t) + c(x_1 - x_2) \\ \epsilon\dot{y_2} &= f_y(x_2, y_2) \end{aligned} \tag{4.3}$$

Here, c denotes coupling strength, D denotes the noise strength and b is a constant bias. η_1 and η_2 are uncorrelated Gaussian noises with mean zero and variance 1. The inputs I_1 and I_2 are used to drive the individual subsystems.

Figures 4.8 and 4.9 shows the timeseries of the two state variables of the subsystems (x_1 and x_2), superposed with the expected logical outcomes for both AND and OR logic. We again observe that consistent logic response is obtained for a moderate noise strength while the consistency is lost both at high and low values of noise. We also observe that x_1 and x_2 both yield the same logic and consistent output can be obtained from either of them. This is a non-trivial feature, as one memristor receives input I_1, while the other receives input I_2. However the output as determined by either state variable x_1 or x_2 is a logic function of both I_1 and I_2. Further, due to the inherent symmetry of the memristive circuit the other variables y_1 and y_2 yield the complementary logic i.e. if $b = -1$, while x_1 and x_2 produce AND logic, y_1 and y_2 yield NAND.

4.3.2 Experimental Verification

To solidify the above computational result, we construct two identical copies of the memristive circuit, resistively couple them and demonstrate the occurrence of coupling induced

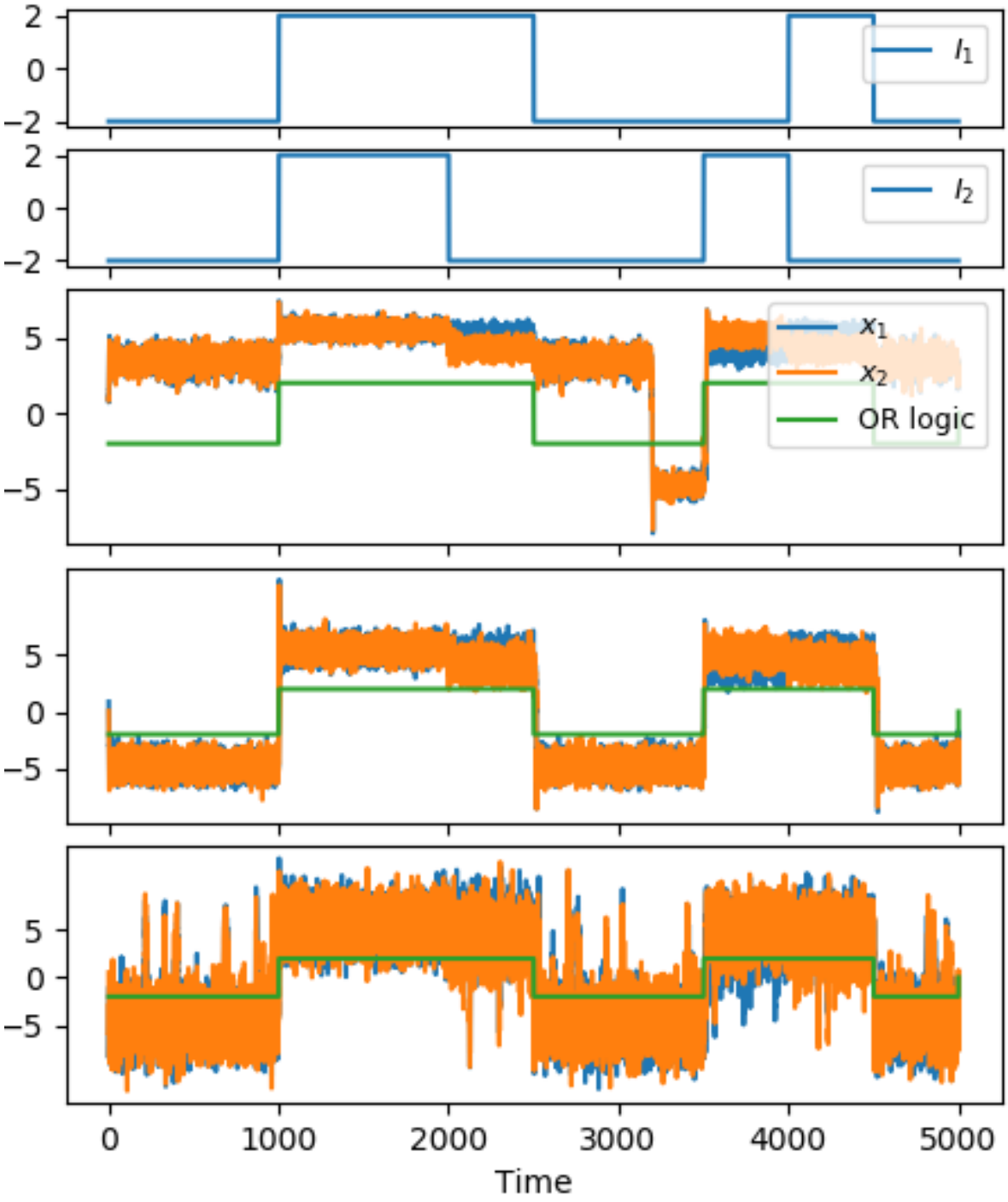

Figure 4.8: Timeseries of variables $x_1(t)$ and $x_2(t)$ obtained by simulating Eqns. 4.3, for three values of noise strength D, $D = 0.5$, $D = 1$, $D = 2.5$, with bias $b = +1$ yielding **OR/NOR logic**. Coupling strength $c = 1$. The corresponding input streams I_1 and I_2 are also shown. Here $x_1(t) > 0$ (or $x_2(t) > 0$) corresponds to logic output 1 and $x_!(t) < 0$ (or $x_2(t) < 0$) corresponds to logic output 0. The parameter values used for the simulation are: $g = 0.1$, $\alpha_1 = 1.86$, $\alpha_2 = 0.325$, $\alpha_3 = 0.65$ and $\epsilon = 0.69$.

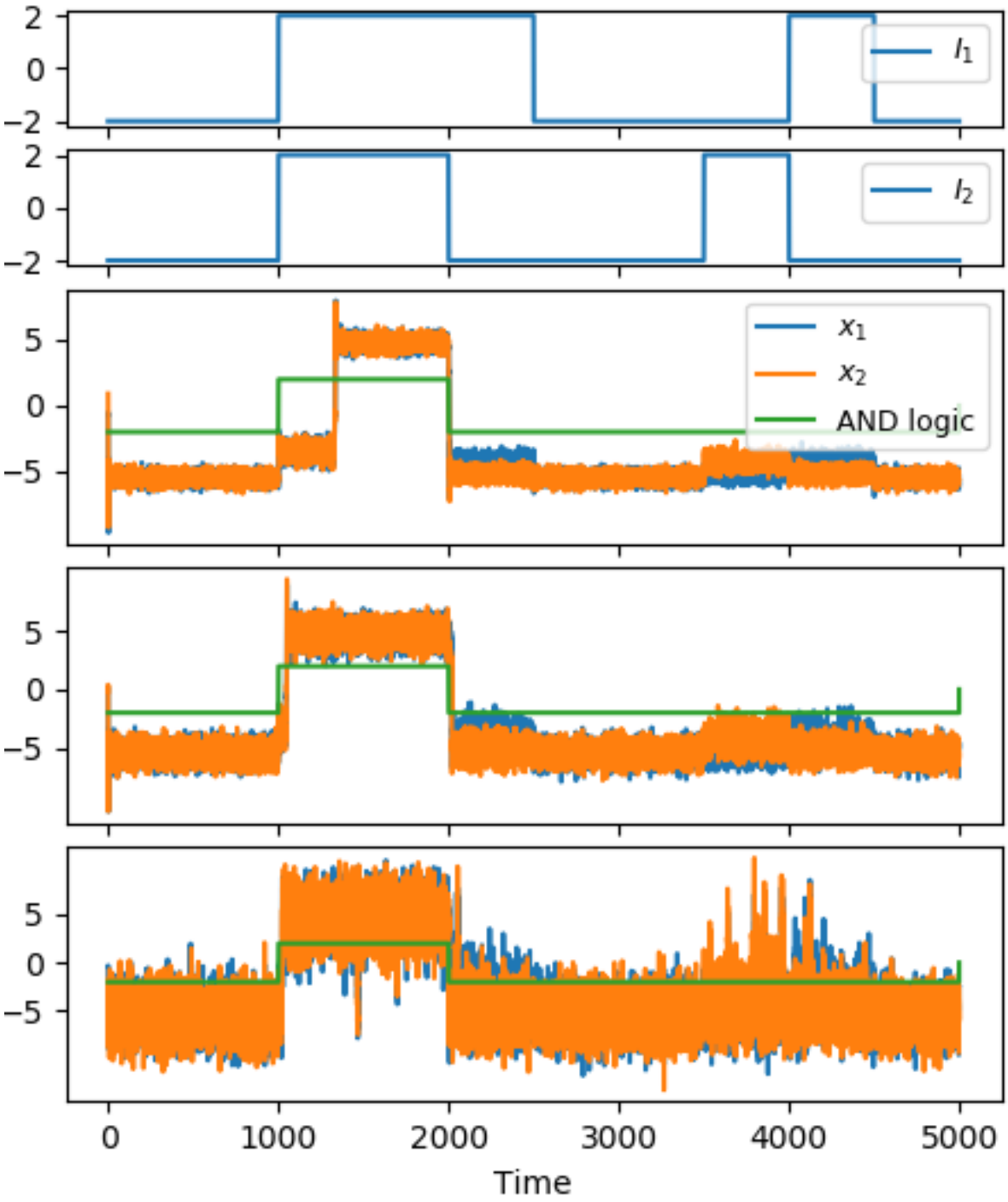

Figure 4.9: Timeseries of variables $x_1(t)$ and $x_2(t)$ obtained by simulating Eqns. 4.3, for three values of noise strength D, $D = 0.5$, $D = 1$, $D = 2.5$, with bias $b = -1$ yielding **AND/NAND logic**. Coupling strength $c = 1$. The corresponding input streams I_1 and I_2 are also shown. Here $x_1(t) > 0$ (or $x_2(t) > 0$) corresponds to logic output 1 and $x_!(t) < 0$ (or $x_2(t) < 0$) corresponds to logic output 0. The parameter values used for the simulation are: $g = 0.1$, $\alpha_1 = 1.86$, $\alpha_2 = 0.325$, $\alpha_3 = 0.65$ and $\epsilon = 0.69$.

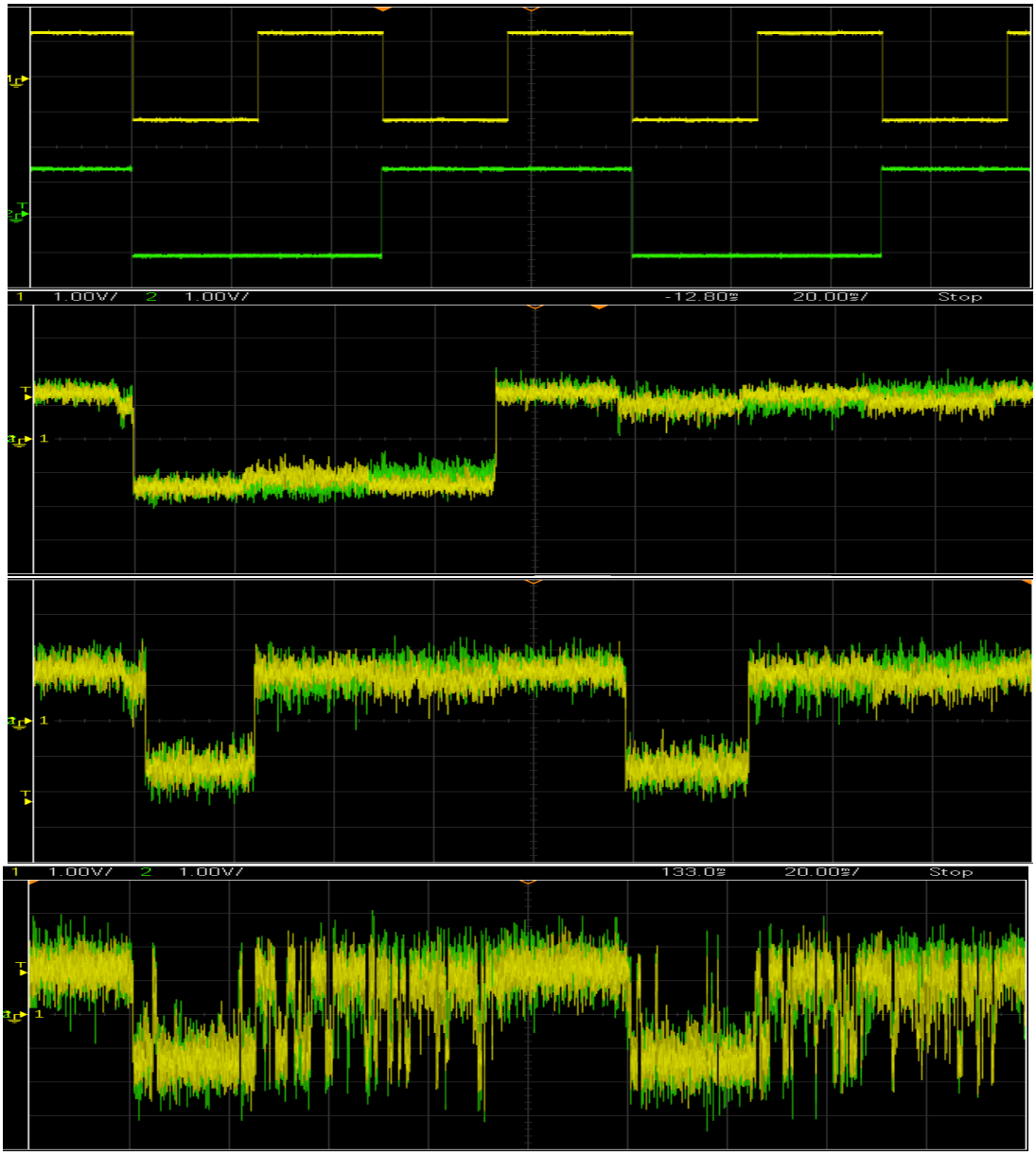

Figure 4.10: Waveforms obtained from hardware implementation of the coupled memristive circuit, showing the voltage across capacitors C_1 (yellow) and C_2 (green) for different noise levels: $D = 1V$ (second) $D = 1.8V$ (third) and $D = 2.8V$ (bottom). (Noise bandwidth 18 kHz) (cf. Fig.4.12). The top panel shows the two input streams I_1 (yellow) and I_2 (green). I_1 and I_2 take value -0.5 V when logic input is 0 and value $+0.5$ V when logic input is 1. Here the bias b is set to $b = +150$ $mVpp$. Clearly the third panel (moderate noise) yields a consistent OR **logic output**. The noise signal is drawn from Agilent or Keysight 33522A, Function/Arbitrary Waveform Generator. The oscilloscope used is Agilent or Keysight DSOX2012A. The scale of the traces are 1 V/Div (Y-axis) and 20 mS /Div (X-axis).

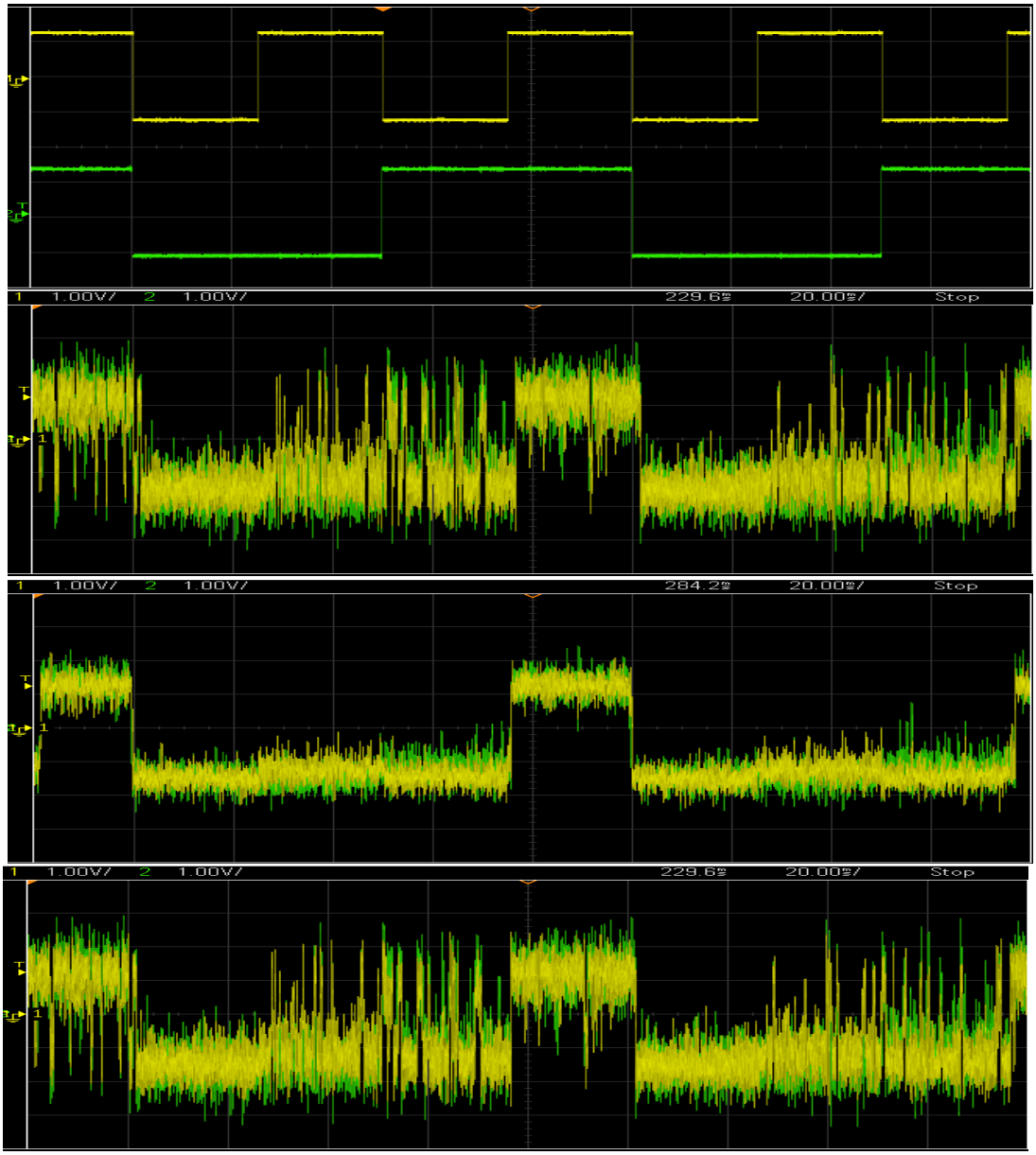

Figure 4.11: Waveforms obtained from hardware implementation of the coupled memristive circuit, showing the voltage across capacitors C_1 (yellow) and C_2 (green) for different noise levels: $D = 1V$ (second) $D = 1.8V$ (third) and $D = 2.8V$ (bottom). (Noise bandwidth 18 kHz) (cf. Fig.4.12). The top panel show the two input streams I_1 (yellow) and I_2 (green). I_1 and I_2 take value $-0.5\ V$ when logic input is 0 and value $+0.5\ V$ when logic input is 1. Here the bias b is set to $b = -150\ mVpp$. Clearly the third panel (moderate noise) yields a consistent AND **logic output**. The noise signal is drawn from Agilent or Keysight 33522A, Function/Arbitrary Waveform Generator. The oscilloscope used is Agilent or Keysight DSOX2012A. The scale of the traces are 1 V/Div (Y-axis) and 20 mS /Div (X-axis).

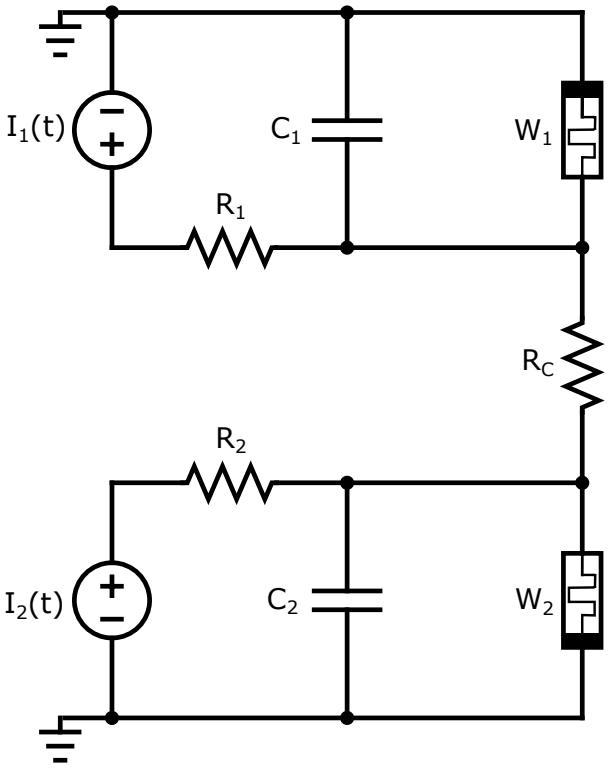

Figure 4.12: Schematic of the coupled memristive circuit. The circuit parameters are fixed as: $R_1 = R_2 = 2.4\,k\Omega$, $C_1 = C_2 = 10\,nF$ and coupling resistance $R_c = 5.57\,k\Omega$. The equivalent circuit for memristors W_1 and W_2 are same as elaborated in Fig. 4.1b.

logical stochastic resonance. The schematic circuit diagram of the construction is shown in Fig. 4.12. Here the active voltage controlled memristor W is the same as shown in Fig. 4.1b.

The oscilloscope trails of the voltage across capacitors C_1 and C_2 are shown in Figs. 4.10 and 4.11. It is evident that the experimental results are completely consistent with those observed in numerical simulations.

4.3.3 Quantitative measure of reliability

We again quantitatively identify the regions of parameter space where reliable logic operations occur, using the same rigorous metric described in section 2.3. Specifically, we use $P(logic)$ to demarcate the regions in parameter space where logic operations are obtained consistently. In Figs. 4.13 and 4.14 we see that a broad range of noise (D) and bias (b) strengths yield completely reliable logic operations (i.e. $P(logic) \sim 1$), with positive values of bias yielding OR/NOR logic and negative values of bias yielding AND/NAND logic. Figures. 4.15 and 4.16 show the regions of reliable operation in the $c - D$ space. Note that there exists a clear band of noise strengths for which consistent operations is obtained. Also, we observe the existence of a minimum threshold of coupling strength c for consistent operation. Coupling strengths larger than this threshold yields faithful logic. We did not find any upper bound in coupling strength c for obtaining $P(logic) \approx 1$, in the explored range of $c \in [0, 5]$.

Further, it is interesting to note from Figs. 4.15 and 4.16 the behaviour of the window of optimal noise strengths for different values of coupling strength c. To make the behavior more apparent, in Fig. 4.17 we show the minimum value of noise strengths $D(low)$ required to produce consistent logic and the maximum value of noise strengths $D(high)$ upto which consistent logic is produced. On increasing coupling strength c, we observe that both $D(low)$ and $D(high)$ show a sharp transition at a critical value, from zero to a finite moderate value, after which it saturates, with $D(high)$ saturating slower and at higher coupling strengths than $D(low)$. So the width of the noise window supporting robust logic operations increases very sharply from zero after a critical coupling threshold and then rapidly saturates at increasing coupling strengths. This clearly indicates that coupling is crucial for obtaining reliable logic outputs, as robust operations are obtained only after sufficiently strong coupling.

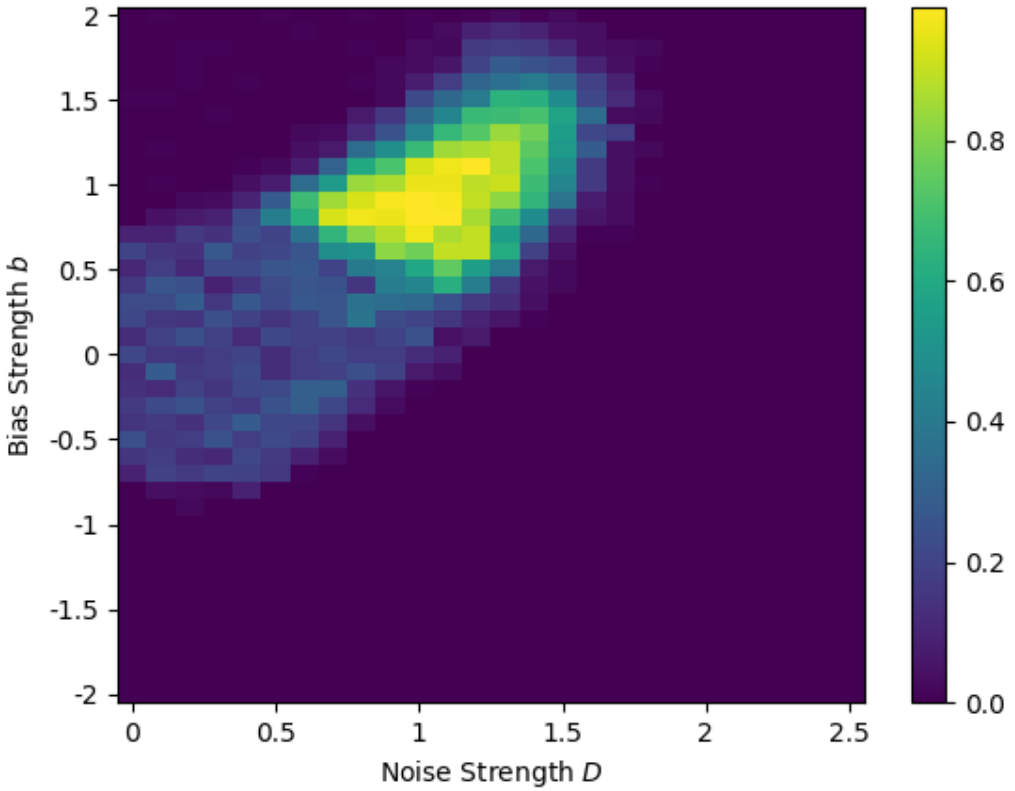

Figure 4.13: Dependence of the probability of obtaining OR logic operation, P(OR), on noise strength D and bias strength b, for coupling strength $c = 1$ and system parameters: $g = 0.1$, $\alpha_1 = 1.86$, $\alpha_2 = 0.325$, $\alpha_3 = 0.65$ and $\epsilon = 0.69$ in Eqns. 4.3.

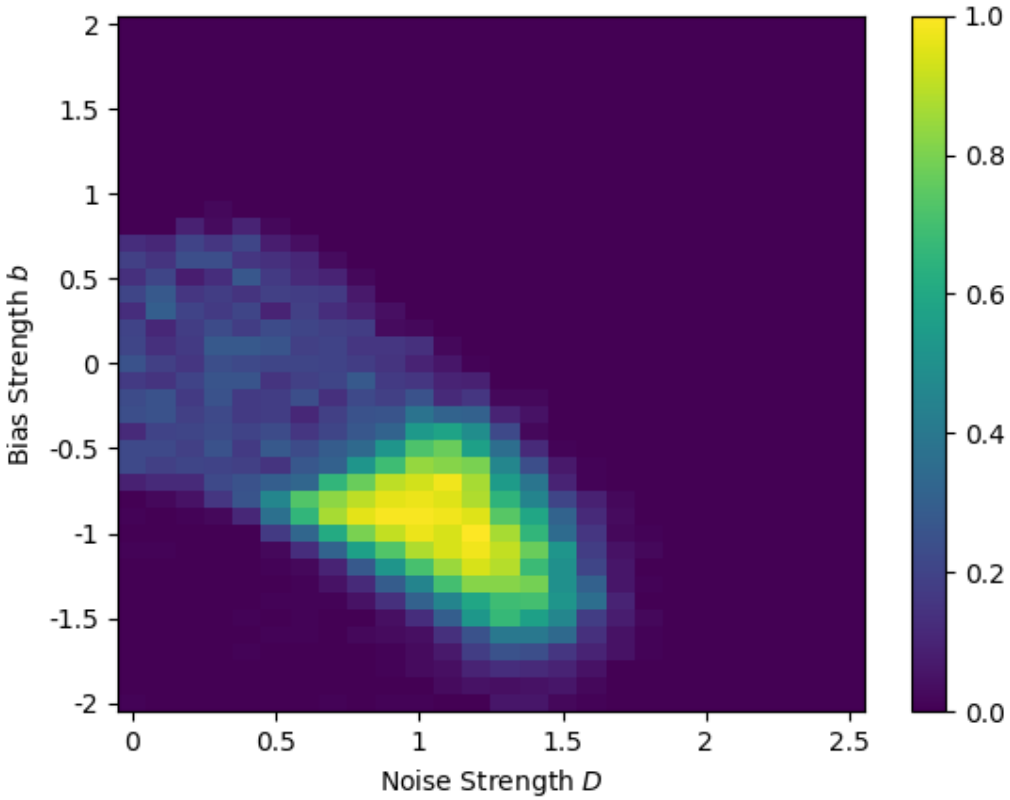

Figure 4.14: Dependence of the probability of obtaining AND logic operation P(AND), on noise strength D and bias strength b, for coupling strength $c = 1$ and system parameters: $g = 0.1$, $\alpha_1 = 1.86$, $\alpha_2 = 0.325$, $\alpha_3 = 0.65$ and $\epsilon = 0.69$ in Eqns. 4.3.

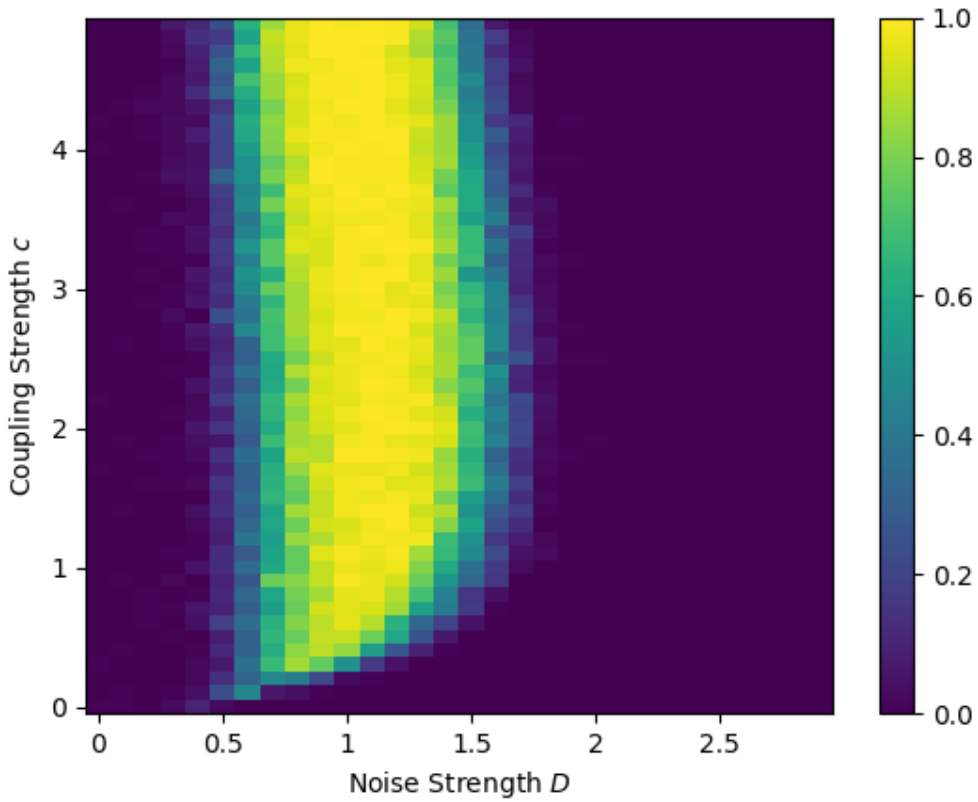

Figure 4.15: Dependence of the probability of obtaining OR logic operation, P(OR), on noise strength D and coupling strength c, for bias $b = 1$ and system parameters: $g = 0.1$, $\alpha_1 = 1.86$, $\alpha_2 = 0.325$, $\alpha_3 = 0.65$ and $\epsilon = 0.69$ in Eqns. 4.3.

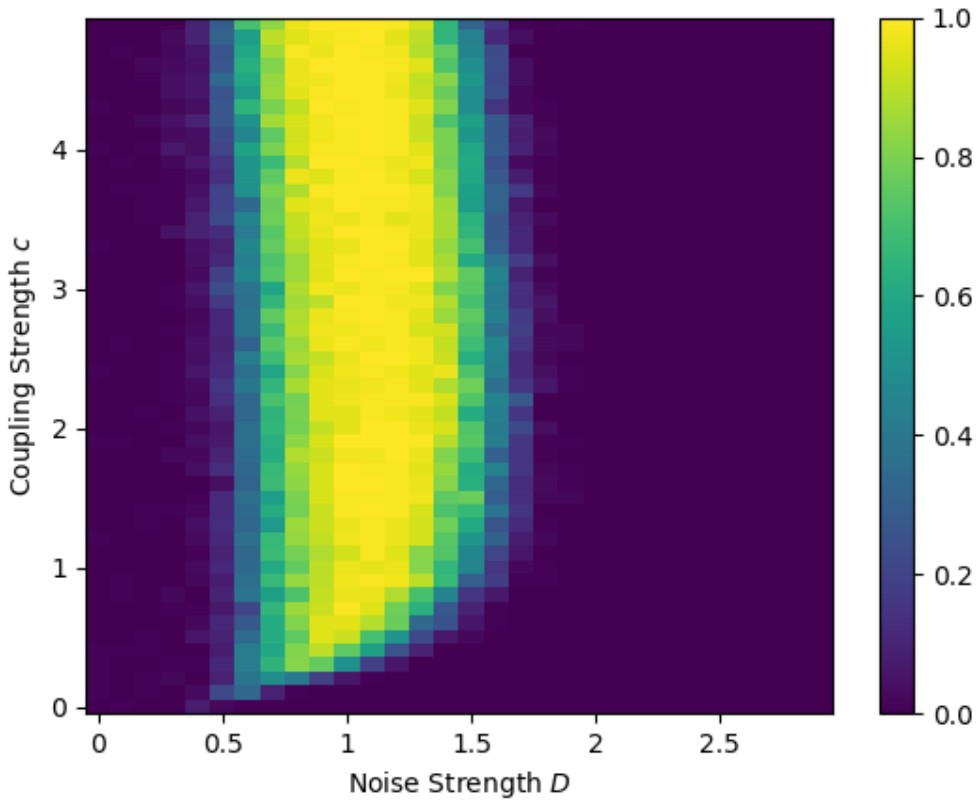

Figure 4.16: Dependence of the probability of obtaining AND logic operation P(AND), on noise strength D and coupling strength c, for bias $b = 1$ and system parameters: $g = 0.1$, $\alpha_1 = 1.86$, $\alpha_2 = 0.325$, $\alpha_3 = 0.65$ and $\epsilon = 0.69$ in Eqns. 4.3.

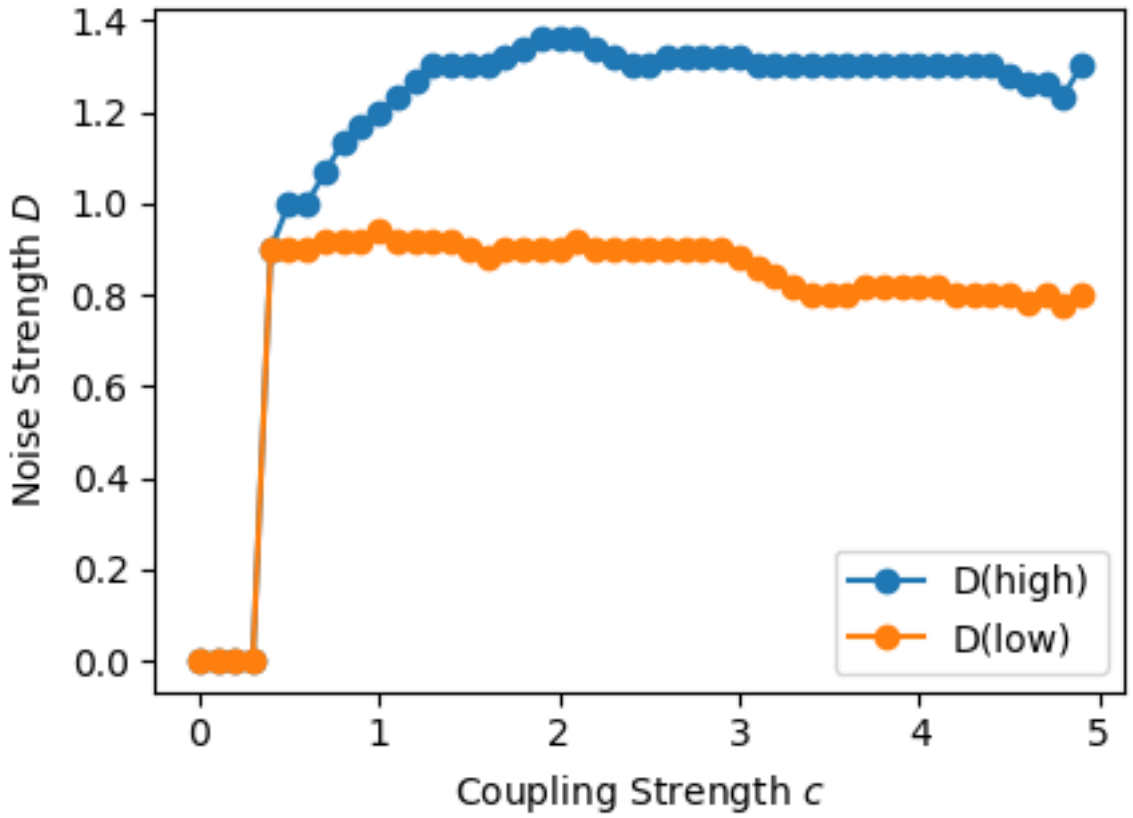

Figure 4.17: Dependence of the minimum noise strength ($D(low)$) and maximum noise strength ($D(high)$) required to obtain a probability $P(logic) > 0.9$ on the coupling strength c. Here the bias $b = +1$.

4.4 Conclusions

In summary, we have implemented logic gates, in a second order autonomous memristive circuit, in the presence of a noise-floor. We have demonstrated that in an optimal band of noise one obtains logic operations extremely reliably. Further, the system yields the complementary logic operation in parallel as well. Lastly the outputs can be morphed to different logic functions by a simple switch of the constant bias. Furthermore we also demonstrated the successful implementation of coupling induced Logical Stochastic Resonance in a coupled system of memristors, and this paves the path for realization of multi-input logic gates without the need of separate adder circuits. All these ideas are demonstrated explicitly through numerical simulations, as well as proof-of-principle circuit experiments. Thus the memristive circuit offers a promising system to implement robust and flexible logic operations and our results may help expand the scope of memristive device-based memcomputing.

Chapter 5

Conclusions and future directions

"Begin at the beginning," the King said, very gravely,
"and go on till you come to the end: then stop."

- Lewis Carroll, *Alice in Wonderland*.

Interplay of noise and nonlinearity in dynamical systems has been an area of research that has garnered long standing interest for multiple reasons. Stochastic processes driving deterministic nonlinear systems produce novel and sometimes counter intuitive phenomena like stochastic resonance which need to be completely understood to effectively model real world systems. Also, in the ever shrinking world of micro-electronics, implicit background noises have almost caught up with the operating voltages of circuits. This is a direct outcome of the major progress in micro-fabrication and the explosive growth in the number of transistors as predicted by Moore's law. With the upper limit to computational power looming in our horizon, it becomes imperative to come up with innovative ways of using noises in novel ways rather than simply trying to suppress them. Thus the understanding of the interaction between dynamic noises and the rich controllable dynamics of simple nonlinear systems have gained utmost importance.

This thesis broadly, is an attempt to further this cause in two ways. First, to introduce the new paradigm of coupling in a simple well understood system, explore the effects of the interplay of coupling and noise and use the understanding to propose and demonstrate a new scheme for producing reliable logic operations using the coupling as the key player. Second, to elucidate the possible use cases of fundamental passive nonlinear circuit elements, like the memristor, that have been recently physically realized, in furthering this new push for dynamics based computing. The direct use of memristors (which themselves are passive memory devices) in tandem with simple resistors and capacitors to produce noise-aided logic, clearly takes us a step closer to neuromorphic computing, where the same building blocks serve as both memory and processing devices.

In the first part (chapter 2) of this thesis we explored the different regimes of behaviour that arise in two diffusively coupled bistable systems, under the influence of uncorrelated noise. Depending on the coupling and noise strengths, we saw four clear regimes of behaviour emerge: (i) no synchrony and no hopping, (ii) synchrony without hopping, (iii) unsynchronized hopping and (iv) synchronized hopping. We characterized these regimes quantitatively using two measures: synchronization error and probability of hopping. Interestingly, the synchronization error decreases monotonically with coupling strength, while the probability of hopping changes non-monotonically with coupling strength, exhibiting an optimal coupling where hopping probability is maximized. In contrast, the probability of hopping increases monotonically with noise strength, while the synchronization shows non-monotonic dependence on noise strength. The delicate interplay of these monotonic and non-monotonic behaviours with respect to coupling and noise, yielded regions of parameter space where either synchrony or hopping, were dominant. This gave rise to the four interesting dynamical patterns, including the non-trivial

synchronized hopping regime.

We confirmed the generality of these findings for different noise distributions, and for a variety of bistable systems. We also experimentally constructed and coupled, two simple piecewise linear circuits and established the robustness of our results. We consolidated the obtained results and moved on to use the results to implement coupling induced Logical Stochastic Resonance that we elaborated in Chapter 3.

These results obtained in chapter 2 can be explored and expanded further in three directions. First is to explore how the regions of behaviour change and morph with a constant bias tilting the wells, as another parameter. Second is to check the influence of various kinds on noise on the system so that we can better understand the behaviour of coupled bistable systems in real world background noise, which usually contains a mixture of noises, both additive and parametric. Third is to expand the spatial extent of the system by increasing the number of bistable units. How a network of coupled bistable systems operate in the presence of noise, is also a question worth pursuing as it will also have direct implications in expanding the scope of cLSR to coupled bistable networks.

In the second part (chapter 3) of this thesis we demonstrate both in simulation and real circuit implementations that when two coupled bistable sub-systems are driven individually by two aperiodic signals encoding a series of binary inputs, I_1 and I_2, in a moderate window of noise strengths and sufficient coupling, the output of the system robustly maps to the 2-input logic of I_1 and I_2. We show that the constant bias in the system can act as a morphing control to switch between the different logic operations possible. We rigorously quantify the probability of obtaining consistent logic P(logic) of different gates, for various values of noise and coupling strengths. We observe that coupling has a crucial role to play in this scheme as the two inputs are individually fed into each subsystem and addition of the two signals isn't required as is the case with Logical stochastic resonance (see 1.4). We call this new scheme of obtaining logic from coupled bistable systems as, coupling induced Logical Stochastic Resonance (cLSR).

The scope and applicability of cLSR can be furthered in two ways. When we explore and understand the behaviour of coupled bistable systems in real world background noises actual, thermal noise in micro-electronic devices can be used to implement noise-aided logic gates and can work robustly with sub-threshold input signals. With the understanding of a network of noisy bistable elements, the scope of cLSR can be further expanded to produce multi-input logic gates.

In the final part (chapter 4) of this thesis we demonstrate the implementation of

both LSR and cLSR using a very simple autonomous memristive circuit. We show that in both schemes reliable logic operations are achieved using the memristive circuit in a wide windows of moderate noise. This was confirmed both using simulations of the non-dimensionalized circuit equations and experimental realizations of the circuits themselves. We rigorously quantify the regions of the parameter space of noise, coupling and bias strengths, where highly reliable logic operations are achieved.

This work on memristive circuits can be further expanded within the scope of neuromorphic computing by exploring two key directions. One, to study how networks of memristive elements interact with one another. Two, inspecting if the memristive counterparts of the capacitor and resistor can be used to implement a circuit equivalent to the one we realized. Thereby, forming a basic logical block in a network of memristive elements.

In conclusion, the work presented in this thesis can act as a seed to further the ideas of noise-based design and dynamics-based computing both of which have a crucial bearing on the future of computation.

Bibliography

[1] Steven H Strogatz. *Nonlinear dynamics and chaos: with applications to physics, biology, chemistry, and engineering*. CRC Press, 2018.

[2] Muthusamy Lakshmanan and Shanmuganathan Rajaseekar. *Nonlinear dynamics: integrability, chaos and patterns*. Springer Science & Business Media, 2012.

[3] Vivek Kohar and Sudeshna Sinha. Noise-assisted morphing of memory and logic function. *Physics Letters A*, 376(8-9):957–962, 2012.

[4] Werner Horsthemke and René Lefever. Noise-induced transitions in physics, chemistry, and biology. *Noise-induced transitions: theory and applications in physics, chemistry, and biology*, pages 164–200, 1984.

[5] Luca Gammaitoni, Peter Hänggi, Peter Jung, and Fabio Marchesoni. Stochastic resonance. *Reviews of modern physics*, 70(1):223, 1998.

[6] K Murali, Sudeshna Sinha, William L Ditto, and Adi R Bulsara. Reliable logic circuit elements that exploit nonlinearity in the presence of a noise floor. *Physical review letters*, 102(10):104101, 2009.

[7] K Murali, I Rajamohamed, Sudeshna Sinha, William L Ditto, and Adi R Bulsara. Realization of reliable and flexible logic gates using noisy nonlinear circuits. *Applied Physics Letters*, 95(19):194102, 2009.

[8] Adi R Bulsara, Anna Dari, William L Ditto, K Murali, and Sudeshna Sinha. Logical stochastic resonance. *Chemical Physics*, 375(2-3):424–434, 2010.

[9] Lei Zhang, Aiguo Song, and Jun He. Effect of colored noise on logical stochastic resonance in bistable dynamics. *Physical Review E*, 82(5):051106, 2010.

[10] Anna Dari, Behnam Kia, Adi R Bulsara, and William L Ditto. Logical stochastic resonance with correlated internal and external noises in a synthetic biological logic block. *Chaos: An Interdisciplinary Journal of Nonlinear Science*, 21(4):047521, 2011.

[11] Siliang Lu, Zhijia Dai, Yongbin Liu, Guoqiang Liu, Hui Yang, and Feifei Wang. Decreasing bit error rate by using enhanced tristable logical stochastic resonance in heavy noise condition. *Chinese Journal of Physics*, 58:179–189, 2019.

[12] Huiqing Zhang, Tingting Yang, Wei Xu, and Yong Xu. Effects of non-gaussian noise on logical stochastic resonance in a triple-well potential system. *Nonlinear Dynamics*, 76(1):649–656, 2014.

[13] Huiqing Zhang, Yong Xu, Wei Xu, and Xiuchun Li. Logical stochastic resonance in triple-well potential systems driven by colored noise. *Chaos: An Interdisciplinary Journal of Nonlinear Science*, 22(4):043130, 2012.

[14] Remo Storni, Hiroyasu Ando, Kazuyuki Aihara, K Murali, and Sudeshna Sinha. Manipulating potential wells in logical stochastic resonance to obtain xor logic. *Physics Letters A*, 376(8-9):930–937, 2012.

[15] Nan Wang and Aiguo Song. Parameter-induced logical stochastic resonance. *Neurocomputing*, 155:80–83, 2015.

[16] Hao Wu, Hui-jun Jiang, and Zhong-huai Hou. Array-enhanced logical stochastic resonance in coupled bistable systems. *Chinese Journal of Chemical Physics*, 25(1):70–76, 2012.

[17] L Zhang, AG Song, and J He. Logic signals driven stochastic resonance in bistable dynamics subjected to 1/f noise floor. *The European Physical Journal B*, 80(2):147–153, 2011.

[18] Yong Xu, Xiaoqin Jin, Huiqing Zhang, and Tingting Yang. The availability of logical operation induced by dichotomous noise for a nonlinear bistable system. *Journal of Statistical Physics*, 152(4):753–768, 2013.

[19] Vivek Kohar, K Murali, and Sudeshna Sinha. Enhanced logical stochastic resonance under periodic forcing. *Communications in Nonlinear Science and Numerical Simulation*, 19(8):2866–2873, 2014.

[20] P Pfeffer, F Hartmann, S Höfling, M Kamp, and L Worschech. Logical stochastic resonance with a coulomb-coupled quantum-dot rectifier. *Physical Review Applied*, 4(1):014011, 2015.

[21] Hiroyasu Ando, Sudeshna Sinha, Remo Storni, and Kazuyuki Aihara. Synthetic gene networks as potential flexible parallel logic gates. *EPL (Europhysics Letters)*, 93(5):50001, 2011.

[22] Animesh Gupta, Aman Sohane, Vivek Kohar, K Murali, and Sudeshna Sinha. Noise-free logical stochastic resonance. *Physical Review E*, 84(5):055201, 2011.

[23] Amit Sharma, Vivek Kohar, Manish Dev Shrimali, and Sudeshna Sinha. Realizing logic gates with time-delayed synthetic genetic networks. *Nonlinear Dynamics*, 76(1):431–439, 2014.

[24] Edward H Hellen, Syamal K Dana, Jürgen Kurths, Elizabeth Kehler, and Sudeshna Sinha. Noise-aided logic in an electronic analog of synthetic genetic networks. *Plos one*, 8(10):e76032, 2013.

[25] Juan Wu, Yong Xu, Haiyan Wang, and Jürgen Kurths. Information-based measures for logical stochastic resonance in a synthetic gene network under lévy flight superdiffusion. *Chaos: An Interdisciplinary Journal of Nonlinear Science*, 27(6):063105, 2017.

[26] Nan Wang and Aiguo Song. Enhanced logical stochastic resonance in synthetic genetic networks. *IEEE transactions on neural networks and learning systems*, 27(12):2736–2739, 2015.

[27] J Zamora-Munt and C Masoller. Numerical implementation of a vcsel-based stochastic logic gate via polarization bistability. *Optics express*, 18(16):16418–16429, 2010.

[28] Kamal P Singh and Sudeshna Sinha. Enhancement of "logical" responses by noise in a bistable optical system. *Physical Review E*, 83(4):046219, 2011.

[29] Bing Zheng, Nan Wang, Haiyong Zheng, Zhibin Yu, and Jinpeng Wang. Object extraction from underwater images through logical stochastic resonance. *Optics letters*, 41(21):4967–4970, 2016.

[30] Diego N Guerra, Adi R Bulsara, William L Ditto, Sudeshna Sinha, K Murali, and P Mohanty. A noise-assisted reprogrammable nanomechanical logic gate. *Nano letters*, 10(4):1168–1171, 2010.

[31] Leon Chua. Memristor-the missing circuit element. *IEEE Transactions on circuit theory*, 18(5):507–519, 1971.

[32] Massimiliano Di Ventra, Yuriy V Pershin, and Leon O Chua. Circuit elements with memory: memristors, memcapacitors, and meminductors. *Proceedings of the IEEE*, 97(10):1717–1724, 2009.

[33] Dmitri B Strukov, Gregory S Snider, Duncan R Stewart, and R Stanley Williams. The missing memristor found. *nature*, 453(7191):80, 2008.

[34] Yuriy V Pershin and Massimiliano Di Ventra. Neuromorphic, digital, and quantum computation with memory circuit elements. *Proceedings of the IEEE*, 100(6):2071–2080, 2011.

[35] V. Manaoj Aravind, K. Murali, and Sudeshna Sinha. Synchronized hopping induced by interplay of coupling and noise. In Walter Lacarbonara, Balakumar Balachandran, Jun Ma, J. A. Tenreiro Machado, and Gabor Stepan, editors, *Nonlinear Dynamics and Control*, pages 325–334, Cham, 2020. Springer International Publishing.

[36] Arkady Pikovsky, Michael Rosenblum, Jurgen Kurths, and Jürgen Kurths. *Synchronization: a universal concept in nonlinear sciences*, volume 12. Cambridge university press, 2003.

[37] Manaoj Aravind, K Murali, and Sudeshna Sinha. Coupling induced logical stochastic resonance. *Physics Letters A*, 382(24):1581–1585, 2018.

[38] István Z Kiss, John L Hudson, J Escalona, and P Parmananda. Noise-aided synchronization of coupled chaotic electrochemical oscillators. *Physical Review E*, 70(2):026210, 2004.

[39] Alexander Neiman. Synchronizationlike phenomena in coupled stochastic bistable systems. *Physical Review E*, 49(4):3484, 1994.

[40] Jeff Hasty, Farren Isaacs, Milos Dolnik, David McMillen, and James J Collins. Designer gene networks: Towards fundamental cellular control. *Chaos: An Interdisciplinary Journal of Nonlinear Science*, 11(1):207–220, 2001.

[41] Edmon Perkins and Balakumar Balachandran. Effects of phase lag on the information rate of a bistable duffing oscillator. *Physics Letters A*, 379(4):308–313, 2015.

[42] Morris M Mano. *Computer system architecture*. Dorling Kindesley Pearson, 2005.

[43] E Tamaseviciute, A Tamasevicius, G Mykolaitis, S Bumeliene, and Erik Lindberg. Analogue electrical circuit for simulation of the duffing-holmes equation. *Nonlinear Analysis: Modelling and Control*, 13(2):241–252, 2008.

[44] Md Abdullah Al Hafiz, Lakshmoji Kosuru, and Mohammad I Younis. Towards electromechanical computation: An alternative approach to realize complex logic circuits. *Journal of Applied Physics*, 120(7):074501, 2016.

[45] Syed NR Kazmi, Md AA Hafiz, Karumbaiah N Chappanda, Saad Ilyas, Jorge Holguin, Pedro MFJ Costa, and Mohammad I Younis. Tunable nanoelectromechanical resonator for logic computations. *Nanoscale*, 9(10):3449–3457, 2017.

[46] Massimiliano Di Ventra and Yuriy V Pershin. The parallel approach. *Nature Physics*, 9(4):200, 2013.

[47] Francesco Caravelli, Fabio Lorenzo Traversa, and Massimiliano Di Ventra. Complex dynamics of memristive circuits: Analytical results and universal slow relaxation. *Physical Review E*, 95(2):022140, 2017.

[48] Valeriy A Slipko and Yuriy V Pershin. Metastable memristive lines for signal transmission and information processing applications. *Physical Review E*, 95(4):042213, 2017.

[49] Quan Xu, Qinling Zhang, Bocheng Bao, and Yihua Hu. Non-autonomous second-order memristive chaotic circuit. *IEEE Access*, 5:21039–21045, 2017.